ANALYSIS OF A BONDED JOINT
USING BULK ADHESIVE PROPERTIES

by

Talia Osiroff

Thesis submitted to the Faculty of the

Virginia Ploytechnic and State University

in partial fulfillment of the requirements for the degree of

Master of Science

in

Engineering Mechanics

APPROVED:

J. Wallace Grant, Chairman

O. Hayden Griffin

David A. Dillard

December, 1988

Blacksburg, Virginia

ANALYSIS OF A BONDED JOINT USING BULK ADHESIVE PROPERTIES

by

Talia Osiroff

J. Wallace Grant, Chairman

Engineering Mechanics

(ABSTRACT)

Adhesives and adhesively bonded structures are being considered as a viable alternative to conventional fastening methods. In order to gain wider acceptance, it is essential to address the issue of the mechanical characterization of adhesive materials and its implementation in the design of bonded joints.

While measuring the in-situ properties of the adhesive in a joint is a difficult task, characterizing its bulk properties is a relatively simpler undertaking. The objective of this study was to propose and verify an experimental procedure that would allow the analytical prediction of the viscoelastic behaviour of a bonded joint, using bulk adhesive properties. The Arcan joint geometry was chosen because of the simple state of stress within the adhesive.

Two automotive adhesives were studied: Ashland Plyogrip

6600/6620, a urethane; and Lord Fusor 320/322, a toughened epoxy. The time dependent characteristics of bulk adhesive specimens were obtained from a series of tensile creep tests conducted on cast adhesive coupons. The viscoelastic behaviour was then utilized in a finite element analysis of bonded joints, in order to predict the deformational behaviour. The final step was to compare the finite element prediction with test results.

For Ashland 6600/6620 urethane, partial agreement between the predicted and the measured results was observed. However, the F.E. prediction of the transient response at each stress level agrees well with the measured transient deformation. The F.E. predictions obtained in the analysis of Lord Fusor 320/322 epoxy deviate from the corresponding test results.

Experimental errors are believed to be the main cause for the deviation of the finite element prediction from the actual test results. These errors affected the accuracy of the viscoelastic characterization of the bulk adhesive as well as the accuracy of the data recorded when testing the Arcan bonded specimens.

The results of the analysis presented in this study indicate that it may be possible to predict the viscoelastic behaviour of any adhesively bonded joint based on viscoelastic characterization of the bulk adhesive.

ACKNOWLEDGEMENTS

The author would like to express gratitude to the direct and indirect support of this work, and wishes to thank:

Her advisor, Dr. Grant, for his guidance, support and patience throughout this study.

General Motors Technical Center, for funding this work.

for his assistance in the laboratory.

Dr. Kurt Gramoll for his useful suggestions and for his help with the computer code he has developed.

The author's parents, and , for their support and understanding.

Most importantly the author would like to thank her husband, , for all his help and support, and her sons, and for they are the best.

TABLE OF CONTENTS

List of Illustrations

List of Tables

Chapter 1

INTRODUCTION

In the 1940's the aircraft industry began promoting the use of adhesives as structural bonding agents. Since that time adhesives have replaced some of the conventional methods of fastening and joining. Nowadays, the aerospace industry is increasing the use of more adhesive bonding in structural components.

Penetration methods, such as drilling holes, cause highly localized stress concentrations. In addition, in structures made of composite materials, the holes damage the fiber reinforcement, thus reducing the strength of the joint and promoting early damage.

Bonded joints reduce the stress concentration, providing greater strength to the assembled parts. This characteristic implies that adhesively bonded joints are potentially more fatigue resistant when subjected to dynamic loads. Adhesives also provide a method of joining together dissimilar materials, even when conventional methods cannot be used due to problems such as electrochemical corrosion between two metals.

There are some disadvantages to the use of adhesives. Being mostly polymers, adhesives are sensitive to temperature, moisture, and

chemical degradation. They exhibit time dependent properties, which demands consideration of the long term durability of the joint.

Stresses and deformations of a bonded structure are functions of the mechanical properties of the components, the geometry of the structure and the type of loads acting on it. It is therefore important to correctly design and predict the behaviour of a bonded joint.

The Finite Element method has been widely used to analyze and determine the stress distributions and displacements in adhesively bonded joints. This type of analysis requires information regarding the viscoelastic properties of the adhesive.

In-situ testing of bonded joints is very difficult to conduct. It is nessesary to use test geometries in which the stress distribution within the bondline is exactly known. Such tests include the Cone and Plate test introduced by Grant and Cooper [12] and the Arcan stiff adherent joint introduced by Arcan and Weissberg [29].

Bulk adhesive tests are relatively easier to conduct. Unfortunately, the correlation between the properties of the bulk material and those of the adhesive in a bonded joint has not been established.

The objective of this effort is to develop a technique in which time dependent material properties, as measured in bulk adhesive specimens, could be introduced into Finite Element analytical methods in order to predict the stresses and deformations of bonded

structures.

Two automotive structural adhesives were evaluated: Ashland Plyogrip 6600/6620, a two part urethane, and Lord Fusor 320/322, a two part toughened epoxy. Relatively thick bondlines were tested to minimize the effects of the interfaces and interphases on the mechanical response of the adhesive.

The three main stages of this study are:

i) Characterization of bulk cast adhesive coupons. The coupons were subjected to tensile creep tests at various stress levels for a period of 1800 seconds, during which the displacements were recorded. The experimental creep compliance curves were modeled using a nonlinear quadratic power law.

ii) Conducting preliminary analysis of the time dependent displacements that occur in an adhesively bonded Arcan joint. In this analysis, the Finite Element code ABAQUS was used. The bulk adhesive creep compliance was incorporated into the analysis.

iii) Performing shear creep tests on adhesively bonded Arcan specimens, in order to compare the predictions of the preliminary Finite Element analysis with the actual behaviour of the joint.

Chapter 2

BACKGROUND INFORMATION

2.1 THEORY OF VISCOELASTICITY

Viscoelasticity is the study of materials whose mechanical response is a function of time and previous history, often referred to as a memory effect.

When a viscoelastic material is subjected to a constant uniaxial load, (a creep test), strain increases with time. At the moment the stress is applied, an instantaneous elastic response, ε_0, is recorded. Following the initial deformation, strain increases with time. Similarly, the tensile creep compliance (D), defined as the time dependent strain divided by the value of the constant stress, exhibits an initial instantaneous response, D_0, followed by an increase in value with time.

When the load is removed, a process of deformation recovery takes place. First an instantaneous elastic response and then creep recovery. The material is said to "remember" its original geometry and recovers with time towards this original configuration. The creep-creep recovery test (illustrated in fig 2.1) is very useful in determinimg the viscoelastic nature and properties of a material. It

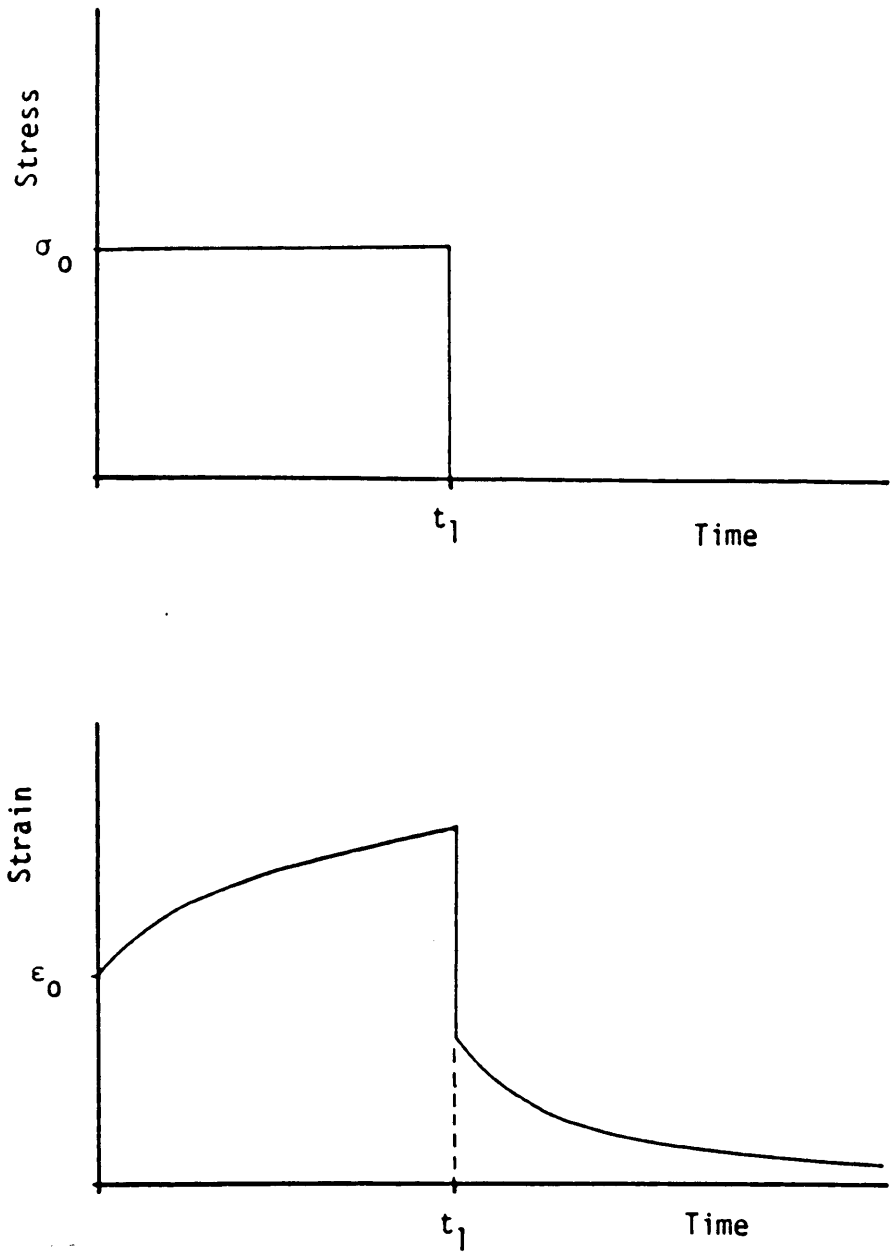

Figure 2.1: Stress and Strain Histories for a Creep - Creep Recovery Test [7].

is also very common, mainly because it is an easy test to perform.

Another test used in the characterization of viscoelastic materials is the stress relaxation test, as illustrated in fig 2.2. In this test the specimen is subjected to a unidirectional step deformation causing the axial strain to be held constant. The result is an initial axial stress which relaxes with time.

Viscoelastic materials can be further divided into linear and nonlinear viscoelastic materials. A procedure to distinguish between the linear and nonlinear behavior of materials is by plotting "isochronous" stress-strain curves. The data from several creep tests at different stress levels is used to create stress-strain curves at constant times. Figure 2.3 illustrates the procedure to obtain isochronous stress-strain curves. The portion of the curves with constant slope corresponds to linear viscoelastic behavior. The portions of the curves with a changing slope represent non linear viscoelastic behavior. Materials may be characterized as linear viscoelastic, nonlinear viscoelastic or in most cases, linear viscoelastic up to a certain stress level and at a certain time.

2.1.1 Linear Viscoelasticity

Linear viscoelastic behavior is most commonly represented with the aid of mechanical analogs, linear springs and dashpots, connected in series or in parallel. Two of the most basic models are the Kelvin

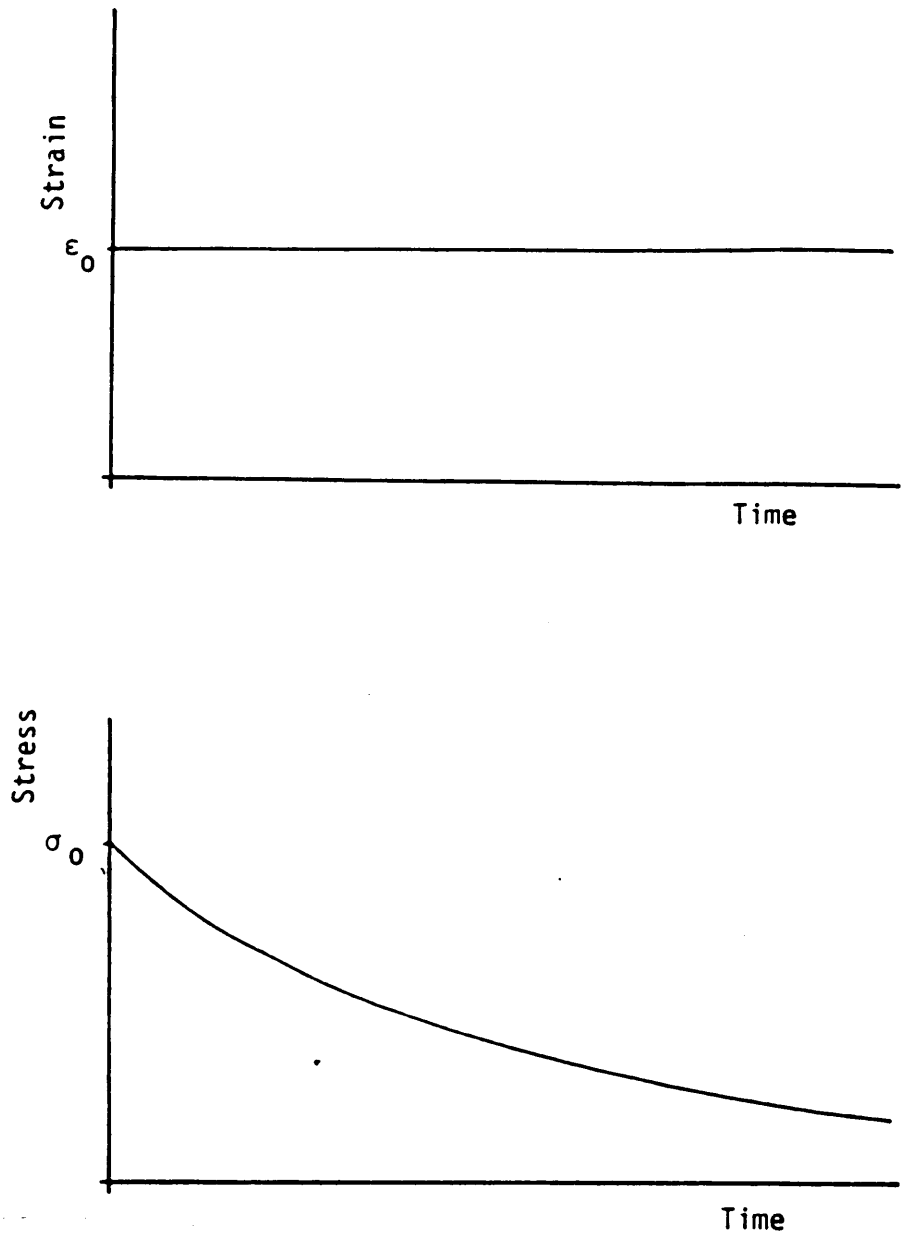

Figure 2.2: Stress and Strain Histories for a Stress Relaxation Test [7].

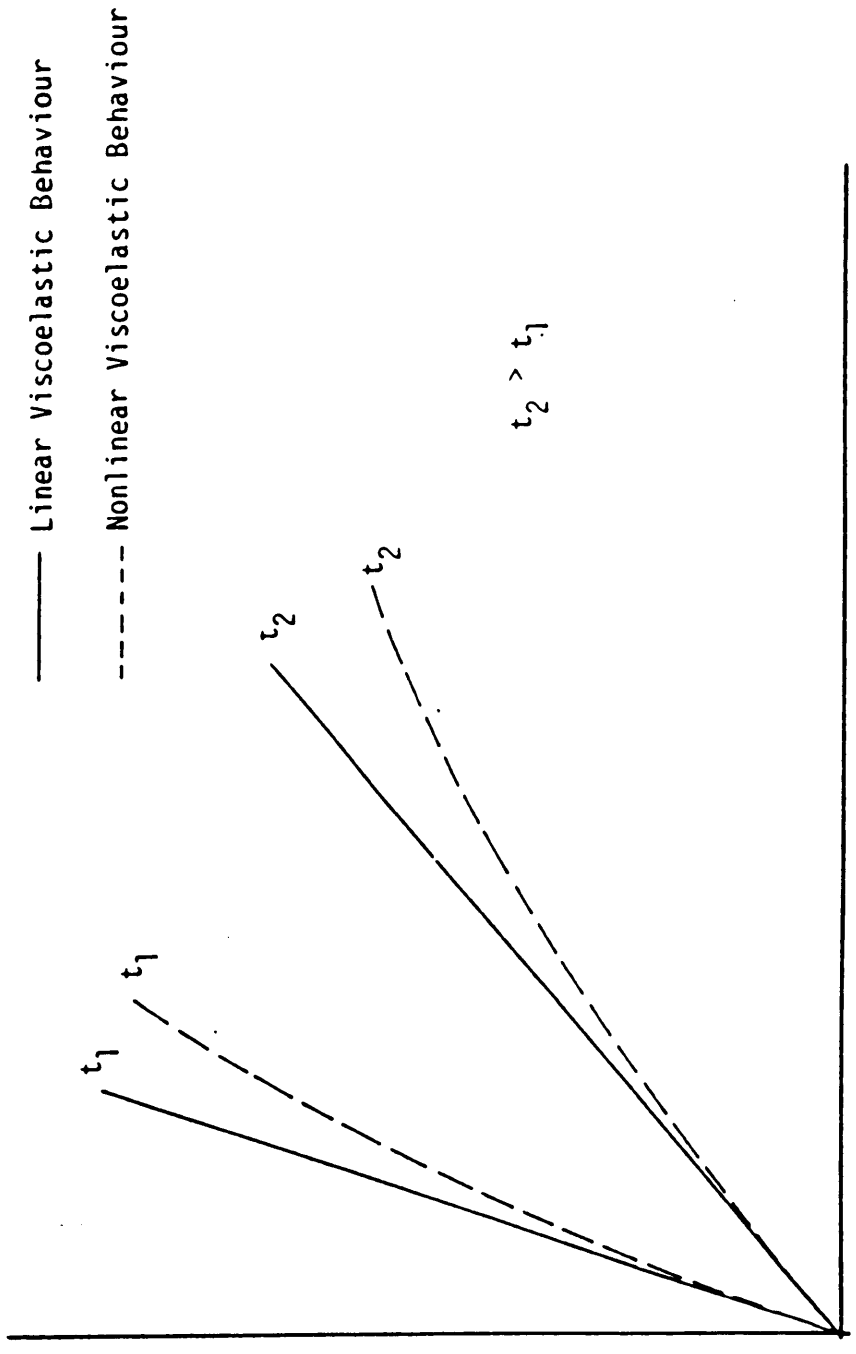

Figure 2.3: Isochronous Stress Strain Curves Illustrating Linear and Nonlinear Viscoelastic Behaviour [7].

solid and the Maxwell fluid (fig 2.4).

Most often, the linear time-dependent response of a given material cannot be realistically modeled with a single Kelvin or a single Maxwell element. However, by combining a sufficient number of the basic elements i.e., springs and dashpots, an accurate representation of the material properties can be achieved.

A series of Kelvin elements with a free dashpot, a free spring or both is commonly used to describe the creep compliance function of a given material over an extended period of times. Each of the multiple Kelvin elements usually accounts for a different period of time.

For a series of Kelvin elements, the creep compliance is given by:

$$D(t) = \sum_{i=1}^{n} \frac{1}{E_i}\left[1 - e^{-E_i t/\mu_i} \right] \qquad (2.1)$$

Where E_i is the stiffness of the i^{th} spring and μ_i is the viscosity of the i^{th} dashpot. If a free spring is added, the model would describe a viscoelastic solid with instantaneous elastic response and no permanent flow. If, on the other hand, a single dashpot is added allowing for a permanent deformation, the model describes a viscoelastic fluid.

The Boltzmann Superposition Principle enables us to find the response of a linear viscoelastic material to any arbitrary stress history. This is done by representing the stress history as series of

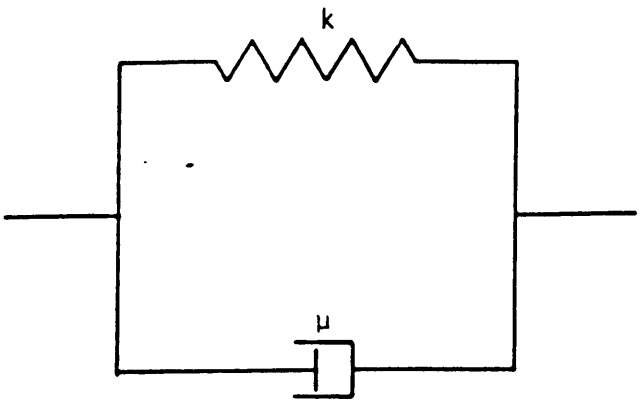

a) Kelvin Viscoelastic Element

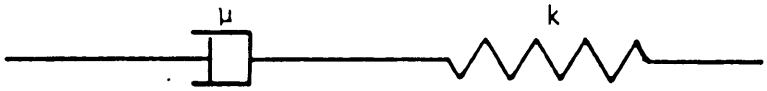

b) Maxwell Viscoelastic Element

Figure 2.4: Simple Mechanical Analogies Used to Model Viscoelastic Behaviour [7].

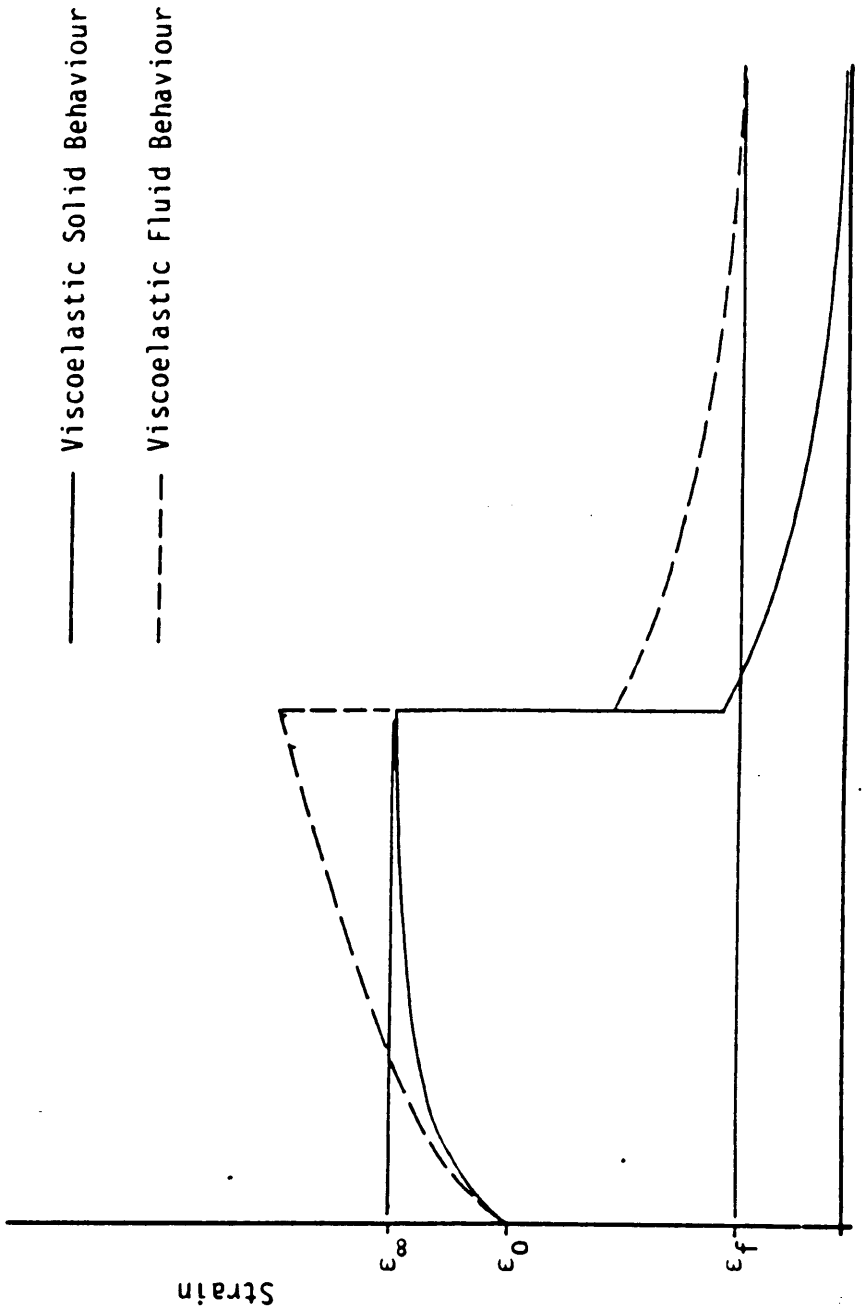

Figure 2.5: Typical Creep -Creep Recovery Behaviour for Viscoelasic Solids and Viscoelastic Fluids [7].

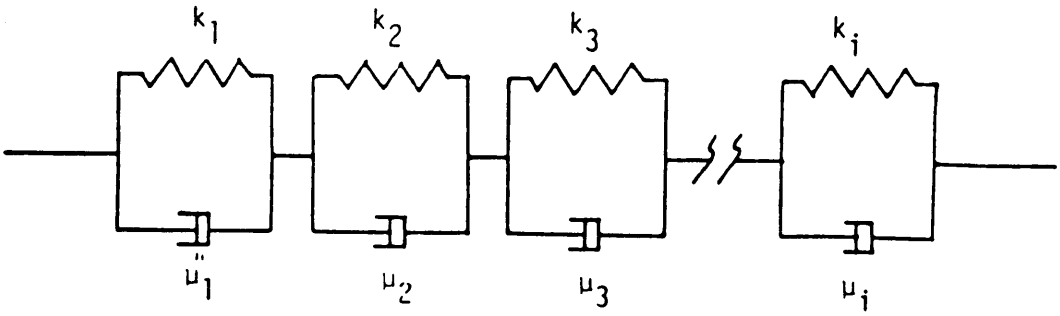

a) Generalized Kelvin Model

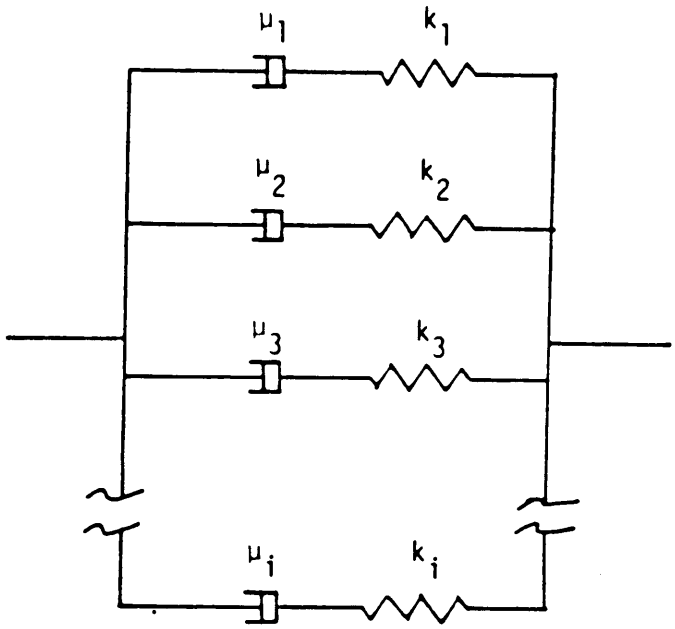

b) Generalized Maxwell Model

Figure 2.6: Generalized Viscoelastic Models [7].

small steps in stress.

$$\varepsilon(t) = \int_{0^-}^{t} D\,(t-\tau)\,\frac{d\sigma}{d\tau}\,d\tau \qquad (2.2)$$

Where:

D (t) is the compliance function of the material

t is the time at the end of each step

τ is a dummy time variable

σ is the stress level at each step

The linear viscoelastic response of a wide variety of materials can be empirically described using a simple power law:

$$D(t) = D_0 + mt^n \qquad (2.3)$$

Where D_0 is the instantaneous compliance and the constants m and n are considered the material properties representing the time dependent behavior. Findley [24-275], has successfully used the power law representation to characterize the linear viscoelastic performance of many polymers.

2.1.2 Nonlinear Viscoelasticity

Although it is not common practice, nonlinear viscoelastic materials can be modeled by modifying the generalized Kelvin and

Maxwell models. This is done by using nonlinear springs and dashpots. Thus, the relaxation times τ_i are not constant for each element and are a function of the stress level. Nonlinearity can also be accounted for by using nonlinear functions to describe the stress.

Green and Rivlin [23] introduced the multiple integral to account for nonlinearity in viscoelastic behavior.

$$\varepsilon(t) = \int_{-\infty}^{t} D_1(\, t-\tau\,)\, \frac{d\sigma(\tau)}{d\tau}\, d\tau +$$

$$+ \int_{-\infty}^{t}\int_{-\infty}^{t}\int_{-\infty}^{t} D_3(t-\tau_1, t-\tau_2, t-\tau_3)^{*}\, \frac{\sigma(\tau_1)}{d\tau_1}\, \frac{d\sigma(\tau_2)}{d\tau_2}\, \frac{d\sigma(\tau_3)}{d\tau_3}\, d\tau_1 d\tau_2 d\tau_3 + \ldots \qquad (2.4)$$

The first term in equation (2.4) describes the linear viscoelastic behavior, whereas the second one introduces the nonlinearity.

In order to use this model, there is a need to determine experimentally a large number of kernel functions, which makes the use of this model difficult and impractical.

The power law, used to describe linear viscoelastic materials, can be modified to include nonlinearity due to stress level by assuming the instantaneous compliance, D_0, and the constant, m, to be functions of stress.

Findley [24-27] suggested the following hyperbolic sine functions

$$D_0 = D_0^* \sinh (\sigma/\sigma_D)$$

$$m = m^* \sinh (\sigma/\sigma_m)$$

$$n = \text{constant} \qquad (2.5)$$

This model, often referred to as the Findley power law, is an empirical model which is relatively simple to use. It requires only a few material constants to be determined from experimental data.

Gramoll [6] introduced the "quadratic power law" where the hyperbolic sine functions are replaced with simple quadratic functions of the form

$$D(t,\sigma) = (1 + g\sigma^2)D_0 + (1 + f\sigma^2)mt^n \qquad (2.6)$$

Where D_0 and m are the linear constants, while g and f are nonlinear stress constants. This modification eliminates the numerical difficulties caused by the hyperbolic sine function at high stress levels and also allows one to regain the linear form by setting the values of f and g to be zero.

The Schapery integral model is another nonlinear viscoelastic model which is widely used. The model is derived from the fundamental principles of irreversible thermodynamics. For applied uniaxial

stress, the strain is given by,

$$\varepsilon(t) = g_0 D_0 \sigma + g_1 \int_{-\infty}^{t} \Delta D(\psi - \psi') \frac{d(g_2\sigma)}{d\tau} d\tau \qquad (2.7)$$

where

D_0 and $\Delta D(\psi)$ are the initial and transient compliance for the linear viscoelastic response. The reduced time ψ and ψ' are defined by

$$\psi = \psi(t) = \int_0^t \frac{dt'}{a_\sigma}$$

$$\psi' = \psi'(\tau) = \int_0^\tau \frac{dt'}{a_\sigma}$$

and g_0 , g_1 , g_2 , a are nonlinear stress functions.

The nonlinear stress effects are introduced through the Schapery functions: g_0, g_1, g_2, and the 'stress shift factor' a_σ.

The transient compliance, ΔD is generally represented by a power law: $\Delta D(\psi) = m\psi^n$. Equation (2.7) becomes,

$$\varepsilon(t) = g_0 D_0 \sigma + g_1 m \int_{-\infty}^{t} (\psi - \psi')^n \frac{d(g_2\sigma)}{d\tau} d\tau \qquad (2.8)$$

For the case of a simple creep test where the stress is σ_0, equation (2.8) becomes,

$$\varepsilon(t) = \left[g_0 D_0 + \frac{g_1 g_2 m t^n}{a_\sigma^n} \right] \sigma_0 \qquad (2.9)$$

It is also noticed that by setting the nonlinear parameters to be equal to 1, equation (2.9) reduces to the linear case of equation (2.3). In order to obtain the parameters required by Schapery's model, creep and creep recovery data are used. The procedure to obtain these parameters has four steps.

The first two steps determine the three linear parameters (D_0, m and n) from creep and creep recovery data for the linear stress range. The remaining four functions (g_0, g_1, g_2 and a_σ) are determined in two steps from the creep and creep recovery data in the nonlinear stress range. A detailed description is found in Tuttle [7].

2.2 IN SITU VERSUS BULK MATERIAL PROPERTIES

When analyzing the stress in a bonded joint, we are faced with a severe problem: the lack of material data for adhesives. There is little information on the correlation between bulk and in-situ adhesive properties.

The presence of the adherends changes the mechanical properties of the adhesive in a bonded joint compared with the bulk material properties. This subject has been recently surveyed in detail by Cooper [10].

According to Alfey [13], the differences in the mechanical response of the bulk and the in situ state is caused by the presence of a weak boundary layer that separates the bulk adhesive from the

metal adherends. However, by accounting for parameters such as the geometry of the joint, the curing history and the residual stesses the behaviour of the bulk adhesive and the adhesive in a bonded joint should be similar.

An important factor in understanding the relationship between adhesive properties and thermodynamic state is the excess free volume (the difference between the equilibrium and glassy free volume) [14]. The curing process induces thermal stresses in the joint, due to a difference in the coefficients of thermal expansion between the substances in the bonded joint. These residual stresses may have an effect on the excess free volume and thus affect the properties of the adhesive in-situ.

The mechanical and physical properties of bulk polymers have been reported in detail. Ferry [15] is a good source of such data. Recently, however, there has been an interest in the characterization of bulk adhesive properties as part of an effort to understand the behaviour of adhesives in bonded joints.

Peretz and Weitsman [16], characterized unscrimmed neat FM-73 in terms of Schepery's nonlinear viscoelastic model [17]. The linear viscoelastic shear creep compliance of the same material was determined by Knauss et al. [18]. Lefebvre and Brinson [19] studied the relaxation and cyclic creep response of neat unscrimmed FM-73 and FM-300.

In their investigation of the relationship between bulk and in-situ mechanical properties of adhesives, Dolev and Ishai [20] have

made two important assumptions. The first one is that the basic mechanical properties of an adhesive layer in a bonded joint is similar to the properties of the same adhesive in the bulk state. The second assumption is that for a joint that has been properly surface treated, the failure mode is cohesive.

Stinger [21] contradicts the assumption that bulk and in-situ adhesive properties correlate. Stinger found a strong dependence of the apparent shear modulus in the in-situ state on the bondline thickness when linearly changing the shear stress in a torsional butt-joint specimen. The data presented shows a large scatter due to the inability to measur the bondline thickness with sufficient accuracy. Although Singer concludes that as the bondline thickness increases the plastic strain to failure decreases, this observation may not reflect plasticity in pure shear state since the shear stress varies linearly with radius.

Knollman and Hartog [22] suggested that there is a gradient in shear modulus in the interfacial zone of an epoxy bonded to aluminum. The experimental results show a fairly linear increase of the adhesive shear modulus through the interfacial zone, and at a bondline thickness of approximately 0.008 in. the modulus approaches a constant value. These results reinforce the assumption that the reason for the lack of correlation between the bulk and in-situ mechanical properties is caused by the presence of a weak boundary layer in the adhesive. The possible reason for the variation in shear modulus in the interfacial region is the variation in the residual stresses in the

adhesive, which implies a variation of the free volume through the adhesive.

Ward [31] has studied the effect of molecular orientation on bonded joints, and showed that different orientation of the molecules lead to different dynamic mechanical storage moduli. He suggests that the molecular orientation in a bonded joint, may differ from that of the free polymer due to the geometric constrains.

Through the use of a Rehovibron dynamic mechanical tester, Ward [32], evaluated viscoelastic behaviour of bonded joints. His results indicate that rigid adherends influence the viscoelastic properties of a thin bond line. Relaxation occured at different temperatures in the bulk adhesive and in the bonded adhesive, and the transitions observed were wider in the bonded joint.

Cooper [10] studied the viscoelastic response of adhesives in-situ based on properties obtained from a pure shear test geometry. Cooper suggests that bulk adhesive properties are affected by residual thermal stresses in the bonded joint.

2.3 FINITE ELEMENT ANALYSIS OF BONDED JOINTS

Many studies have been made applying Finite Element Methods to bonded structures. In his work, Roy [9], presents a detailed survey of the finite element analysis of adhesive joints.

The main purpose of this analysis is to quantify the stress

distributions and deformations in adhesively bonded specimens. Several computer codes are currently employed to analyze bonded joints using Finite Element Methods (FEM). Most of these codes can only predict the behavior of linear viscoelastic materials. In this study the following Finite Element codes were considered to model the deformation of bulk adhesives and joints.

2.3.1 VISTA Finite Element Code

VISTA is a FEM program which requires time dependent relaxation data in the form of a Prony series. The shear and bulk relaxation moduli written in this form are,

$$G(t) = G_{\infty} + \sum_{1}^{n} G_n e^{-t/\tau_n} \qquad (2.10)$$

and,

$$K(t) = K_{\infty} + \sum_{1}^{n} K_n e^{-t/\tau_n} \qquad (2.11)$$

where, n = number of terms in the series

t = time

$G(t)$ = time dependent shear modulus

$K(t)$ = time dependent bulk modulus

G_{∞} and K_{∞} = values at infinite time

G_n and K_n = coefficients

τ_n = time constants associated with the coefficients

VISTA calls for relaxation data as material property information. In order to simplify the experimental procedure, most of the time dependent material properties are obtained from creep tests. Thus, a method of converting from creep data to relaxation data is desired.

2.3.2 NOVA Finite Element Code.

NOVA, a nonlinear viscoelastic analysis code was developed by S. Roy and J N Reddy [9]. In this program the adhesive layer is modeled using Schapery's nonlinear single integral. Isotropic viscoelastic materials can be characterized in terms of the tensile creep compliance or the shear creep compliance. These compliance functions are represented by Prony series. The effect of stress level and temperature on the viscoelastic response is accounted for by the nonlinear shift factor.

In the current version of NOVA, the nonlinear material functions g_0, g_1, g_2 and a_σ for FM-73 have been defined in a subroutine named SHFACT. Thus, the program is currently calibrated to analyze FM-73 bulk adhesive and joints. Should analysis of another material be required, the subroutines describing the material properties need to be redefined and calibrated.

The program can conduct plane stress, plane strain or axisymmetric analyses of bonded joints subjected to mechanical or thermal loads that vary with time. NOVA also contains a nonlinear

Fickean moisture diffusion model and a delayed failure criterion.

2.3.3 ABAQUS Finite Element code

ABAQUS is a Finite Element code used at Virginia Polytechnic Institute and State University under academic contract with Hibbitt, Karlsson and Sorensen, Inc. The version currently available and used in this study is 4.5.

The program is designed for the numerical modeling of structural response. It consists of a number of libraries which allow for generality and flexibility in modeling.

A series of procedures provide solutions to static and dynamic stress problems. The element library is capable of modeling linear and nonlinear geometries. Through the material library, the program offers options for description of linear and nonlinear, isotropic and anisotropic material models.

A higher degree of flexibility is introduced through the subroutine option, where subroutines written by the user for a specific case are added to the internal main program.

2.4. ARCAN ADHESIVE SHEAR SPECIMEN

The use of Finite Element methods in the analysis of bonded joints requires previous knowledge of the mechanical properties of the

adhesive and adherends. It is difficult to obtain a complete characterization of the adhesive properties through in-situ testing of bonded joints. The principal obstacle is that the exact stress distribution within the bondline must be known. Most joint geometries result in complex states of stress within the bondline, making it impossible to characterize the adhesive from the measured deformations. A geometry with a uniform state of stress is ideally suited for this task.

A nearly uniform, pure shear, test specimen for adhesives was developed by M. Arcan and V. Weissberg [29]. This test is a modification of the Mixed Mode Fracture Specimen developed by M. Arcan [28].

The specimen geometry is presented in fig (2.7). The loading frame, or the grips, are made of a very stiff material. The specimen itself, is made out of two adherends bonded together to form a butterfly arrangement. Three pins on each side secure the butterfly to the frame. The tensile force, (p), is applied to the frame through the loading holes located on the frame.

The present configuration and design of the specimen allows for extreme versatility in measurements of shear properties of the adhesive and studies of mixed mode fracture of the joint.

By performing linear elastic finite element analysis, Arcan and Weissberg showed that a state of constant shear stress, almost free of other stress components, exists in the adhesive layer at a distance of approximately 1% of the bond length away from the free corner.

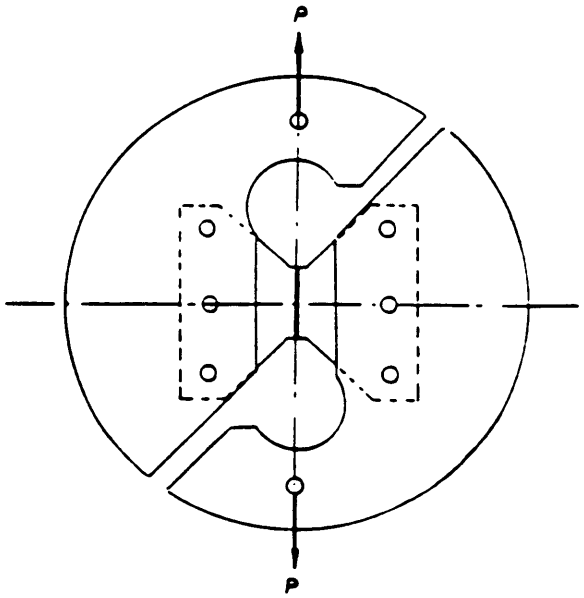

Figure 2.7: The Arcan Specimen - Showing the Loading Frame [12].

Finite element analysis of the same configuration conducted by Grant and Cooper [12] confirms the existance of a state of almost pure shear stress in the bondline.

CHAPTER 3

EXPERIMENTAL PROCEDURES AND RESULTS

3.1 Bulk Material Testing

Bulk testing of adhesives in this study required casting the bulk adhesive in sheet form. The cast sheets were cut into coupons 1 in. x 11 in. in size. The average thickness was 0.05 in. These coupons were subjected to a uniaxial creep load. The creep compliance curves obtained from these test were fitted with a quadratic power law equation, as proposed by Gramoll [6].

3.1.1 Specimen preparation

Much effort was put into establishing a technique for casting defect-free sheets of bulk adhesive. The main objective is to obtain homogeneous and consistent castings. The main problem is to eliminate the voids that are trapped during the mixing of the components or in the casting process. Both components of the adhesives utilized in this work are highly viscous, and the pot life of the mixed components is very short.

All techniques used to mix, degas, and cast bulk samples have to be very fast. The degasing procedure had to be powerful so as to pull out the air bubbles before the mixture starts to set (rapid increase of viscosity). Various methods were considered. Techniques such as mixing in a vacuum mixer to prevent trapping air, or curing in a vacuum oven did not produce uniform bubble free specimens. Preheating the components to reduce their viscosity did not improve the quality of the cast product.

The following procedure, which utilizes parts of the above techniques, has produced relatively bubble-free samples. The procedure is as follows:

(1) Prepare the mold by covering the aluminum plates withteflon coated cloth. Place spacers on plate for desiredthickness of cast sheet.

(2) Line a paper cup with two polyethylene bags (such as sandwich bags), one inside the other. The second bag is a safety bag in case the inside bag breaks.

(3) Place the cup on a scale and weigh out the desired quantities of each part of the two-component mixture, placing the paste or viscous liquids directly into the inside bag.

(4) Remove bags from cup, carefully squeezing out the extra air, and tape the bags shut.

(5) Knead the bags until thoroughly mixed, usually two to three minutes.

(6) Cut the corner from the bags and extrude into a previously prepared 250 ml polyethylene bottle with cap in place. This bottle has its bottom cut off about 1/2 to 3/4 of an inch from the bottom.

(7) Place the bottle in a centrifuge bucket cap down (cap supports the bottle on bottom of bucket).

(8) Place in centrifuge and counterbalance with another sample or similar weight.

(9) Centrifuge for 5 min at 2000 RPM (radius ≅ 10 in), this process causes any remaining bubbles to rise to the surface.

(10) After removing the bottle, place the cut off bottom into the cut end of the bottle and use as a plunger to extrude the mixture.

(11) Remove cap and extrude onto the aluminum plate, previously covered with teflon coated cloth, being careful not to entrap any air in the extrusion process. The best technique is to extrude into a big blob. Don't try to spread the material on the plate during the extrusion process.

(12) Apply pressure to the adhesive with an identical teflon covered aluminum plate, flattening to almost desired thickness.

(13) Place weight on upper plate.

(14) Cure and post cure between aluminum plates as specified by manufacturer.

A number of curing procedures were considered. The time and temperature used in the curing and post curing steps determine the final properties of the adhesive. The choice of cycle also depends on the desired range of properties, available facilities, manufacturing circumstances, etc. For example, due to the structure of the mold in which the sheets of adhesive were cast, it was not possible to oven cure the sheets immediately after casting. During an attempt to conduct such cure cycle the mould leaked. Instead, the castings were allowed to set overnight and then were fully cured. With the guidance of the adhesive manufacturers, the following cure cycles were performed:

ADHESIVE	CURE (room temp)	POST CURE
Ashland Plyogrip 6600/6620	24 hours	15min at 200^{0}F
Lord Fusor 320/322	24 hours	10min at 210^{0}F

The glass transition temperature, T_g, of the urethane adhesive (Asland Plyogrip 6600/6620) is 60^{o}c, while the glass transition temperature for the epoxy adhesive (Lord Fusor 320/322) is 35^{o}c.

3.1.2. Test Procedure

The test procedure used in determininng the time dependent response of the bulk adhesives is described in the following sections.

The first step was to obtain the value of the Ultimate Tensile Stress, (U.T.S), by performing uniaxial tensile tests on "dog bone" specimens of bulk adhesive. The next step was conducting a series of tensile creep tests at various stress levels. The creep tests included a mechanical conditioning procedure.

3.1.2.1. Tensile testing

In order to determine the Ultimate Tensile Strength of the bulk adhesive, at least 3 "dog bone" shaped specimens were cut from each sheet of cured adhesive. These specimens were tested using an M.T.S. servo-hydraulic testing machine at the rate of 1000 lb/min, until the specimen failed. The load, deflection and ultimate tensile strength (U.T.S.) were recorded and, this data was utilized to produce a stress versus strain curve.

3.1.2.2. Creep Testing

In order to obtain a complete creep compliance vs. time spectrum, six different stress levels, 10%, 20%, 30%, 40%, 60%, and 80% of the ultimate tensile stress were applied. All creep tests were conducted on one specimen, starting with the lower stress level.

3.1.2.3 Mechanical Conditioning

When discussing mechanical conditioning, Gramoll [6] reports that some investigators have used mechanical conditioning in order to obtain consistent results, while others argue that mechanical conditioning permanently changes the material by local geometry modifications.

While attempting to obtain consistent creep test results, it was realized that a mechanical conditioning procedure was essential to produce repeatable results. When the conditioning procedure was not used, the results obtained were unacceptable by any standard. After conducting some preliminary experiments the following mechanical conditioning procedure was established;

a) At each stress level at least four conditioning cycles were performed until good repetition was obtained.

b) For the first two cycles the specimen was loaded for 20 minutes and unloaded for 60 minutes.

c) For the following cycles, the 3rd and 4th cycles, the loading time was extended to 30 minutes and the unloading to 90 minutes.

The results (presented in section 3.2.3), indicate that it is reasonable to average the creep data from the third and the fourth conditioning cycles in order to obtain single creep compliance versus time curve at a given stress level.

3.1.2.4 Testing Procedure

The resulting procedure required approximately one working day to complete testing at any given stress level. The specimen was then allowed to recover overnight to completely relax before the next higher level was started the following morning. Thus, to complete the six stress levels would take six successive working days. Some specimens broke during lower stress levels, terminating that test. This was especially true of the epoxy adhesive which had high U.T.S.

At the low stress levels, especially in the polyurethane adhesives, it was necessary to place a dummy extensometer on the specimen to counterbalance the active extensometer. This was surprising, considering the light weight of this apparatus. Nevertheless, when the dummy extensometer was introduced, the data became consistent. The dummy extensometer was utilized throughout all subsequent testing.

Total specimen length was 11 inches. Approximately one and a half inches of the total specimen length was inserted into the grip at each end. Thus, the test section length between grip ends was never less than 8 inches.

It became necessary to consider all the aspects discussed above, as well as the conditioning cycles to produce consistent results.

3.1.3 Test Results

The test results for both adhesives tested are presented in this section. The creep compliance curves were calculated based on the measured displacements in each specimen.

There are two sets of results, the first set contains the results obtained for the urethane adhesive, Ashland Plyogrip 6600/6620. The second set contains the results for the epoxy adhesive, Lord Fusor 320/322.

3.1.3.1 Tensile Test Results

The Ultimate Tensile Stress obtained from tensile tests performed on three specimens for each adhesive were averaged giving the following values:

ADHESIVE	UTS (psi)
Ashland 6600/6620 (urethane)	1000
Lord Fusor 320/322 (epoxy)	3435

3.1.3.2 Mechanical Conditioning

The first set of figures for a particular adhesive (fig 3.1

through 3.6, and 3.9 through 3.15) show the change in strain versus time, for the third and fourth conditioning cycles. The curves show good agreement between the two cycles (within experimental error).

3.1.3.3 Creep Compliance

The results of the third and fourth cycles were averaged to obtain a creep compliance versus time plot, which is shown as the next curve (or set of curves) in the series for a particular adhesive (fig 3.7 and 3.16 through 3.18). It should be noted that t_0, the initial time, was evaluated at five times the loading time.

3.1.3.4 Isochronous Stress Strain Curves

The next set of figures in the series show the isochronous stress strain curves for the above mentioned adhesives (fig 3.8 and 3.19).

3.1.4 DISCUSSION

3.1.4.1 Ashland Plyogrip 6600/6620

Ashland 6600/6620 is a very flexible urethane adhesive. Placing an extensometer on specimens of this adhesive causes bending due to the weight of the extensometer resulting in incorrect deflection

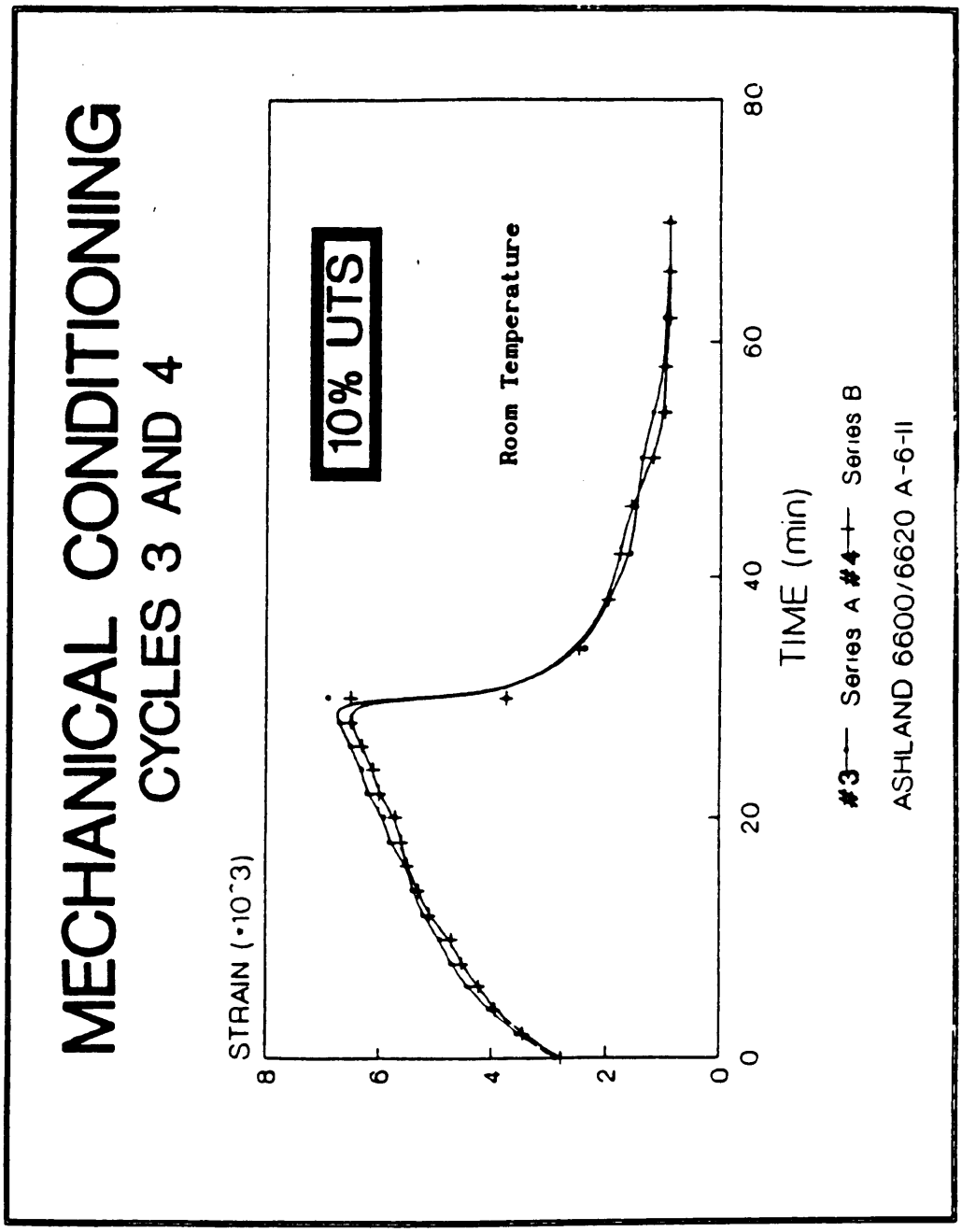

Figure 3.1: Mechanical Conditioning; third and fourth cycles. Ashland Plyogrip 6600/6620.

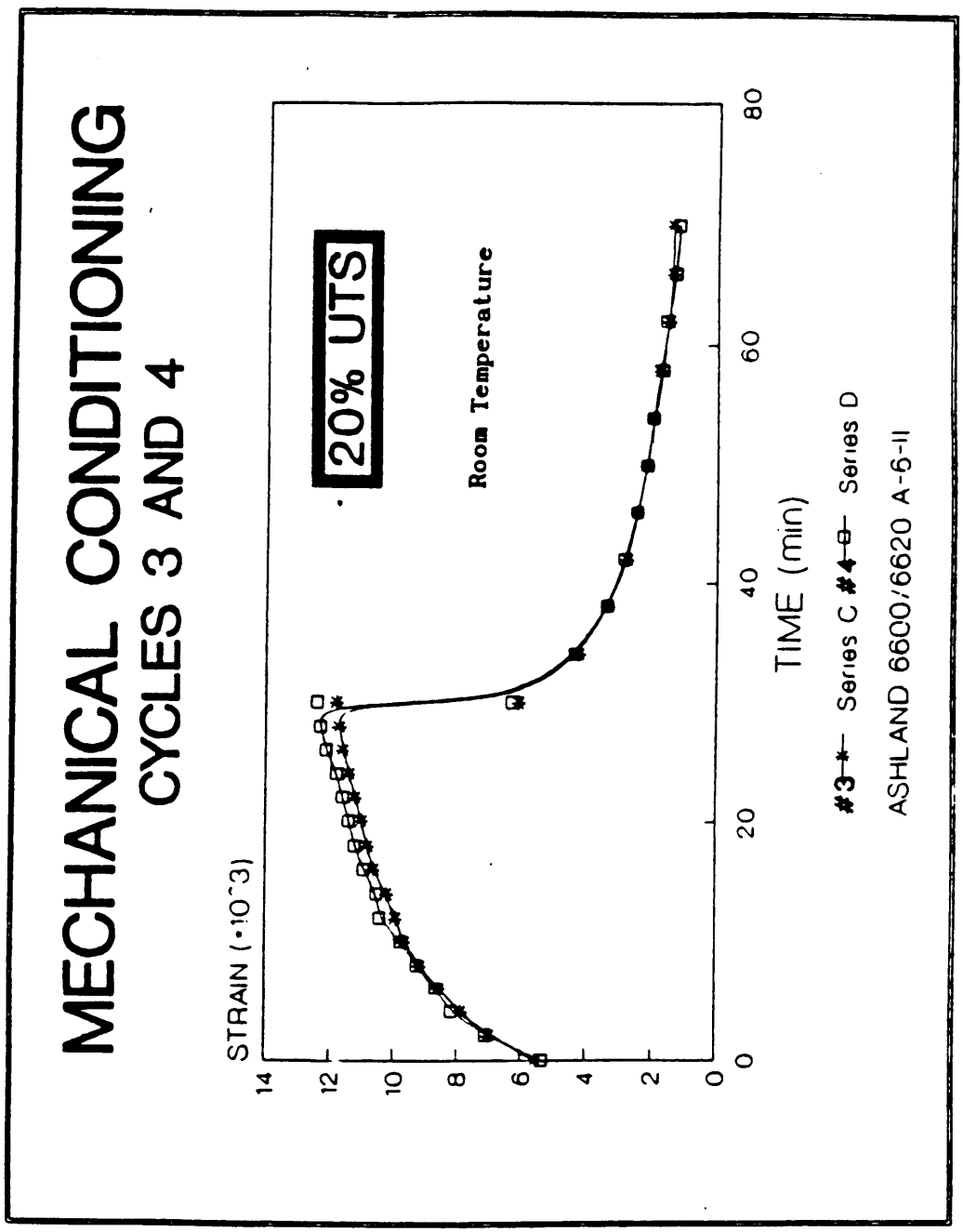

Figure 3.2: Mechanical Conditioning: third and fourth cycles, Ashland Plyogrip 6600/6820.

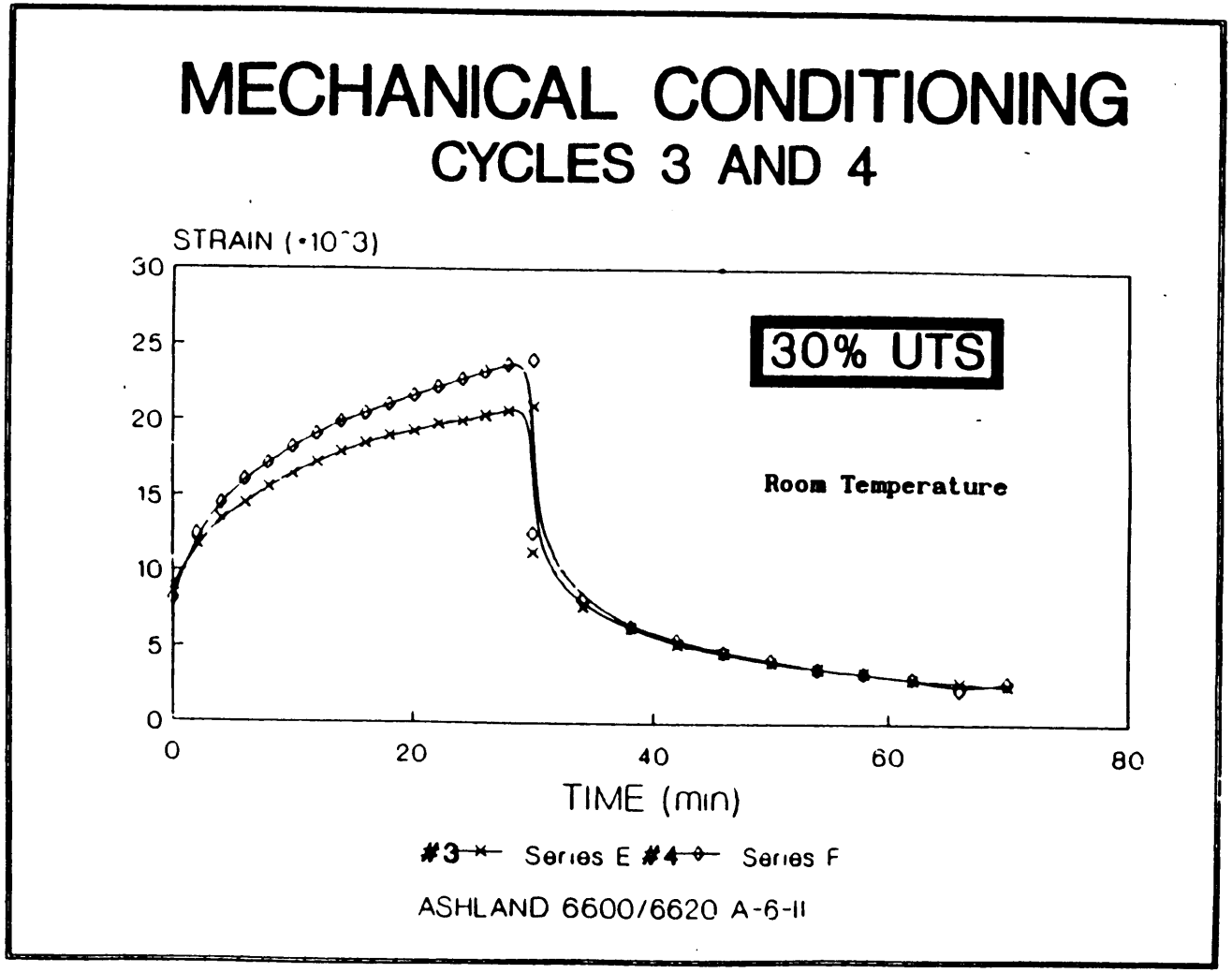

Figure 3.3: Mechanical Conditioning; third and fourth cycles, Ashland Plyogrip 6600/6620.

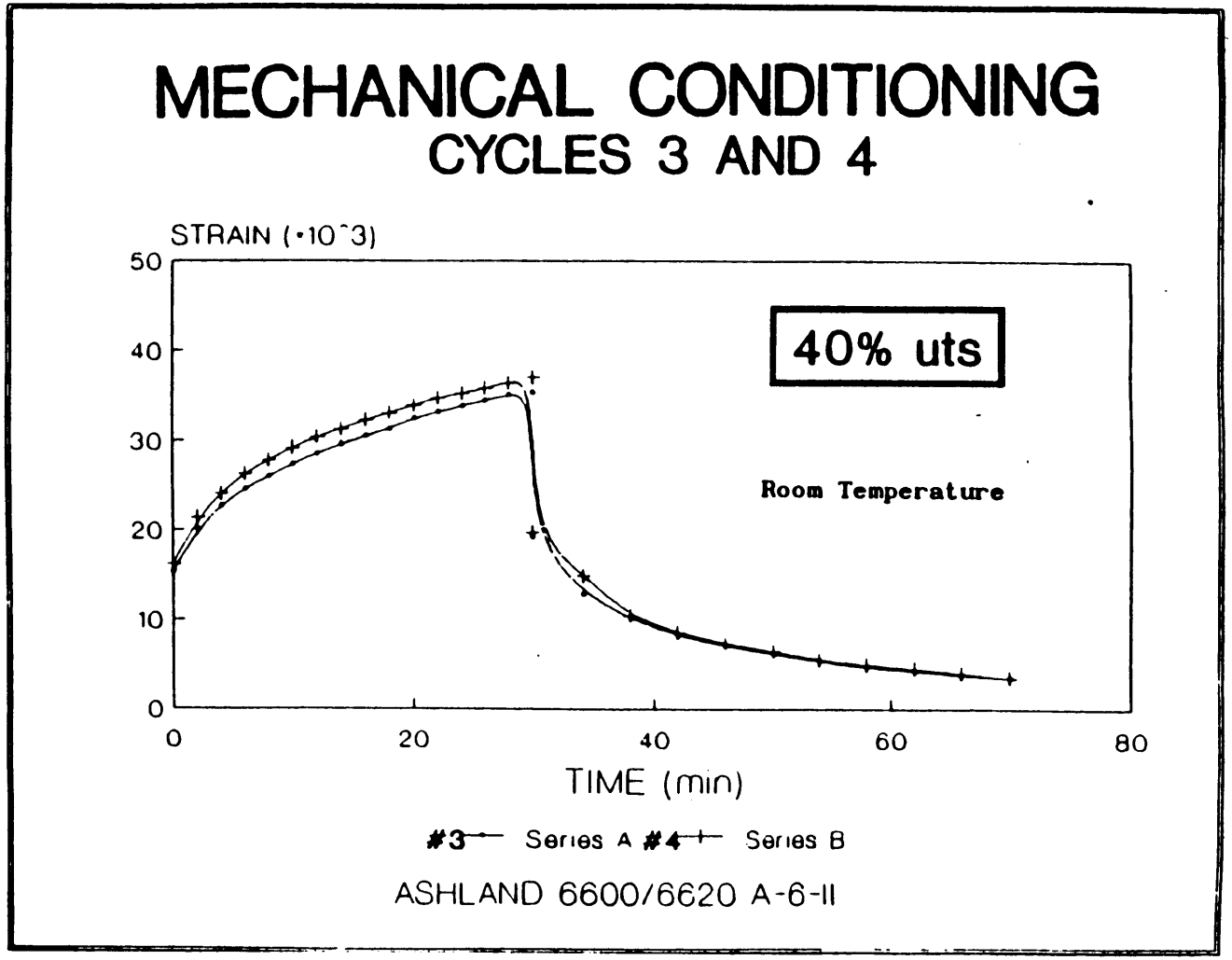

Figure 3.4: Mechanical Conditioning; third and fourth cycles, Ashland Plyogrip 6600/6620.

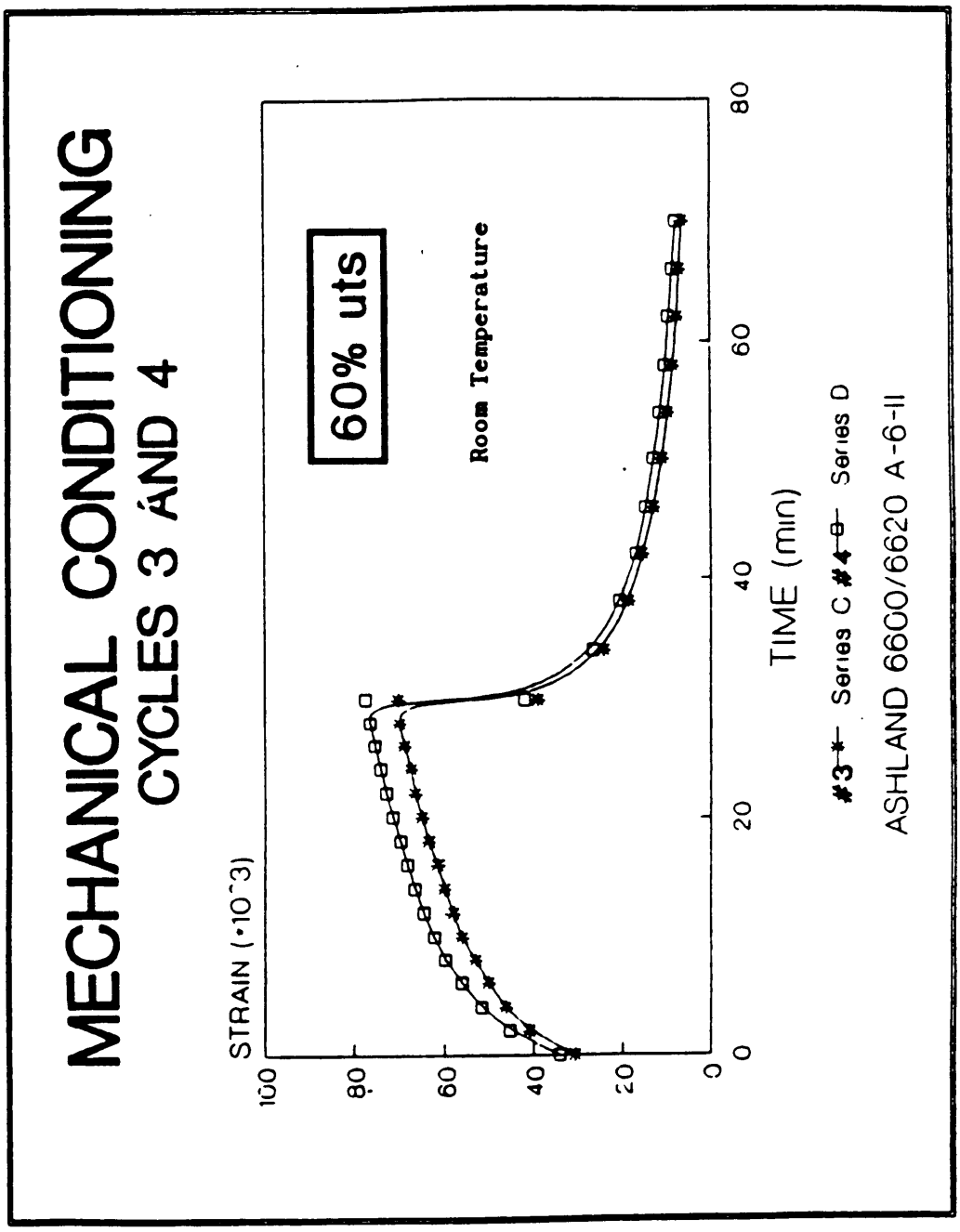

Figure 3.5: Mechanical Conditioning; third and fourth cycles. Ashland Plyogrip 6600/6620.

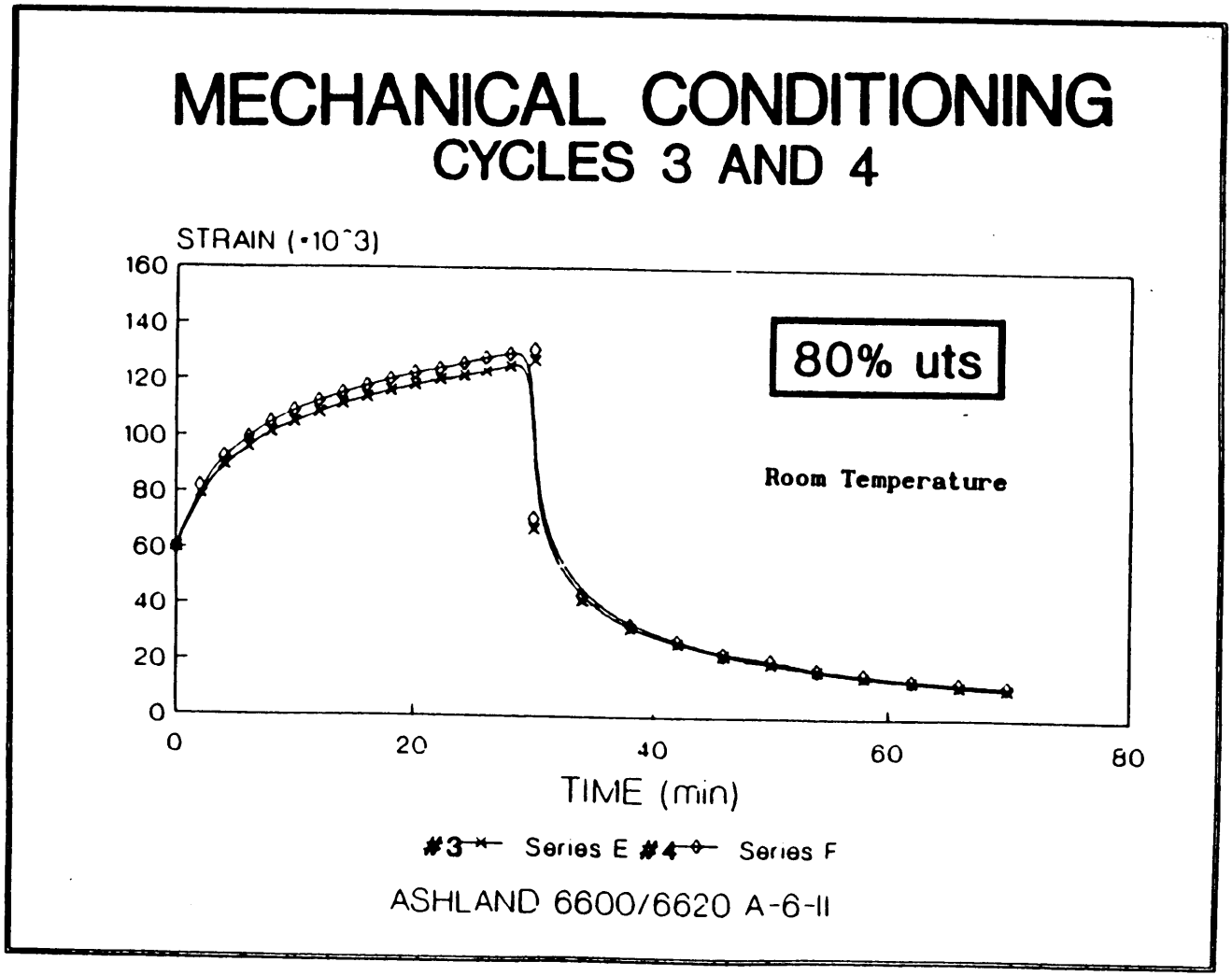

Figure 3.6: Mechanical Conditioning; third and fourth cycles, Ashland Plyogrip 6600/6620.

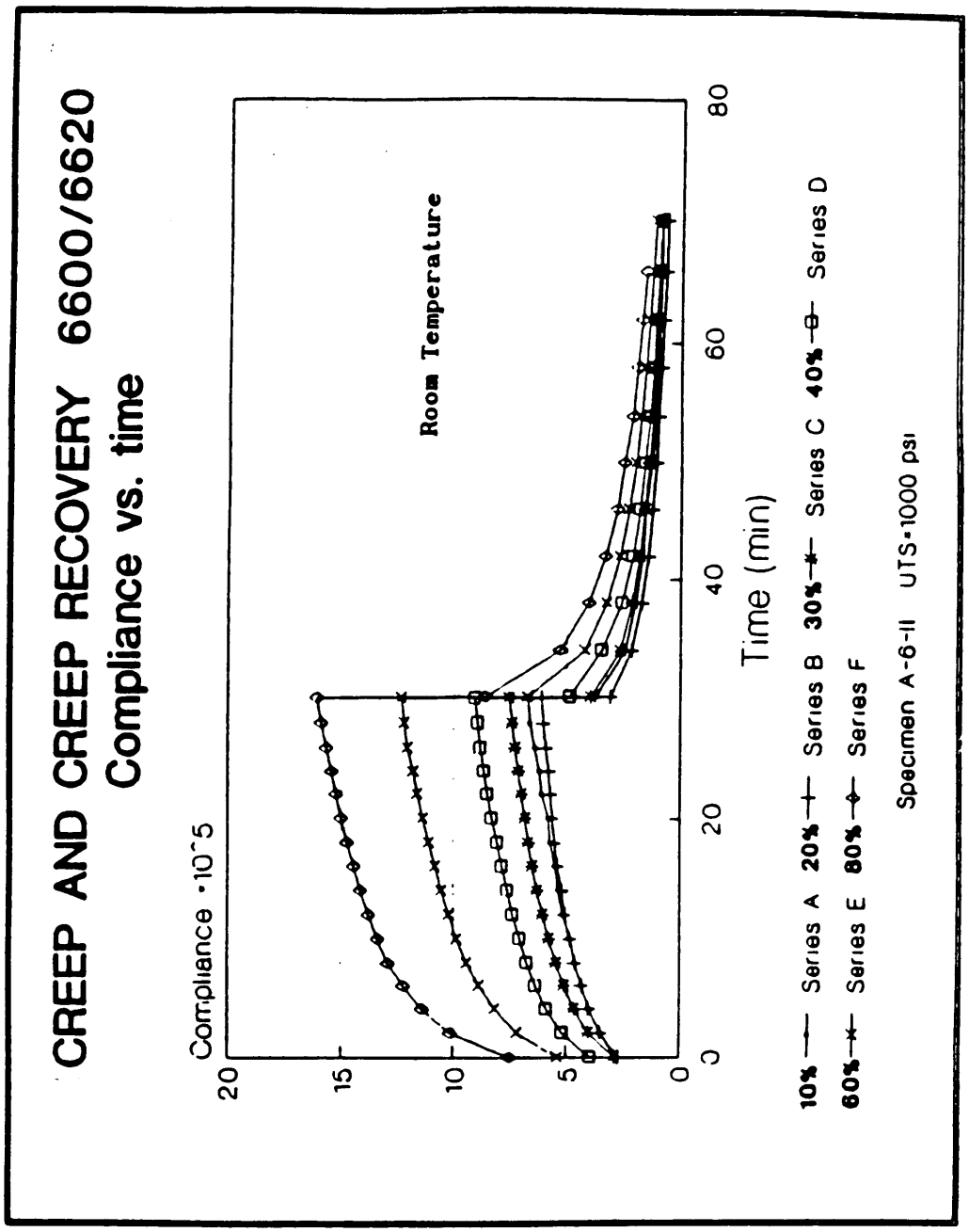

Figure 3.7: Creep and Creep Recovery for Ashland Plyogrip 6600/6620.

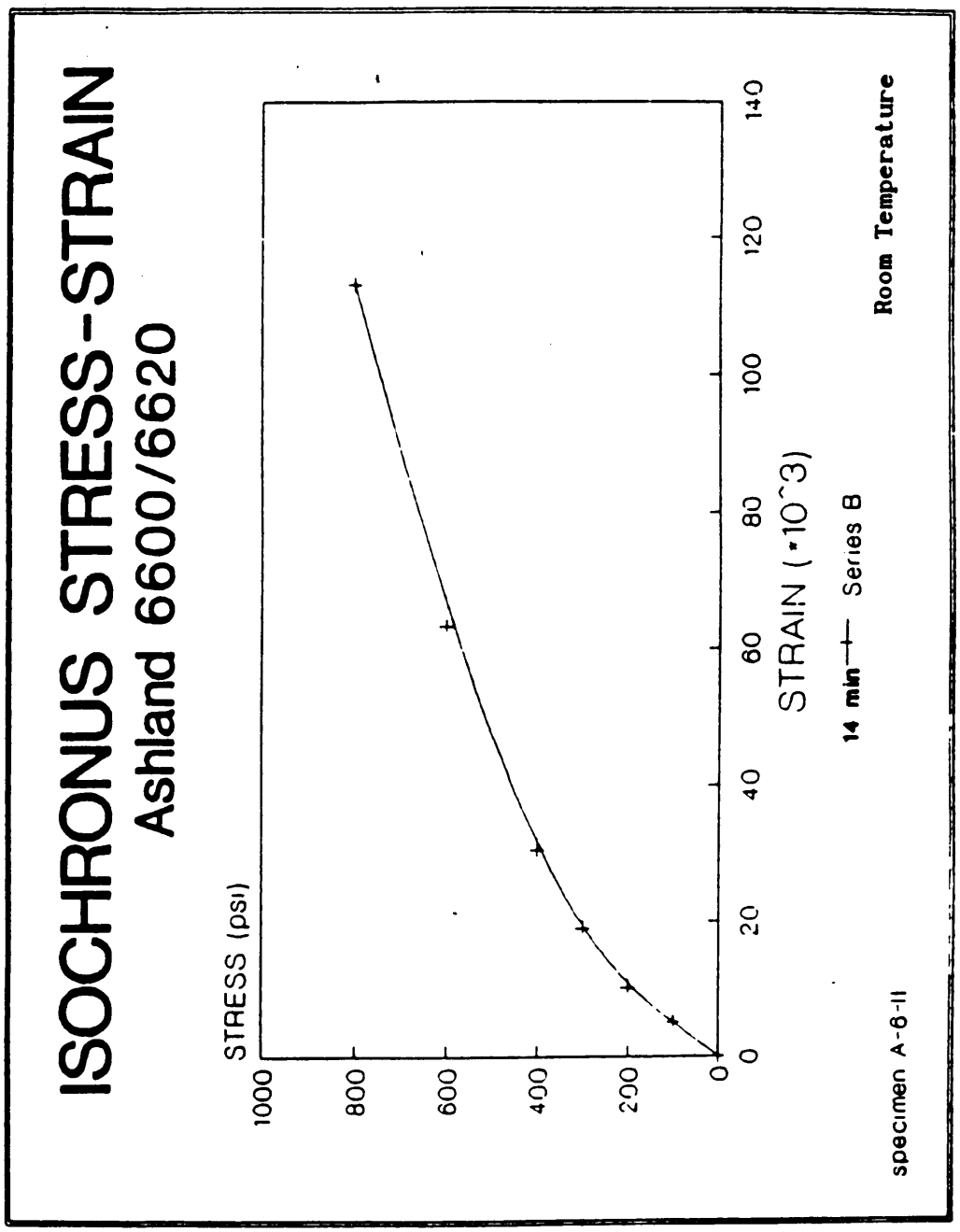

Figure 3.8: Isochronous Stress Strain Curve for Ashland Plyogrip 6600/6620.

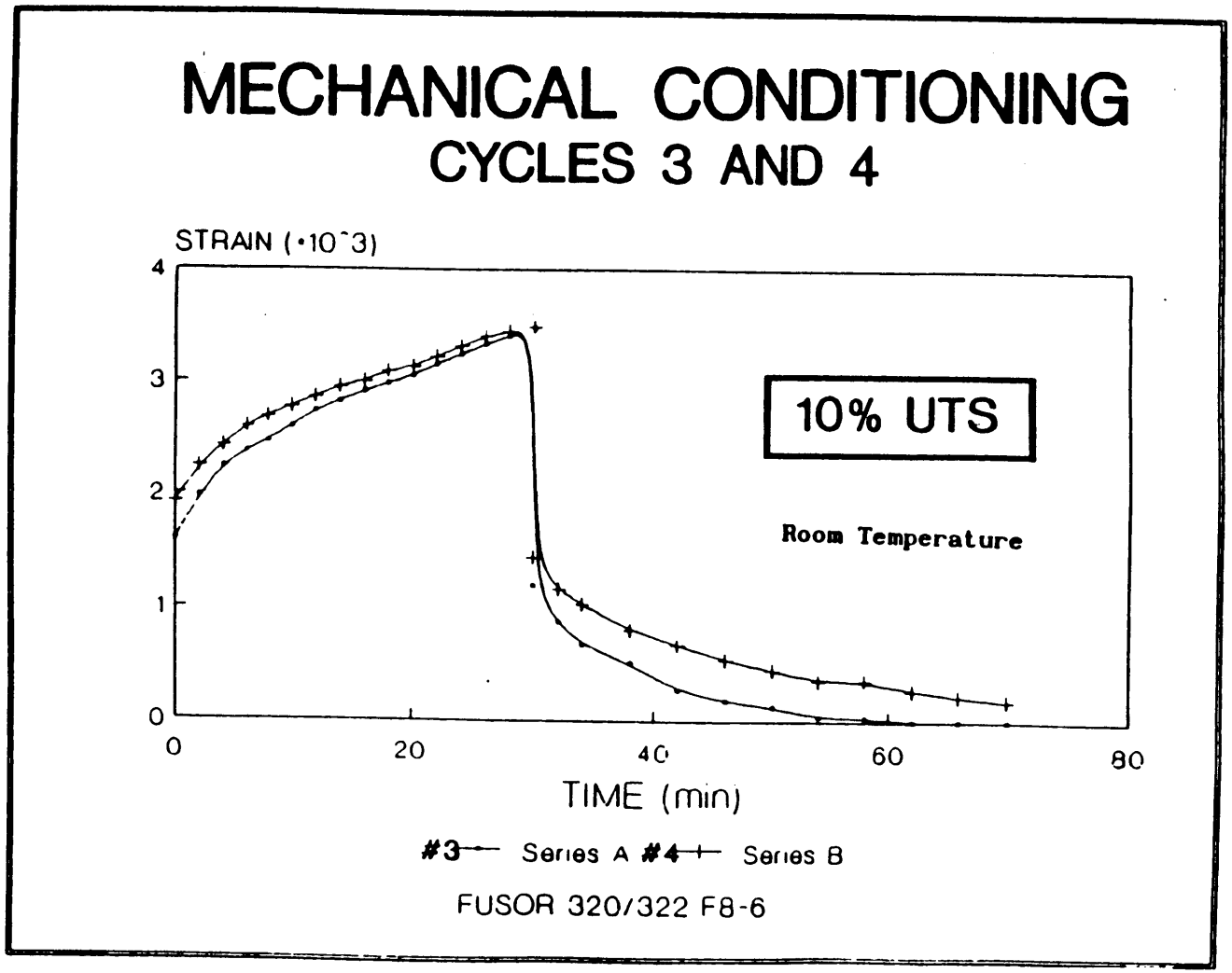

Figure 3.9: Mechanical Conditioning; third and fourth cycles, for Lord Fusor 320/322 (F8-6).

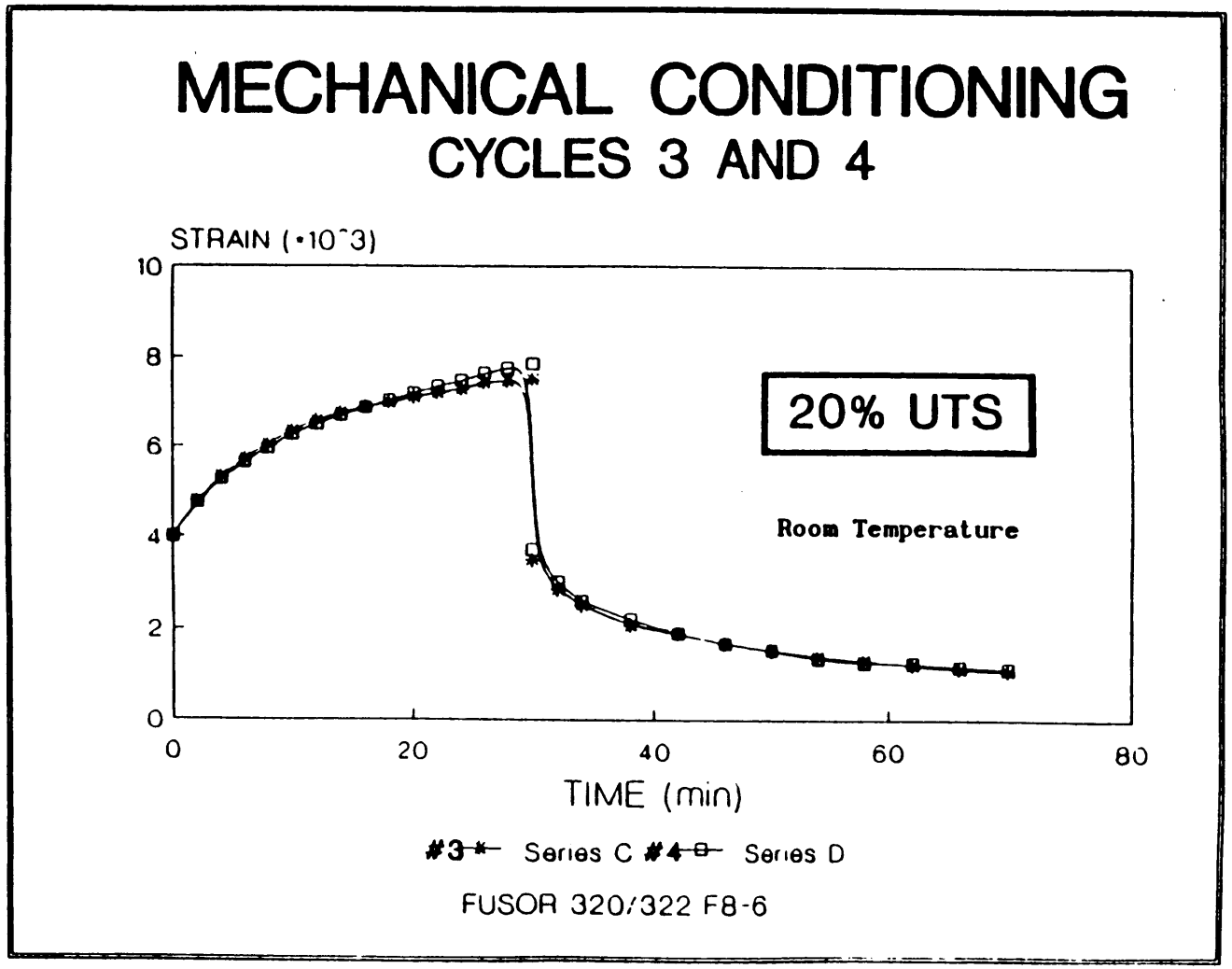

Figure 3.10: Mechanical Conditioning; third and fourth cycles, for Lord Fusor 320/322 (F8-6).

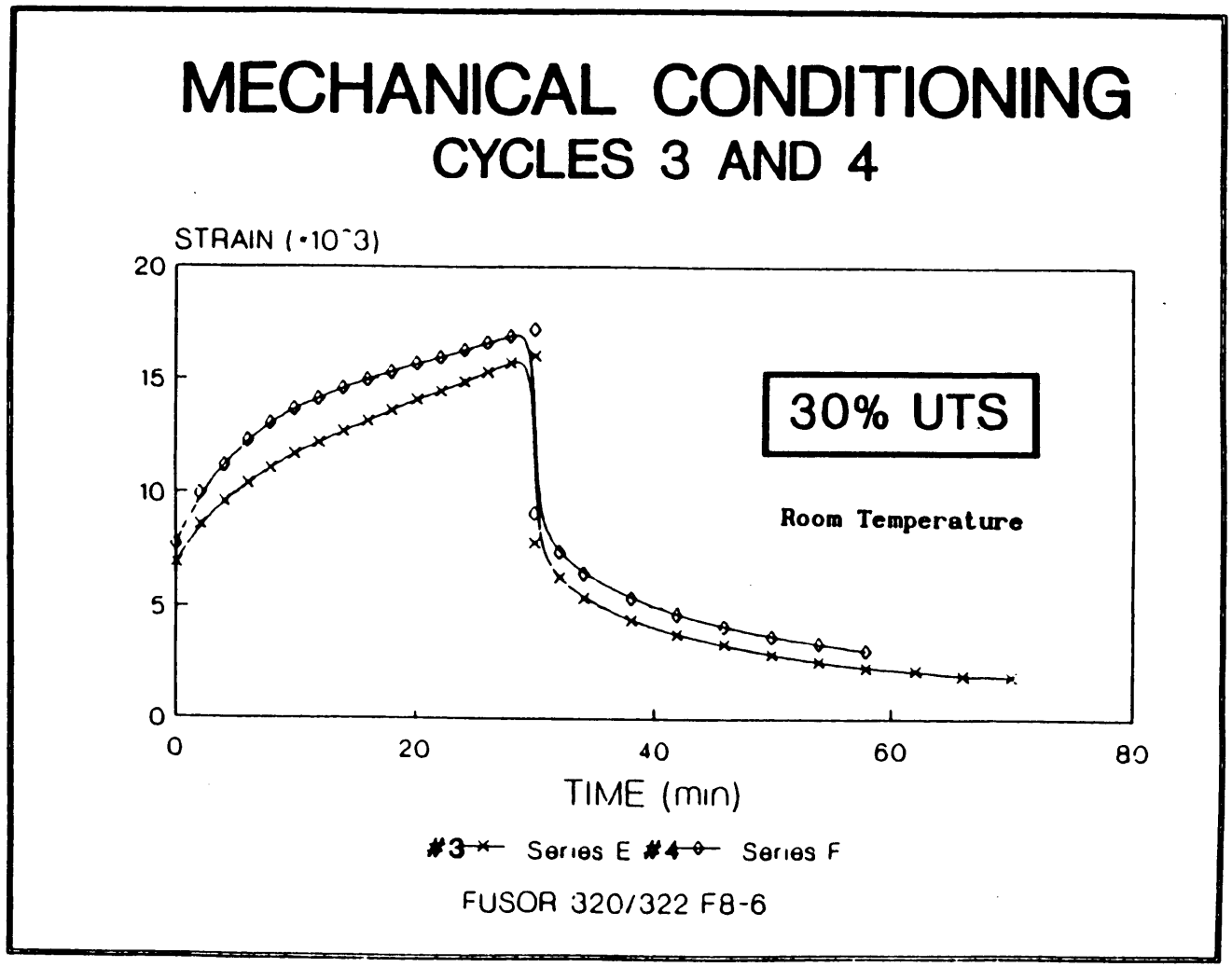

Figure 3.11: Mechanical Conditioning; third and fourth cycles, for Lord Fusor 320/322 (F8-6).

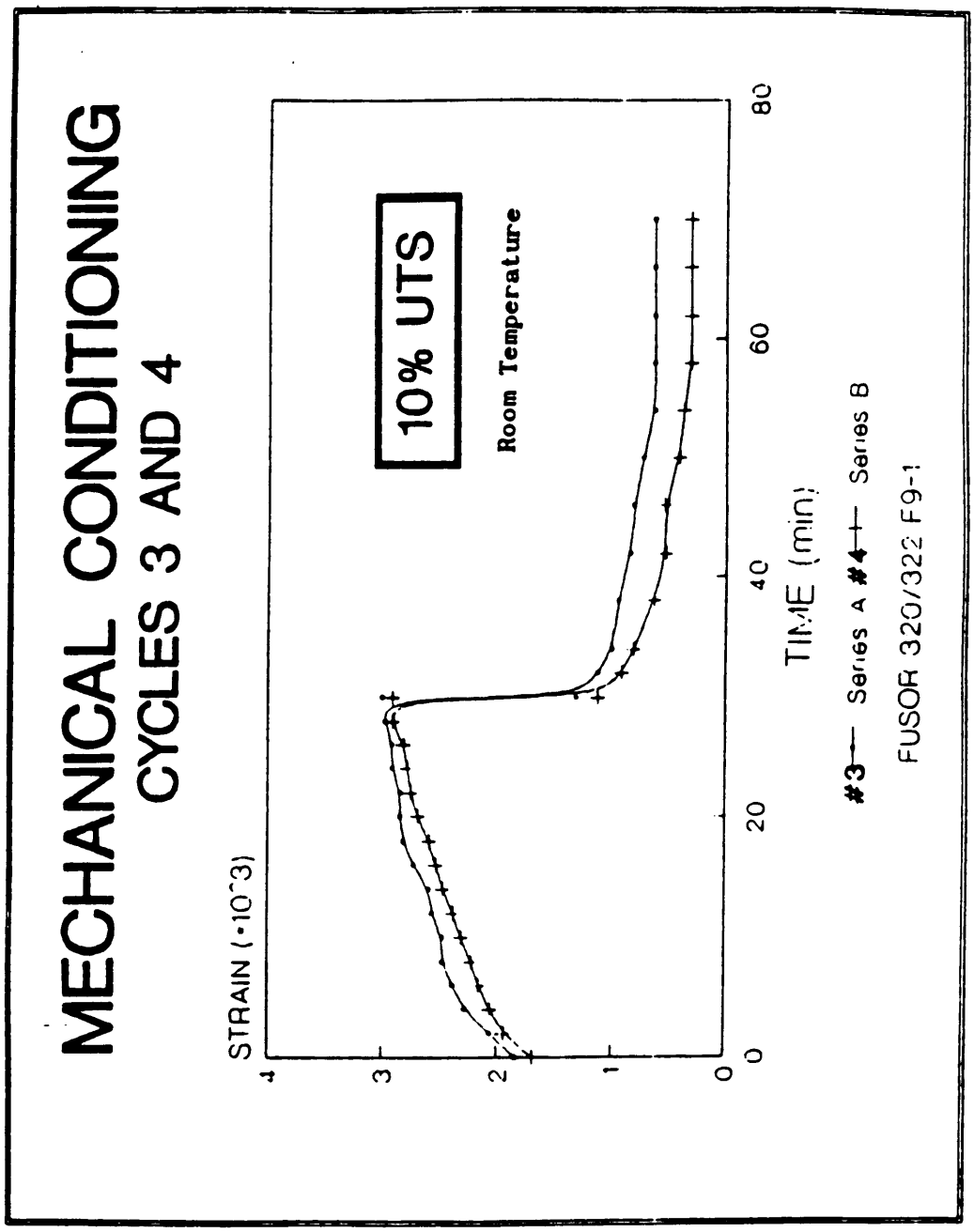

Figure 3.12: Mechanical Conditioning: third and fourth cycles, for Lord Fusor 320/322 (F9-1).

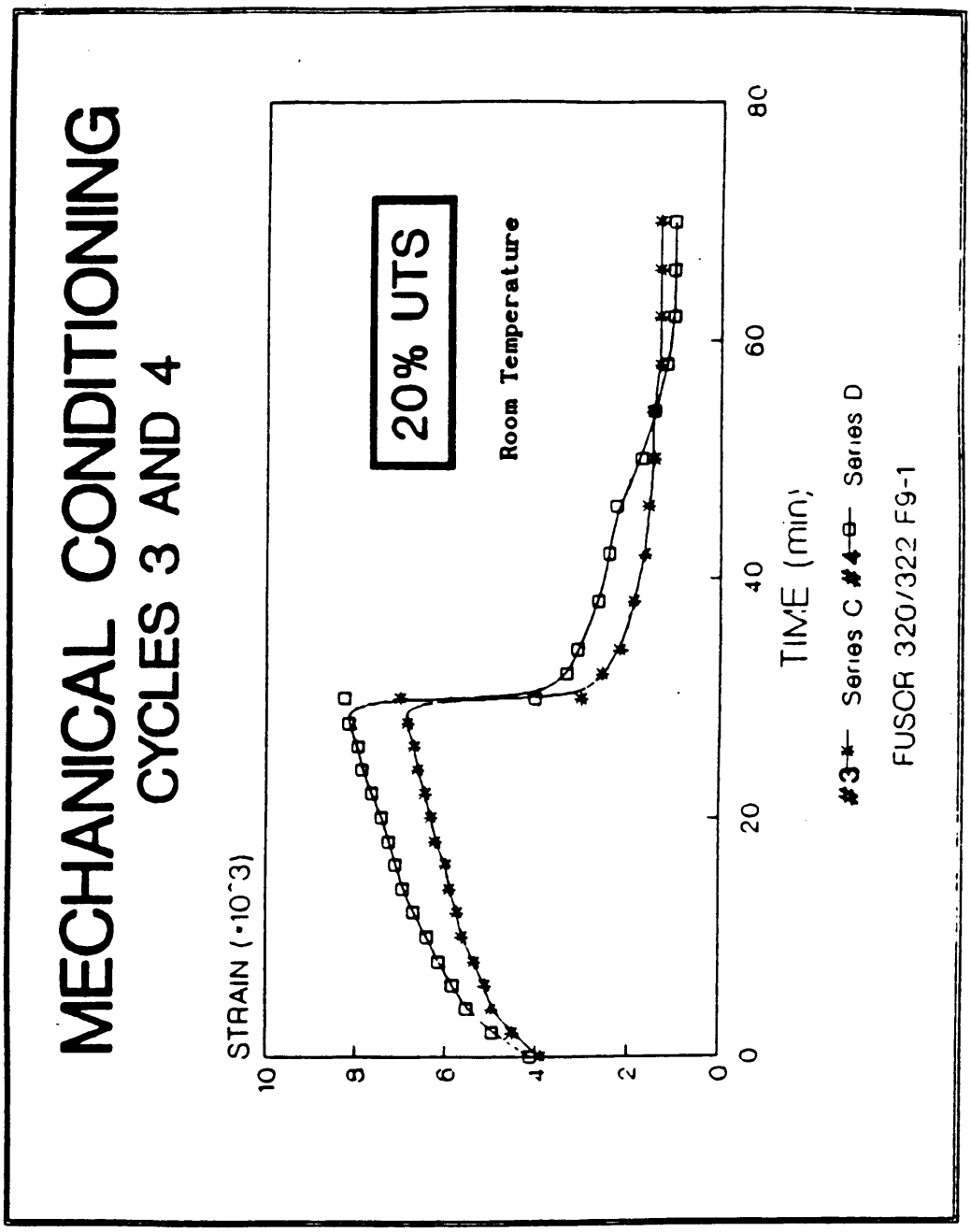

Figure 3.13: Mechanical Conditioning: third and fourth cycles, for Lord Fusor 320/322 (FG-1).

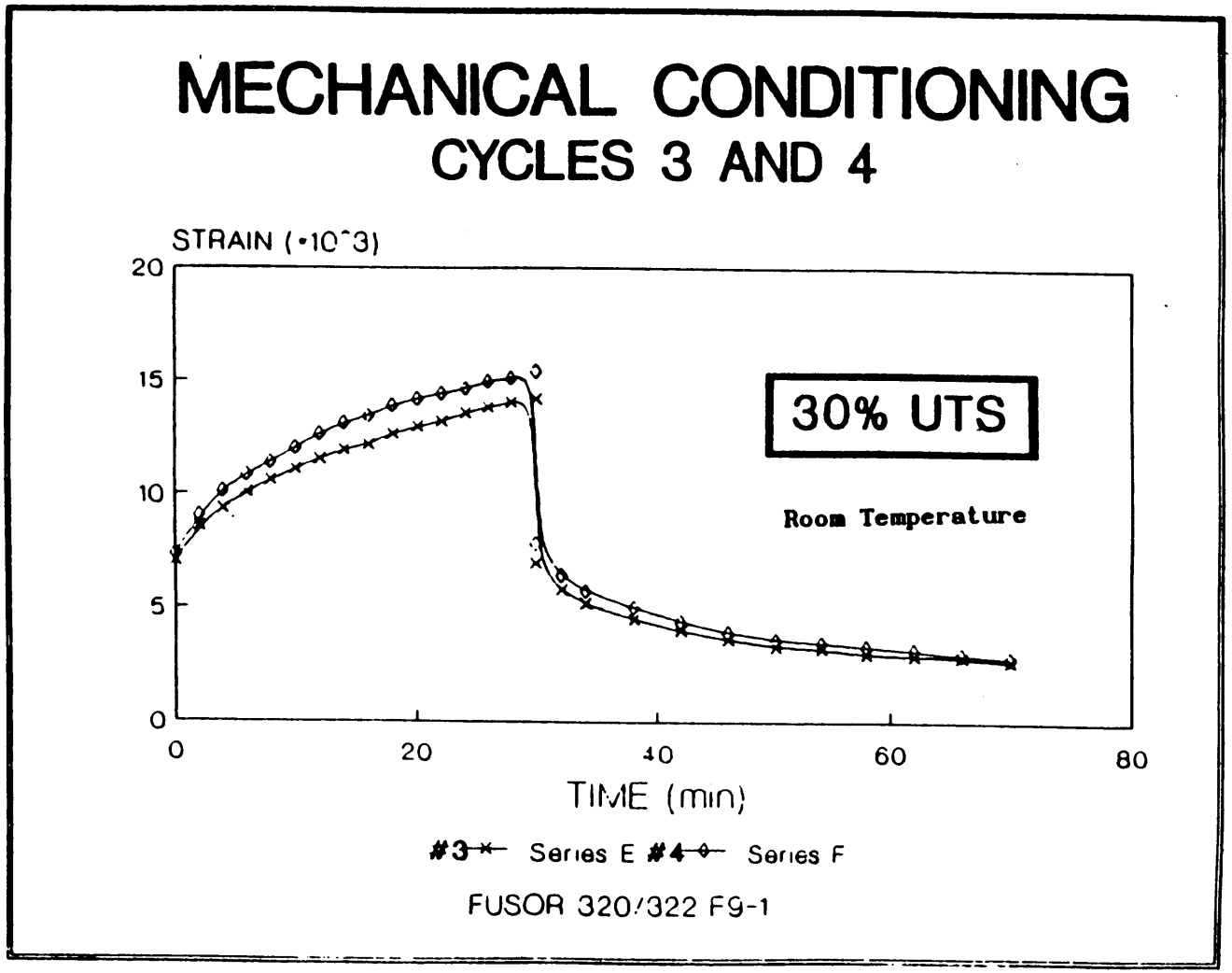

Figure 3.14: Mechanical Conditioning; third and fourth cycles, for Lord Fusor 320/322 (F9-1).

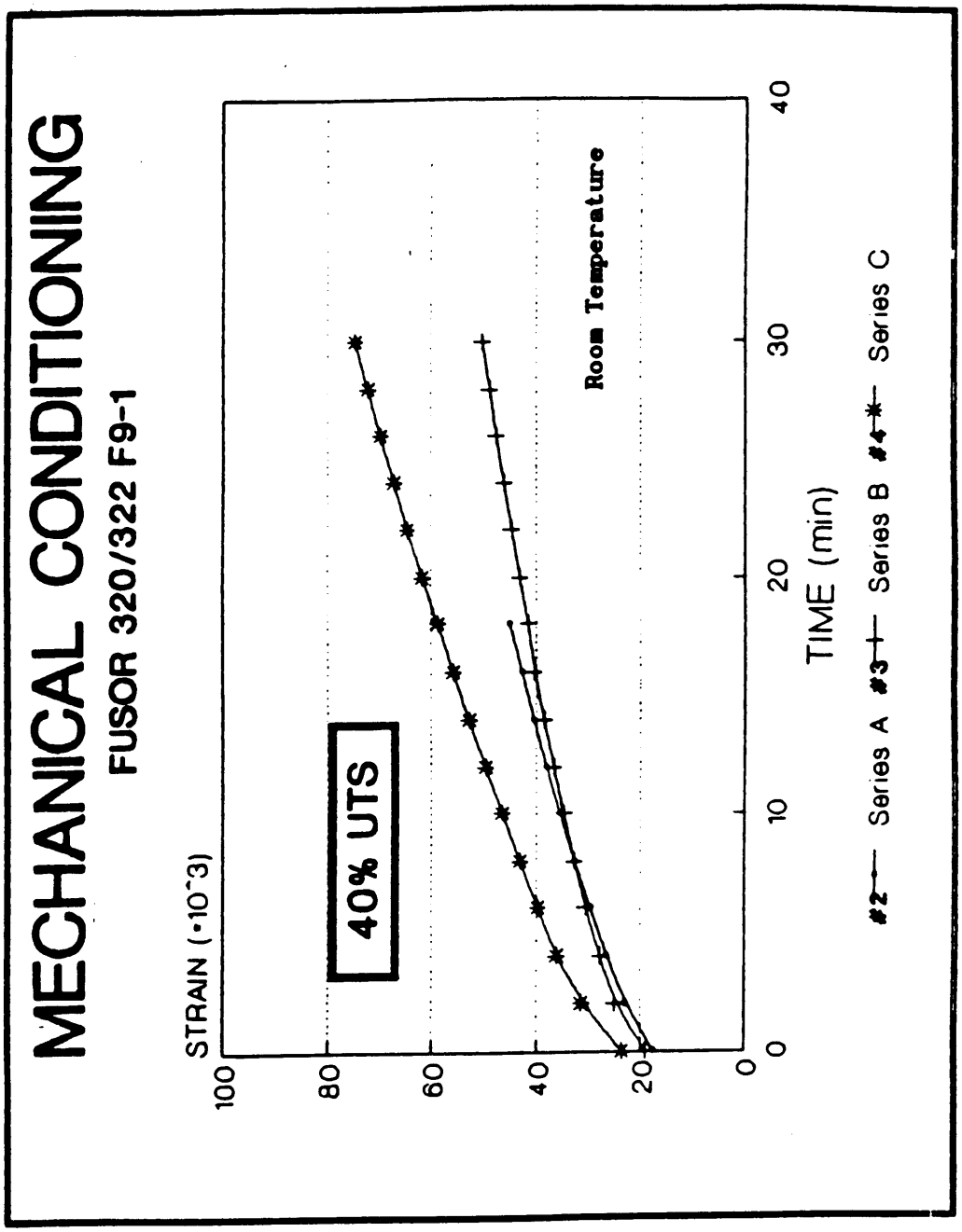

Figure 3.15: Mechanical Conditioning: third and fourth cycles, for Lord Fusor 320/322 (F9-1).

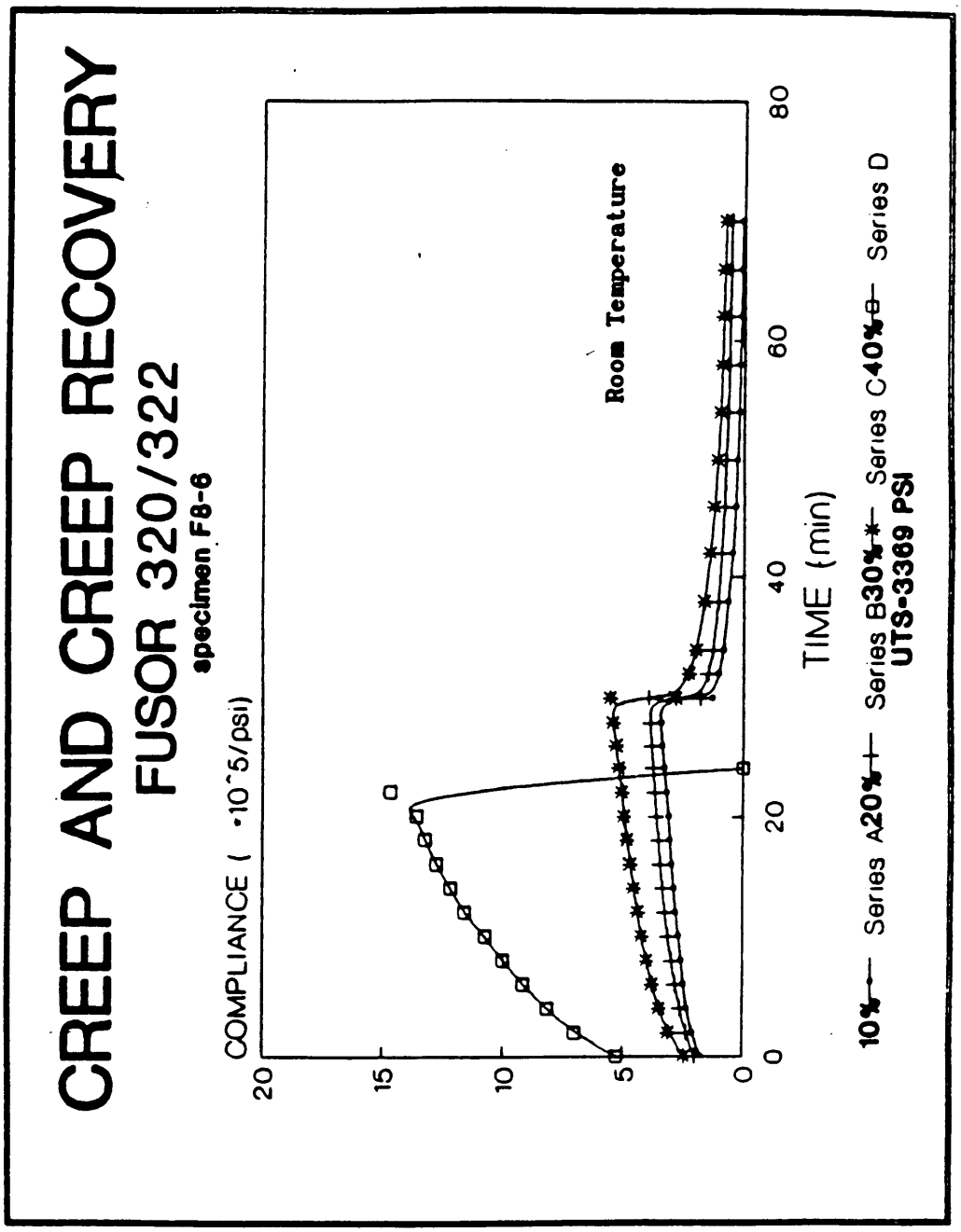

Figure 3.18: Creep and Creep Recovery
for Lord Fusor 320/322 (F8-6)

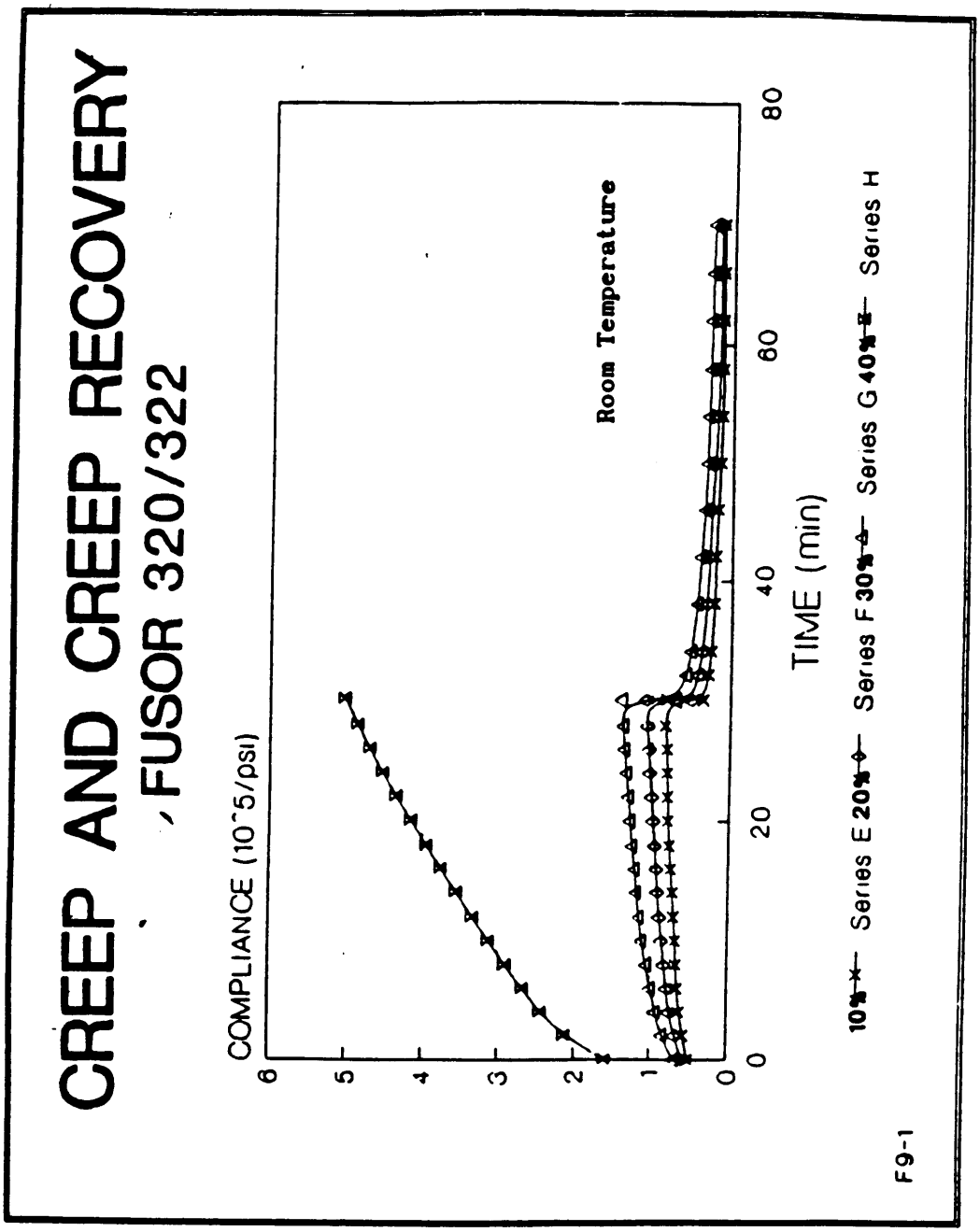

Figure 3.17: Creep and Creep Recovery for Lord Fusor 320/322 (F9-1)

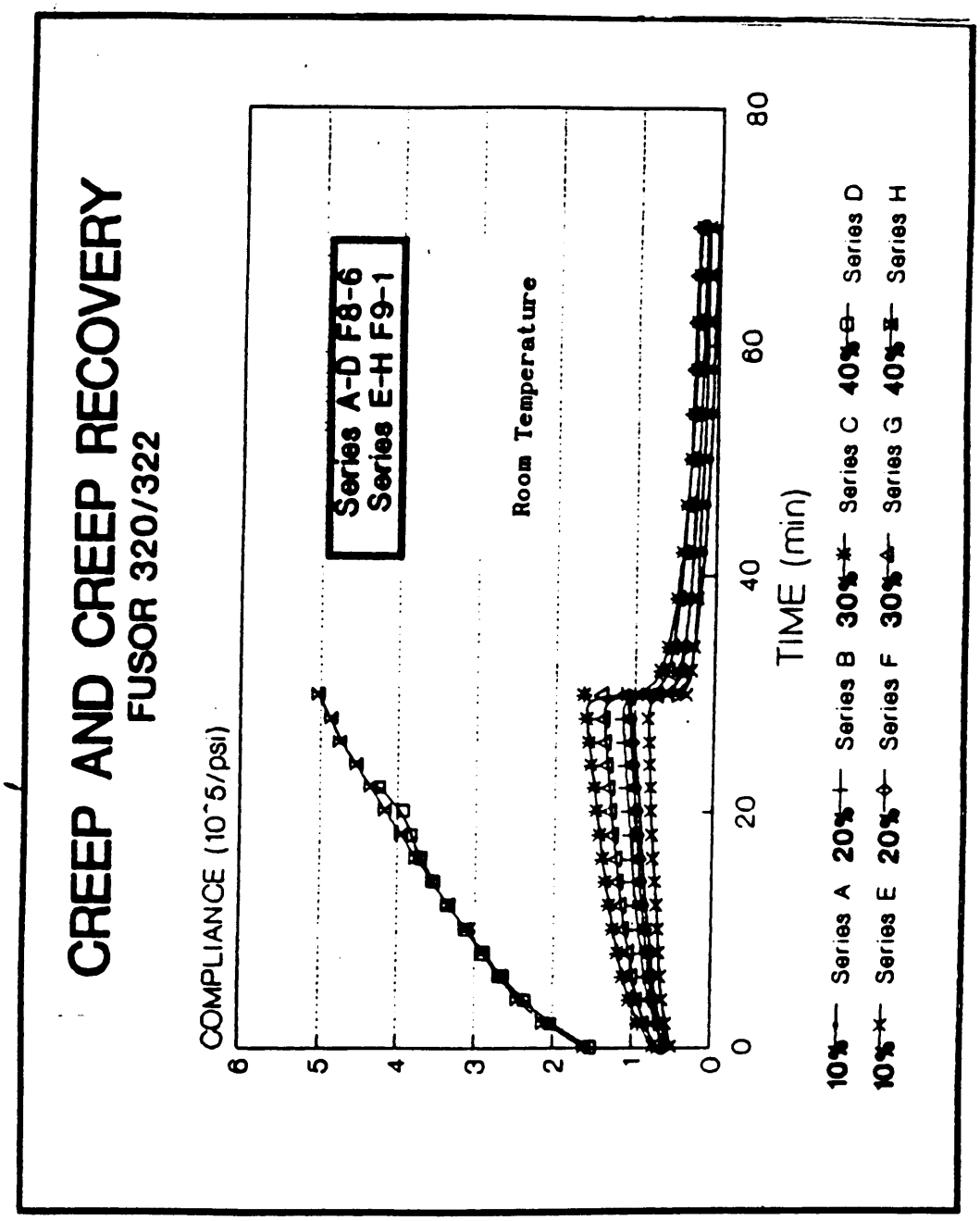

Figure 3.18: Creep and Creep Recovery for Lord Fusor 320/322 (F8-6 and F9-1)

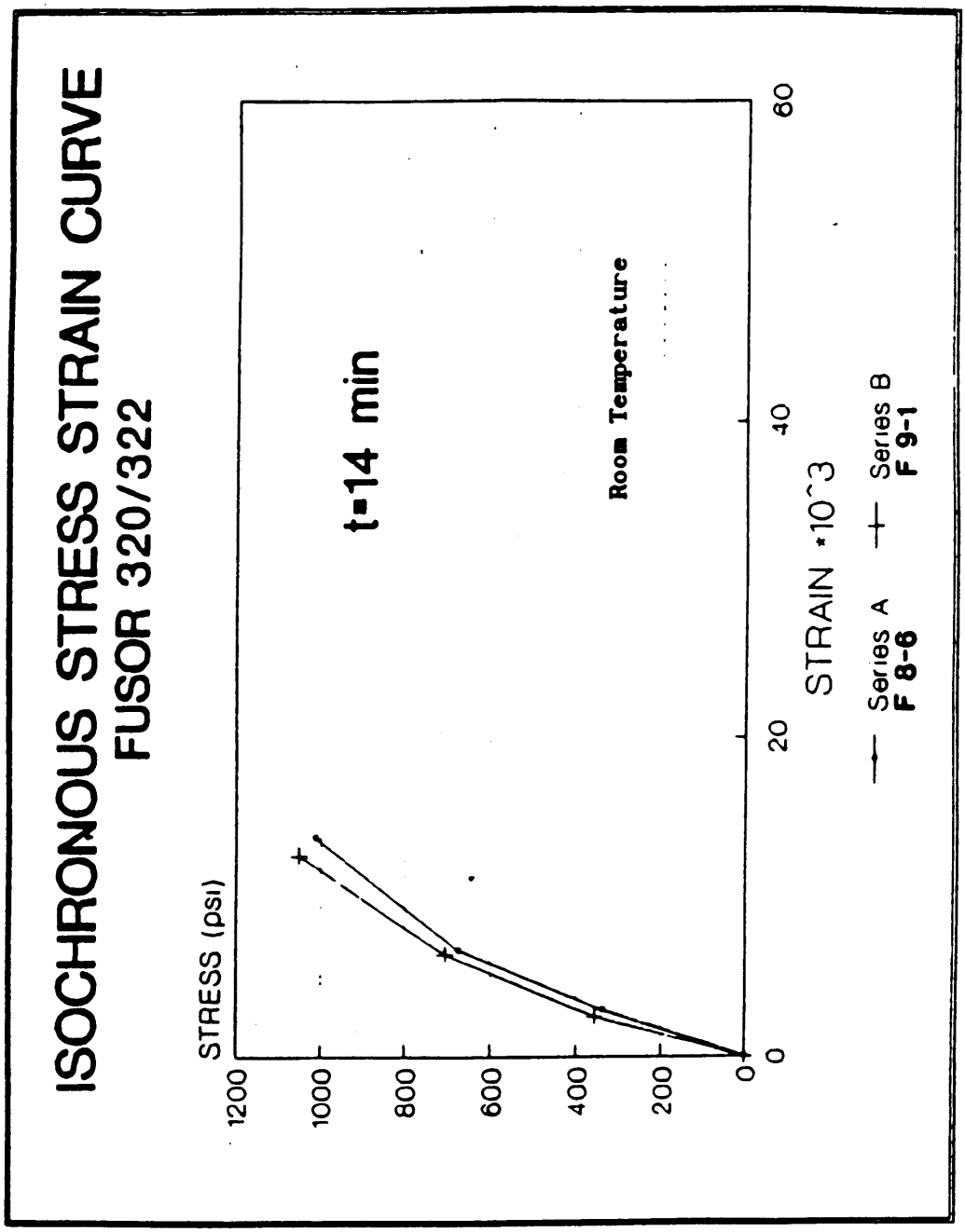

Figure 3.19: Isochronous Stress Strain Curve for Lord Fusor 320/322.

readings. This problem was overcome by placing a second extensometer on the other side of the specimen. The weight of the extensometers is neglible compared to the applied loads.

It is easily seen in figure 3.7, the creep compliance versus time curves, that up to 20% of the Uitimate Tensile Stress, the adhesive exhibits linear viscoelastic behavior. At higher stress levels the adhesive behaves as a nonlinear viscoelastic material. This phenomenon is also obvious in the isochronous stress strain plot. The specimen did not break, even after performing creep cycles at 80% of the ultimate tensile stress.

The creep compliance versus time curves were then curve fitted to a quadratic power law form using the curve fitting program CFIT written by Gramoll [6].

The first step was to represent each of the creep compliance curves with an expression of the form

$$D(t,\sigma) = D_0^* + m^* t^n \qquad (3.1)$$

Where D_0^*, m^* and n are a set of constants for each stress level. The value of n was determined in this step, assuming that n is independent of stress level (constant). This average value of n was used to repeat the curve fit procedure at each stress level with the power law eq. (3.1) by forcing the exponent n to be the constant value.

Secondly, the new values of D_0^* and m^* for each stress level were fitted to a quadratic equation, as described in eq. (3.2) and (3.3).

$$D_0^* = (1 + g\sigma^2)D_0 \left[\frac{in^2}{lb}\right] \tag{3.2}$$

$$m^* = (1 + f\sigma^2)m \left[\frac{in^2}{lb\ sec}\right] \tag{3.3}$$

where f and g are constants that introduce the nonlinearity. Knowing the values of all five constants n. D_0, m, g and f, the overall result is the following (at room temperature):

$$D(t,\sigma) = (1 + g\sigma^2)\ 6.817E\text{-}6 + (1 + f\sigma^2)6.08E\text{-}6\ t^{0.29343}\left[\frac{in^2}{lb}\right] \tag{3.4}$$

where

$$g = 1.0663E\text{-}5 \left[\frac{in^4}{lb^2}\right]$$

$$f = 1.6134E\text{-}6 \left[\frac{in^4}{lb^2}\right]$$

A summary of the curve fitting results is presented in tables 3.1 and 3.2, and in figures 3.20 through 3.22.

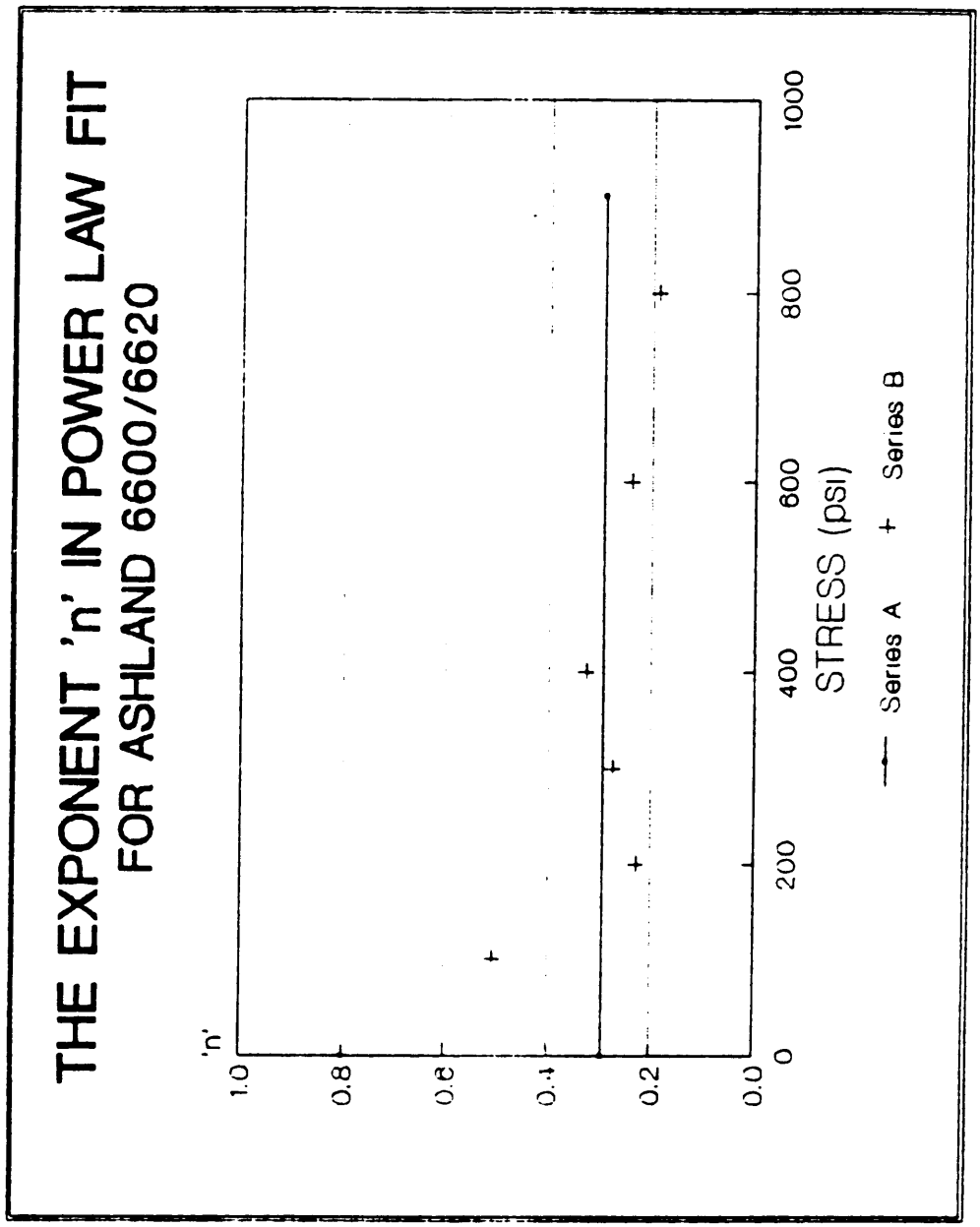

Figure 3.20: The Exponent 'n', in a Power Law Fit for Ashland Plyogrip 6600/6620.

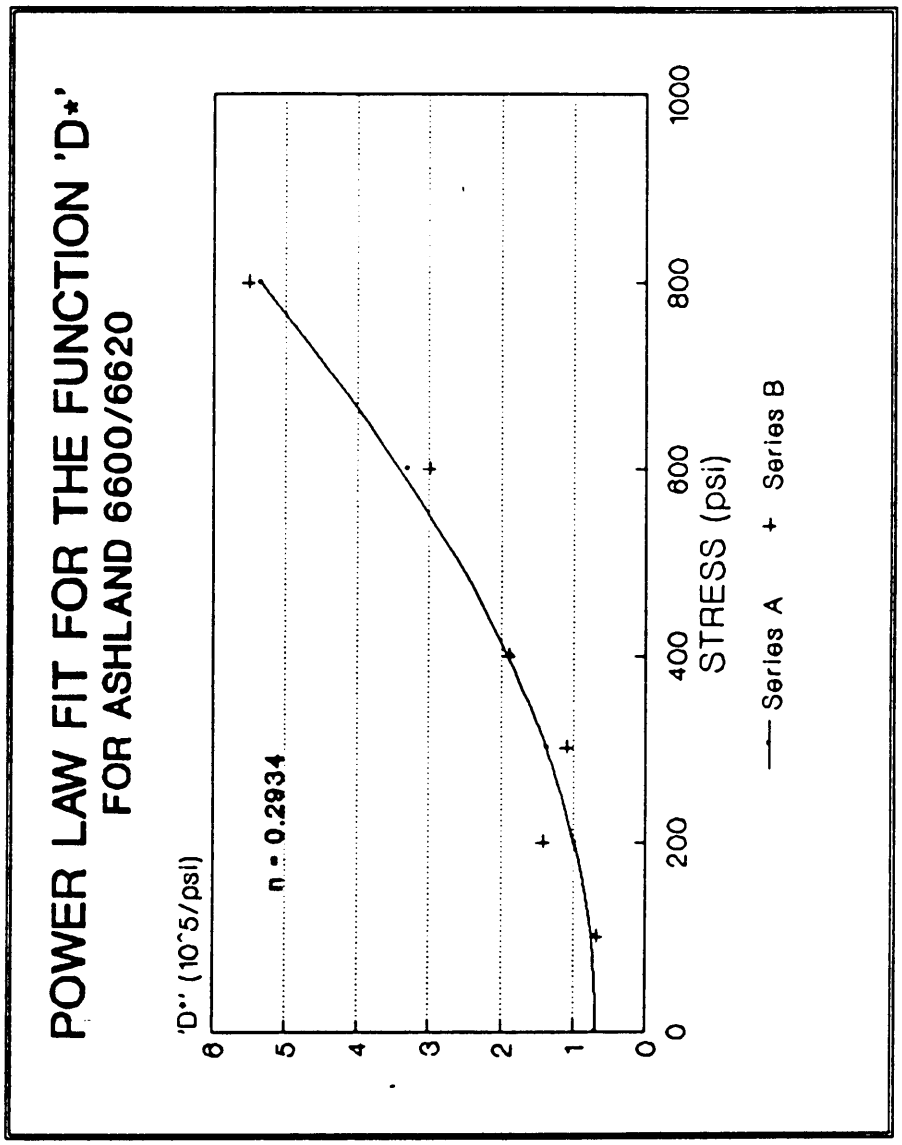

Figure 3.21: The Function 'D_o^*', in a Power Law Fit for Ashland Plyogrip 6600/6620.

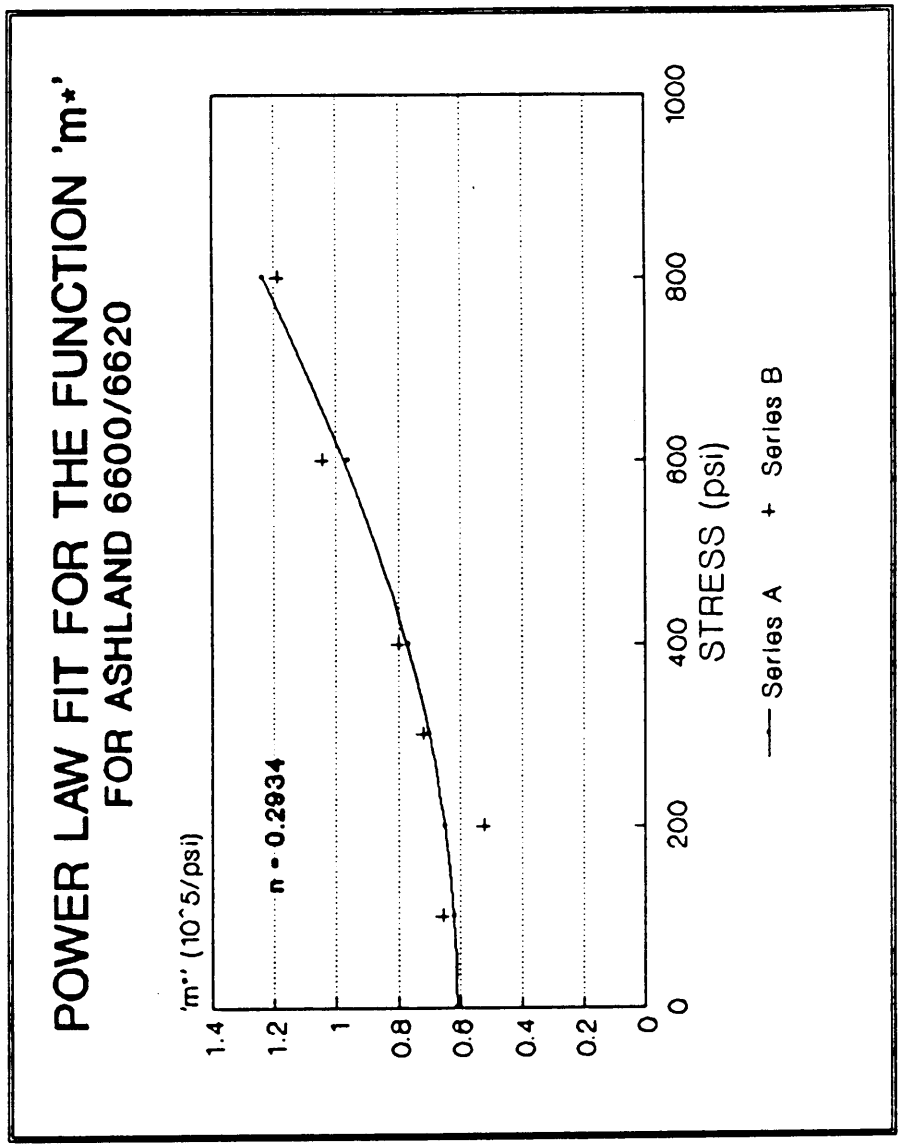

Figure 3.22: The Function '$m^{\bullet}$', in a Power Law Fit for Ashland Plyogrip 6600/6620.

Table 3.1: The Value of the Exponent 'n' in a Power Law Fit for Ashland 6600/6620.

Stress [psi]	'n' Exponent	Coefficient of Variation [%]
100	0.5056	0.7814
200	0.2276	0.5562
300	0.2739	0.3996
400	0.3272	0.3142
600	0.2386	0.2366
800	0.1876	0.0691

n = 0.2934 (Coefficient of Variation = 38.876%)

Table 3.2: Power Law Fit for D_0^* and m^* for Ashland 6600/6620.

STRESS [psi]	D_0^* $\left[\frac{in^2}{lb}\right]$	m^* $\left[\frac{in^2}{lb\ sec}\right]$	Coefficient of Variation [%]
100	0.664E-5	6.566E-6	1.6641
200	1.406E-5	5.241E-6	0.6856
300	1.089E-5	7.165E-6	0.4224
400	1.885E-5	7.969E-6	0.3735
600	2.988E-5	10.43E-6	0.4002
800	5.507E-5	11.86E-6	0.6831

$$D_0^* = (1 + 10.663E\text{-}6 * \sigma^2) * 6.817E\text{-}6 \quad (C.O.V = 13.733\%)$$

$$m^* = (1 + 1.6134E\text{-}6 * \sigma^2) * 6.08E\text{-}6 \quad (C.O.V = 10.067\%)$$

3.1.4.2 Lord Fusor 320/322

When casting Fusor 320/322, a toughened epoxy, it was virtually impossible to eliminate all of the air bubbles in the finished bulk specimen. The "C-scan" ultrasonic technique was used to detect the presence of large voids. The better specimens (with no voids in the testing section) were chosen for testing.

When testing a specimen (F8-6) of this adhesive the following behavior was observed:

a) The adhesive exhibits a near linear viscoelastic behavior for 10% and 20% of the UTS (fig 3.16 and 3.19).

b) The difference in the values for creep compliance at 40% UTS and the values at 30% UTS was very large. The values measured at 40% UTS were about 2.5 times the values at 30% UTS, whereas the values at 30% UTS were 1.5 times the values obtained at 10% and 20% of UTS.

c) During the third cycle at 40% of the UTS, the specimen broke at the site of an air bubble, within the gage length.

In order to confirm the observed behavior and reduce the possibility of experimental error in the above results, another specimen was fabricated, F9-1. The new specimen was cast from a fresh batch of adhesive. The test procedure used on specimen F9-1 was the same as the one used on F8-6. Specimen F9-1 broke during the fourth cycle at 40% UTS at the site of an air bubble. The strains measured

during the second and third cycles at 40% UTS are almost the same as the previous specimen (fig 3.18 and 3.19). The measurements taken during the fourth cycle (just before failure occurred) show a large increase in strain. When comparing the results of F8-6 and F9-1 (fig 3.18 and 3.19), good agreement is found for the tests conducted at 10%, 20%, and 30% of the UTS. Also, there is good agreement in the results of the "failure cycles", that is the results measured just before failure occurred.

The observed behavior indicates that the presence of air bubbles/voids results in sites of local stress concentration, a significant increase in creep compliance and early failure. Preliminary observation suggests that the size of the air bubble dictates the stress level at which failure occurs. No specific study of the effects of voids on the quasi-static or creep response of the cast adhesives was performed.

The creep compliance versus time curves for the two specimens tested were averaged and curve fitted with a quadratic power law. A summary of the curve fitting procedure is presented in tables 3.3 through 3.4 and, figures 3.23 through 3.25; resulting in the following relationship:

$$D(t,\sigma) = (1 + g\sigma^2)4.559E\text{-}6 + (1 + f\sigma^2)7.317E\text{-}6\ t^{0.53743}\left[\frac{in^2}{lb}\right] \quad (3.5)$$

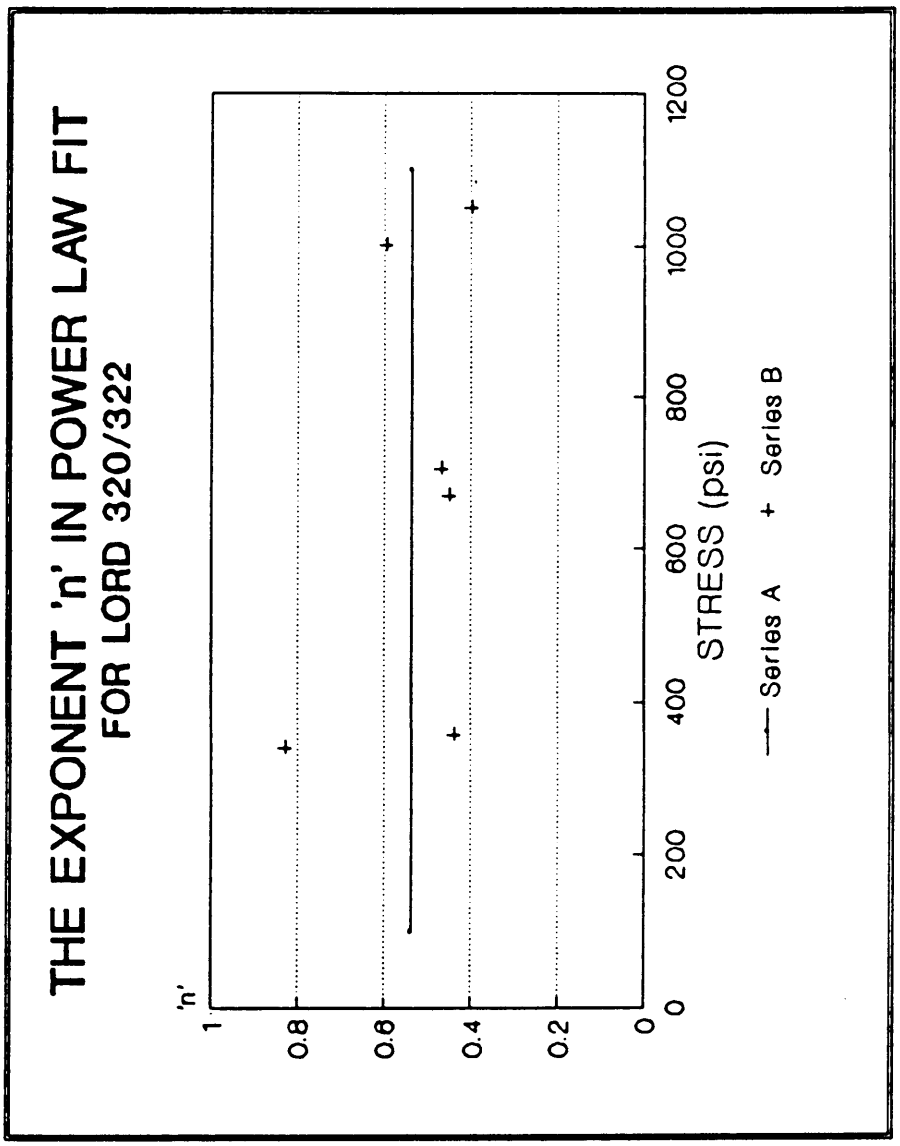

Figure 3.23: The Exponent 'n', in a Power Law Fit for Lord Fusor 320/322.

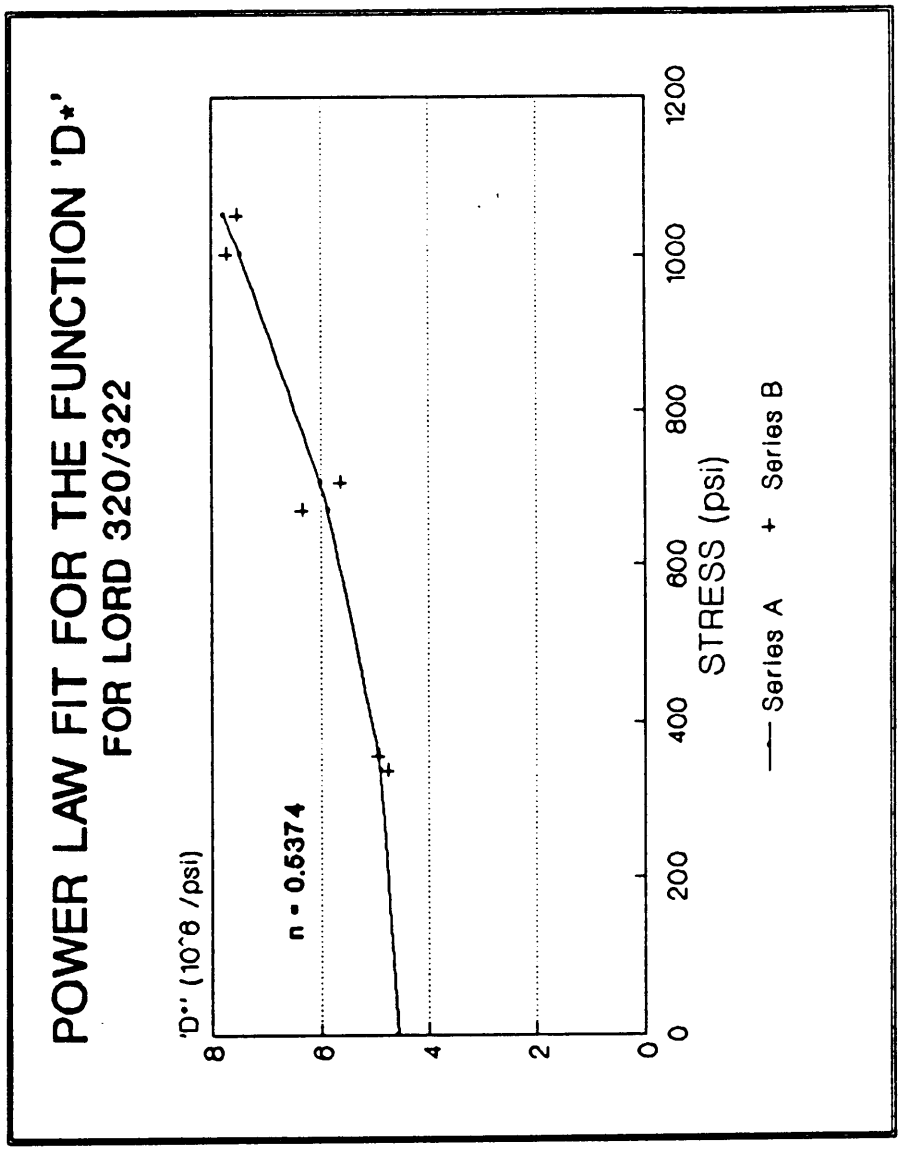

Figure 3.24: The Function 'D_0^*', in a Power Law Fit for Lord Fusor 320/322.

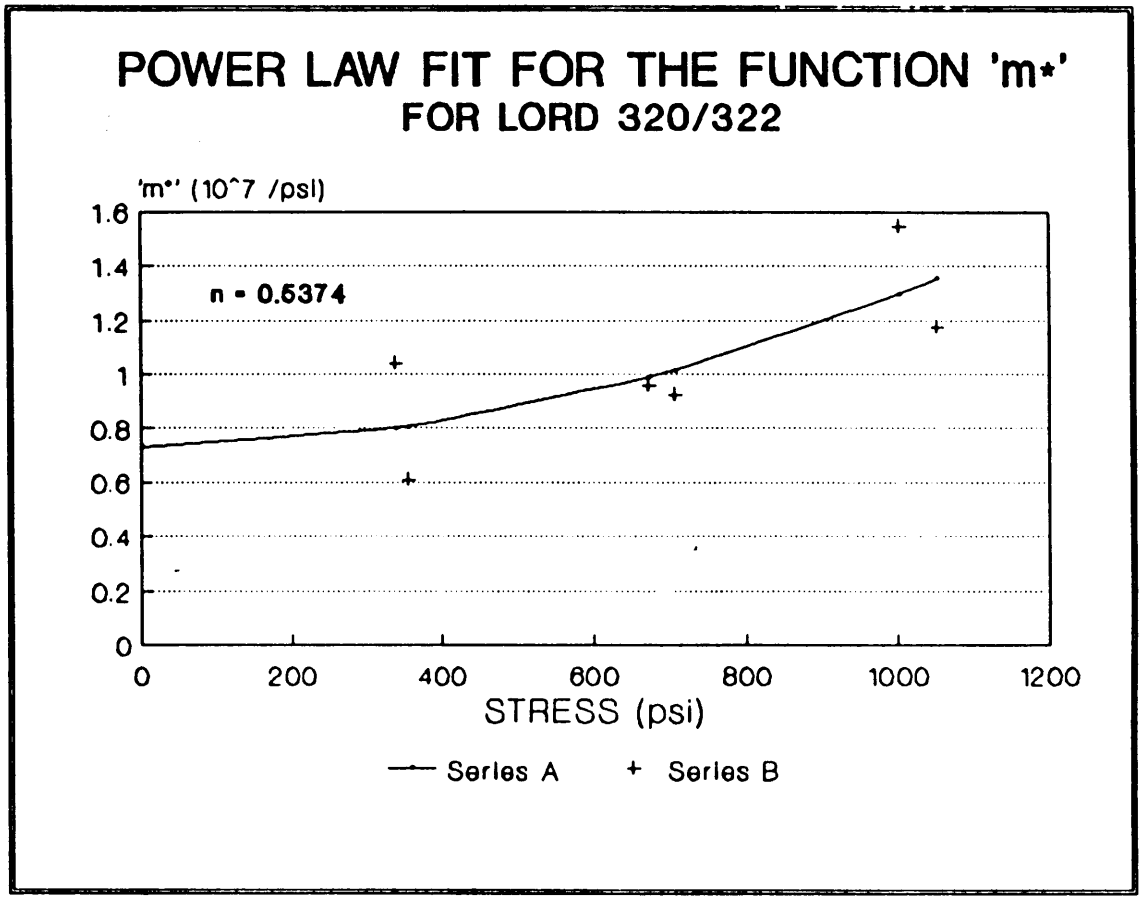

Figure 3.25: The Function '$m^{\bullet}$', in a Power Law Fit for Lord Fusor 320/322

Table 3.3: The Value of the Exponent 'n' in a Power Law Fit for Lord 320/322.

Stress [psi]	'n' Exponent	Coefficient of Variation [%]
337 (F8-6)	0.8276	3.9108
355 (F9-1)	0.4365	1.2335
679 (F8-6)	0.4092	0.1568
705 (F9-1)	0.4671	0.2971
1004 (F8-6)	0.5942	0.1914
1051 (F9-1)	0.3996	0.2060

n = 0.5374 (Coefficient of Variation = 33.253%)

Table 3.4: Power Law Fit for D_0^* and m^* for Lord 320/322.

STRESS [psi]	D_0^* $\left[\frac{in^2}{lb}\right]$	m^* $\left[\frac{in^2}{lb\ sec}\right]$	Coefficient of Variation [%]
337 (F8-6)	4.766E-6	1.037E-7	4.3366
355 (F9-1)	6.331E-6	0.958E-7	0.6856
670 (F8-6)	6.331E-6	0.958E-7	0.1882
705 (F9-1)	5.616E-6	0.922E-7	0.3974
1004 (F8-6)	7.700E-6	1.546E-7	0.1943
1051 (F9-1)	7.519E-6	1.173E-7	0.4071

$$D_0^* = (1 + 6.327E\text{-}7 * \sigma^2) * 4.559E\text{-}6 \quad (C.O.V = 5.703\%)$$

$$m^* = (1 + 7.669E\text{-}7 * \sigma^2) * 7.317E\text{-}6 \quad (C.O.V = 21.44\%)$$

where,

$$g = 6.327E\text{-}7 \left[\frac{in^4}{lb^2}\right]$$

$$f = 7.669E\text{-}7 \left[\frac{in^4}{lb^2}\right]$$

3.2 THE ARCAN SPECIMEN

Shear creep tests were performed using the Arcan specimen geometry to evaluate the performance of in-situ adhesives. The testing procedure is similar to that used in the bulk adhesive coupon characterization.

3.2.1 Specimen Preparation

The Arcan specimens and the bonding mold used to assure aligned bonding were machined from steel. Drawings of the specimen and the mold are presented in figures 3.26 through 3.29 . The bondline thickness was 0.06 inches.

The bonding surfaces were grit-blasted, and then the specimens were degreased and cleaned thoroughly. The areas that were not to be bonded were protected with a temperature-resistant Kapton masking tape.

The bonding molds consists of two mold plates and four 3/8 inch

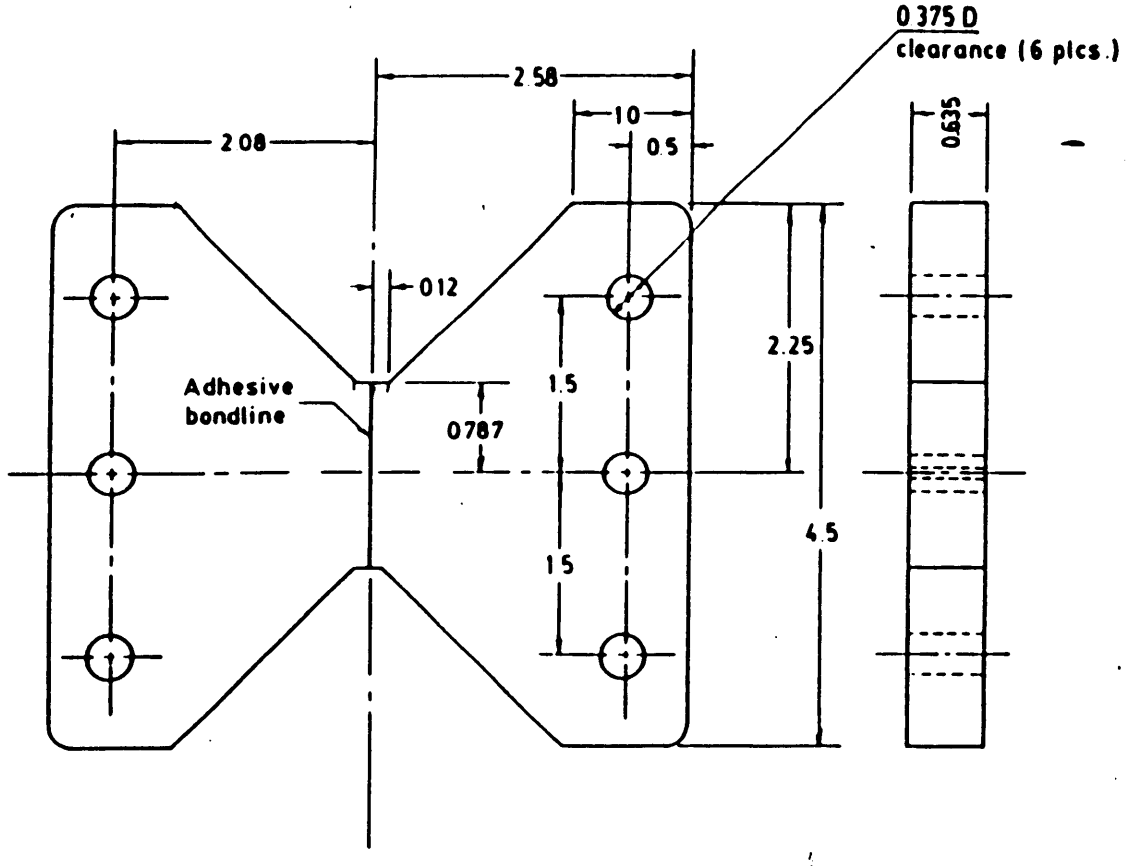

Figure 3.26: The Arcan Specimen - Showing the Butterfly Joint [10].

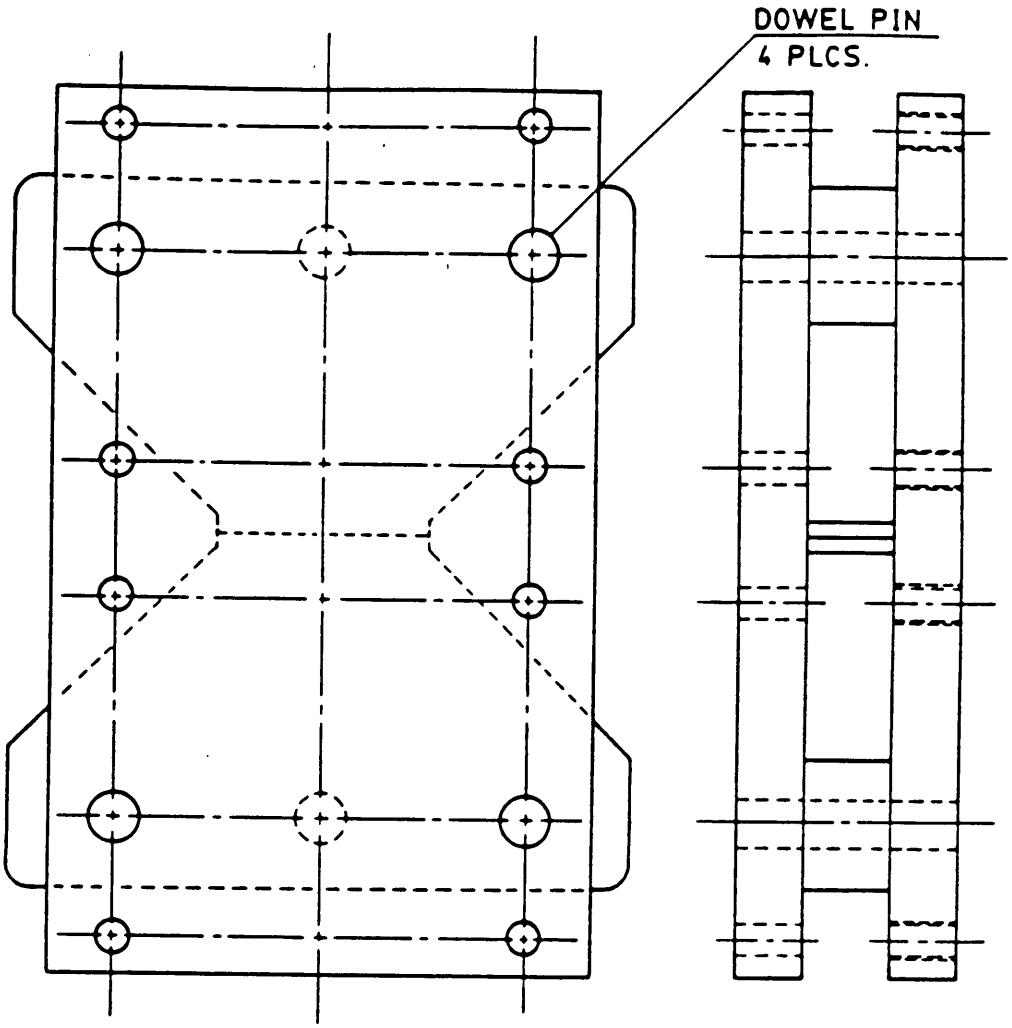

Figure 3.27: Arcan Specimen Held in Place During Cure by the two Mold Half Plates [10].

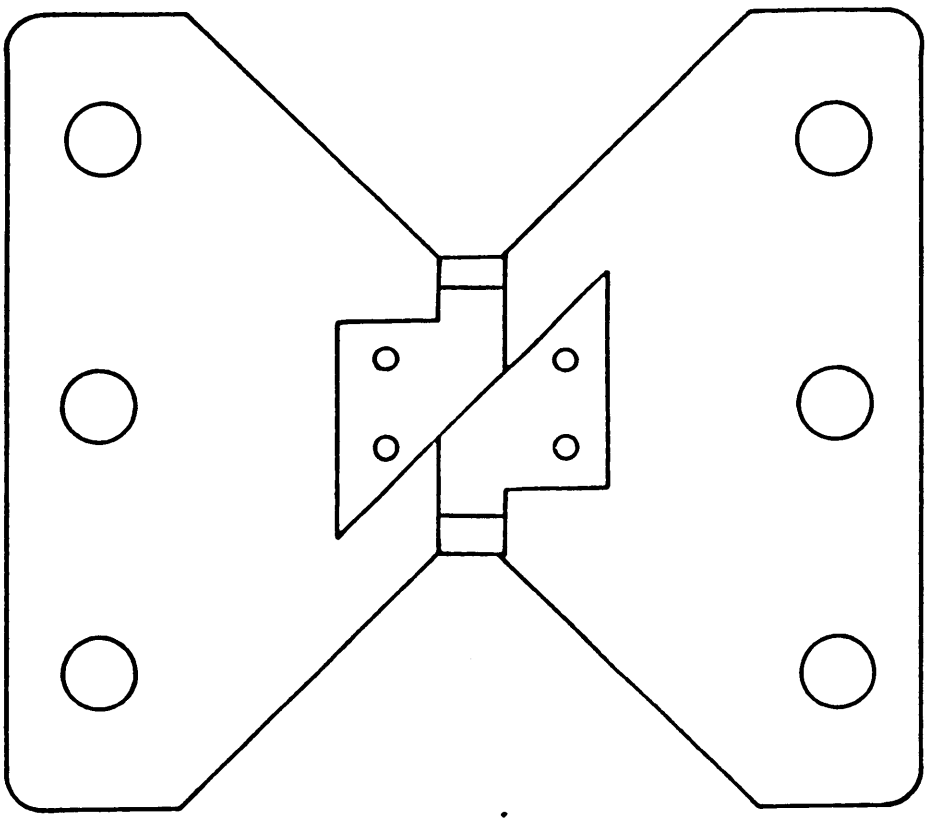

Figure 3.28: Extensometer Fixture Mounted on Arcan Specimen.

dowel pins. The pins assure alignment of the specimen and also control bondline thickness.

The specimens were cured according to the same curing cycle as for the bulk adhesive specimens. The pins were removed before the post-cure, to eliminate stresses in the specimen.

3.2.2 Test Procedure

The specimens were tested using an MTS servo-hydraulic testing system under load control. In order to measure the deformation of the adhesive, an extensiometer was attached to the adherends on both sides of the bondline with the aid of a fixture, as shown in fig 3.28 .

A steel calibration specimen was fabricated and tested in order account for the deformation of the adherends in the joint. Figure 3.30 shows the deformation of the steel specimen as a function of the load.

3.2.2.1 Shear Testing

The Ultimate Shear Stress of the bonded Arcan specimens was measured by uniaxially loading the joints so as to produce near-uniform shear stress within the bondline. At least three Arcan specimens were bonded with each of the adhesives. These specimens were then loaded at a rate of 1000 lb/min, until the specimen failed. The value of the stress applied at the time of failure was taken as the

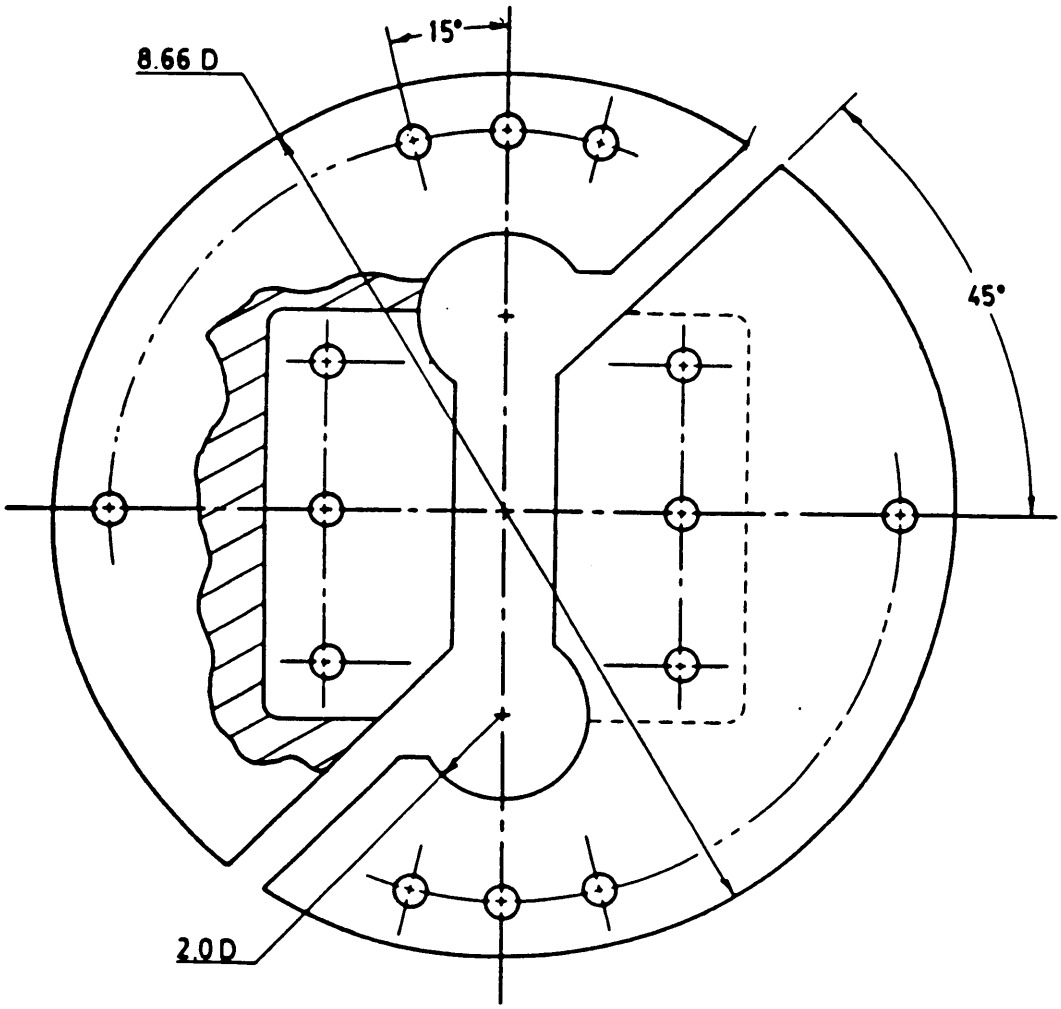

Figure 3.29: Front View of The Load Fixture Used to Grip Arcan Specimen During Testing [10].

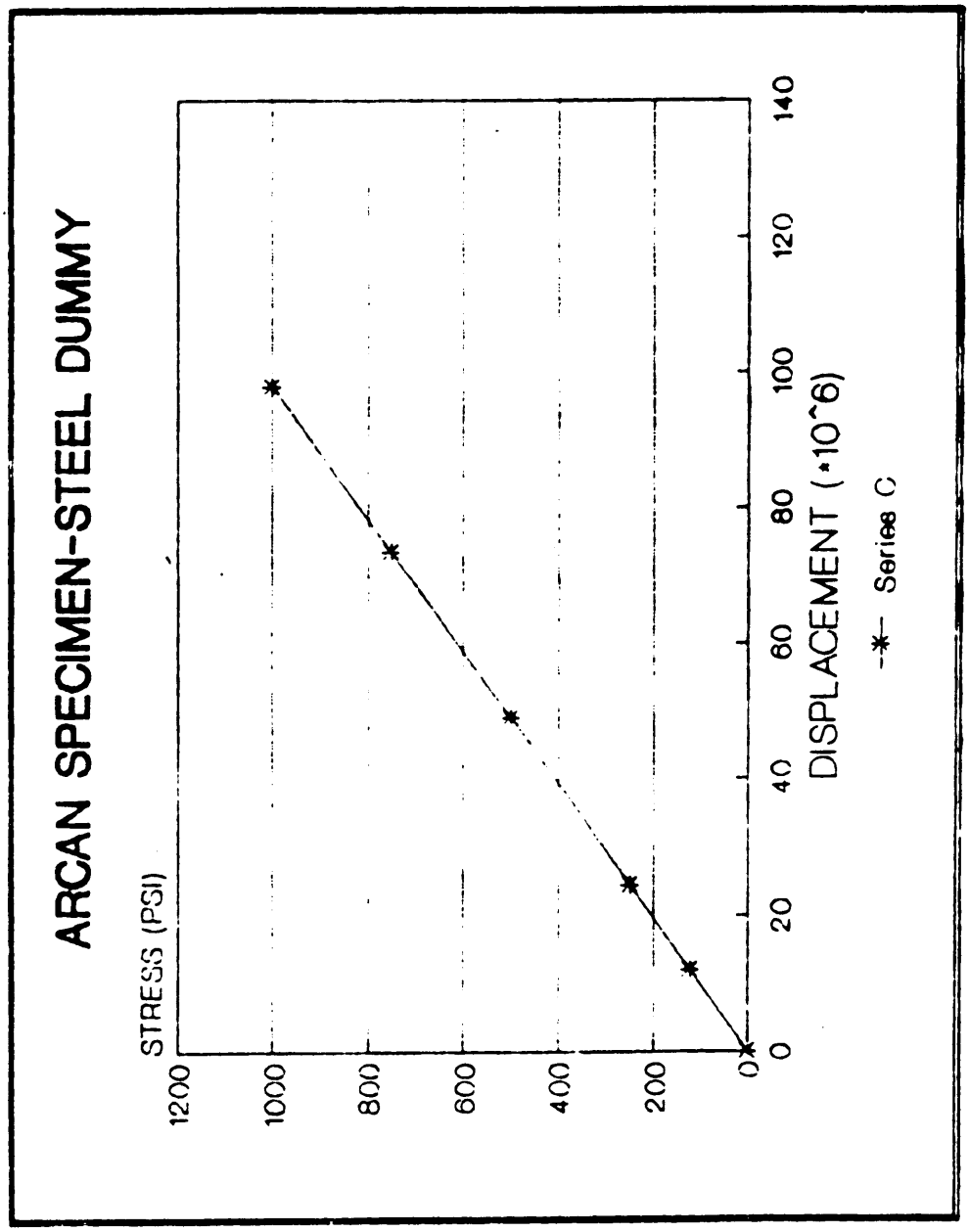

Figure 3.30: Callibration Curve of The Deflection in a Dummy Arcan Specimen.

Ultimate Shear Stress.

3.2.2.2 Creep Testing

Creep tests at various shear stress levels were performed. All creep tests were conducted on a single specimen per material, starting with the lowest stress level.

In order to avoid facing the possibility of inconsistent results, the mechanical conditioning procedure described in section 3.1.3.2 of this chapter, was applied.

Four conditioning cycles were conducted at each stress level, and the results of the third and fourth conditioning cycles were averaged to obtain creep versus time curves.

The procedure of 3.1 was used to gather data for the adhesively bonded Arcan joints. The displacements recorded at low stress levels were small, especially for the joints bonded with the epoxy adhesive.

3.2.3 Results

The following values of the ultimate shear stress were obtained by averaging results of shear tests performed on three specimens for each adhesive.

ADHESIVE	ULTIMATE SHEAR STRENGTH
Ashland Plyogrip 6600/6620 urethane	1097 psi
Lord Fusor 320/322 epoxy	2242 psi

3.2.3.1 Creep Testing Results

The first set of compliance curves, figures 3.31 through 3.36, correspond to the Ashland Plyogrip 6600/6620 urethane adhesive. The second set of compliance curves, figures 3.37 through 3.42, correspond to the Lord Fusor 320/322 epoxy adhesive.

3.2.3.2 Mechanical Conditioning

The first set of figures for each adhesive (figures 3.31 through 3.34 and 3.37 through 3.40) show the change of strain versus time, for the second third and fourth conditioning cycles.

3.2.3.3 Creep Compliance

The curves for the shear creep compliance are presented in figures 3.35 and 3.41 . These curves were obtained by averaging the third and fourth conditioning cycles.

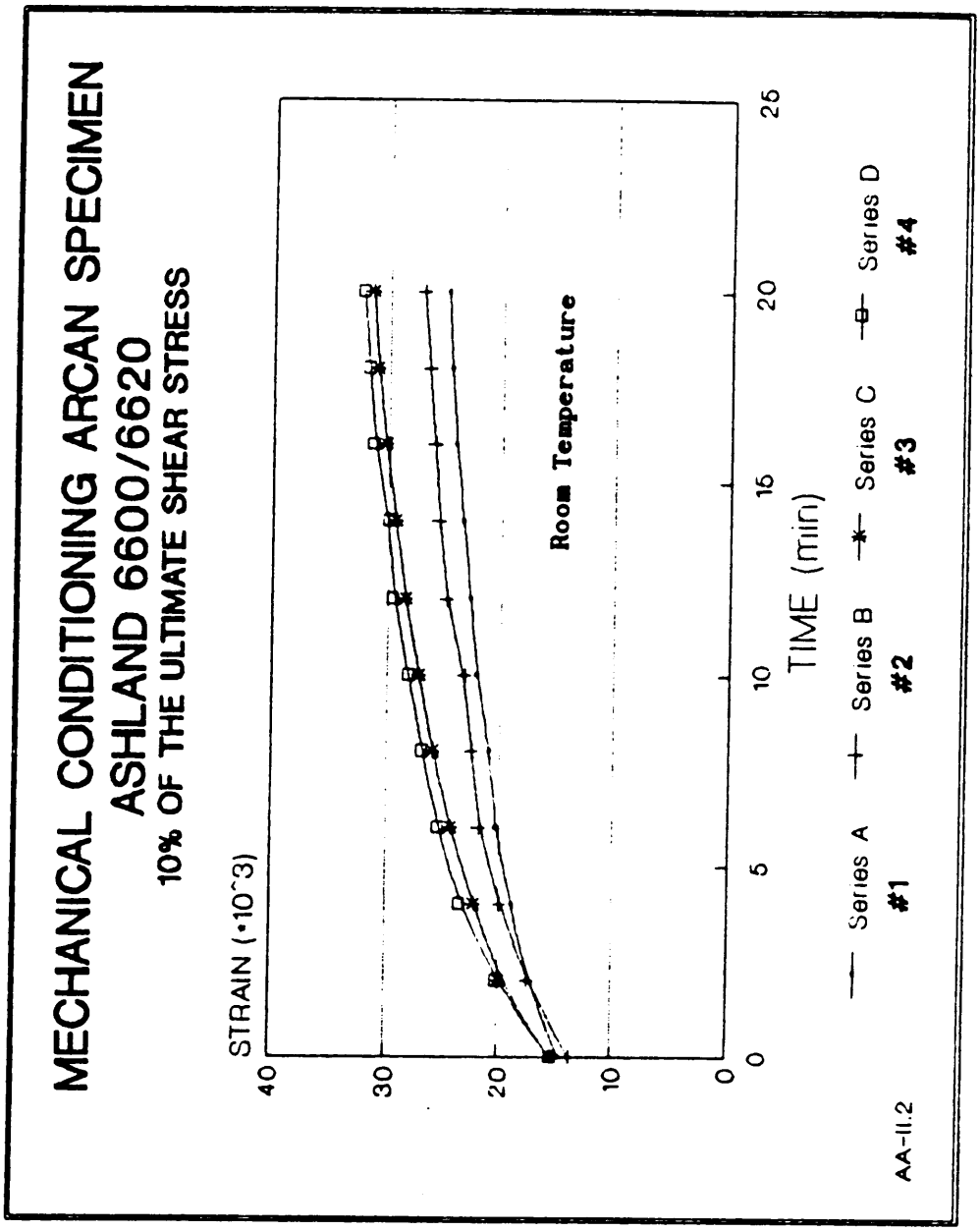

Figure 3.31: Mechanical Conditioning of Arcan Specimen, for Ashland Plyogrip 6600/6620.

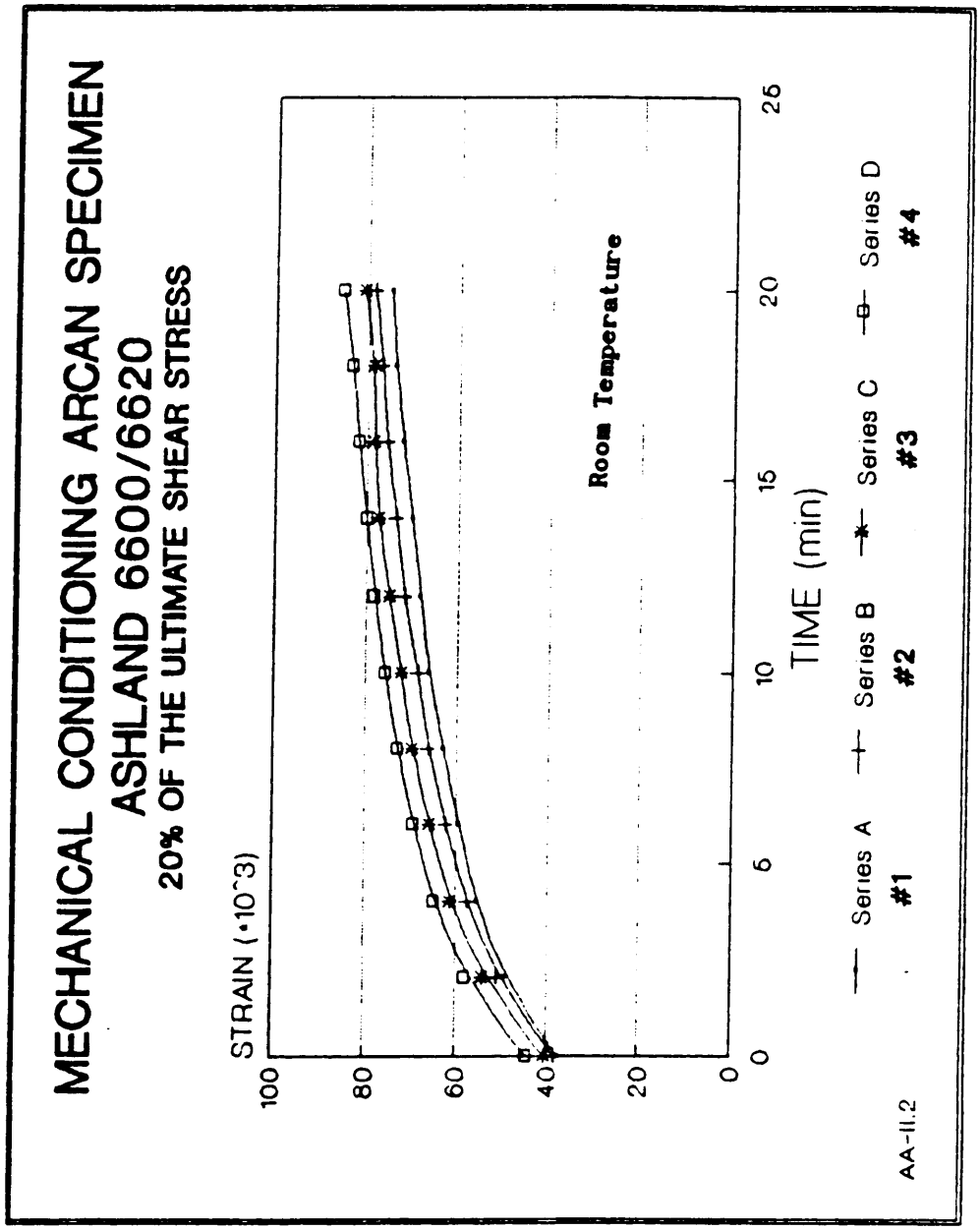

Figure 3.32: Mechanical Conditioning of Arcan Specimen, for Ashland Plyogrip 6600/6620.

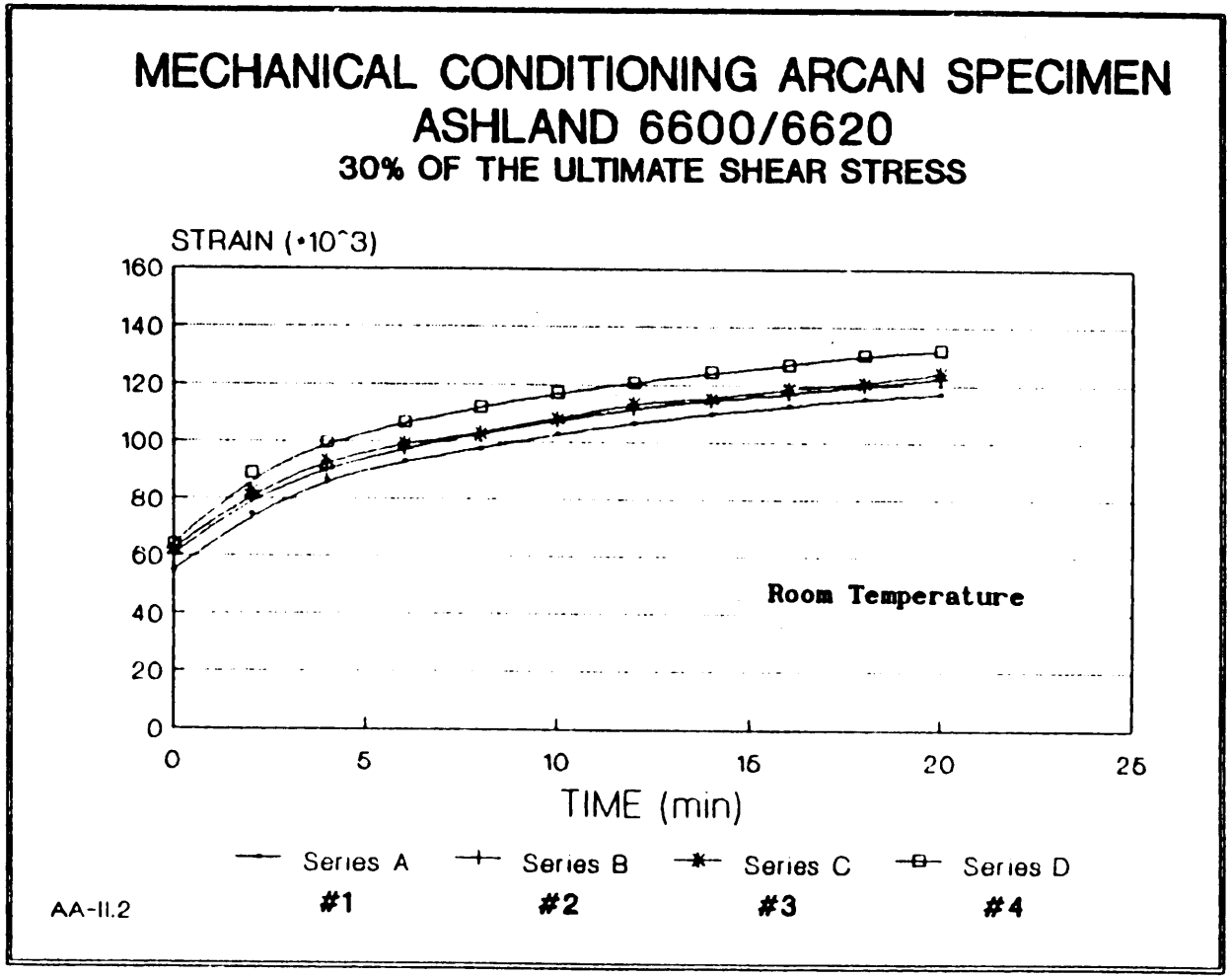

Figure 3.33: Mechanical Conditioning of Arcan Specimen, for Ashland Plyogrip 6600/6620.

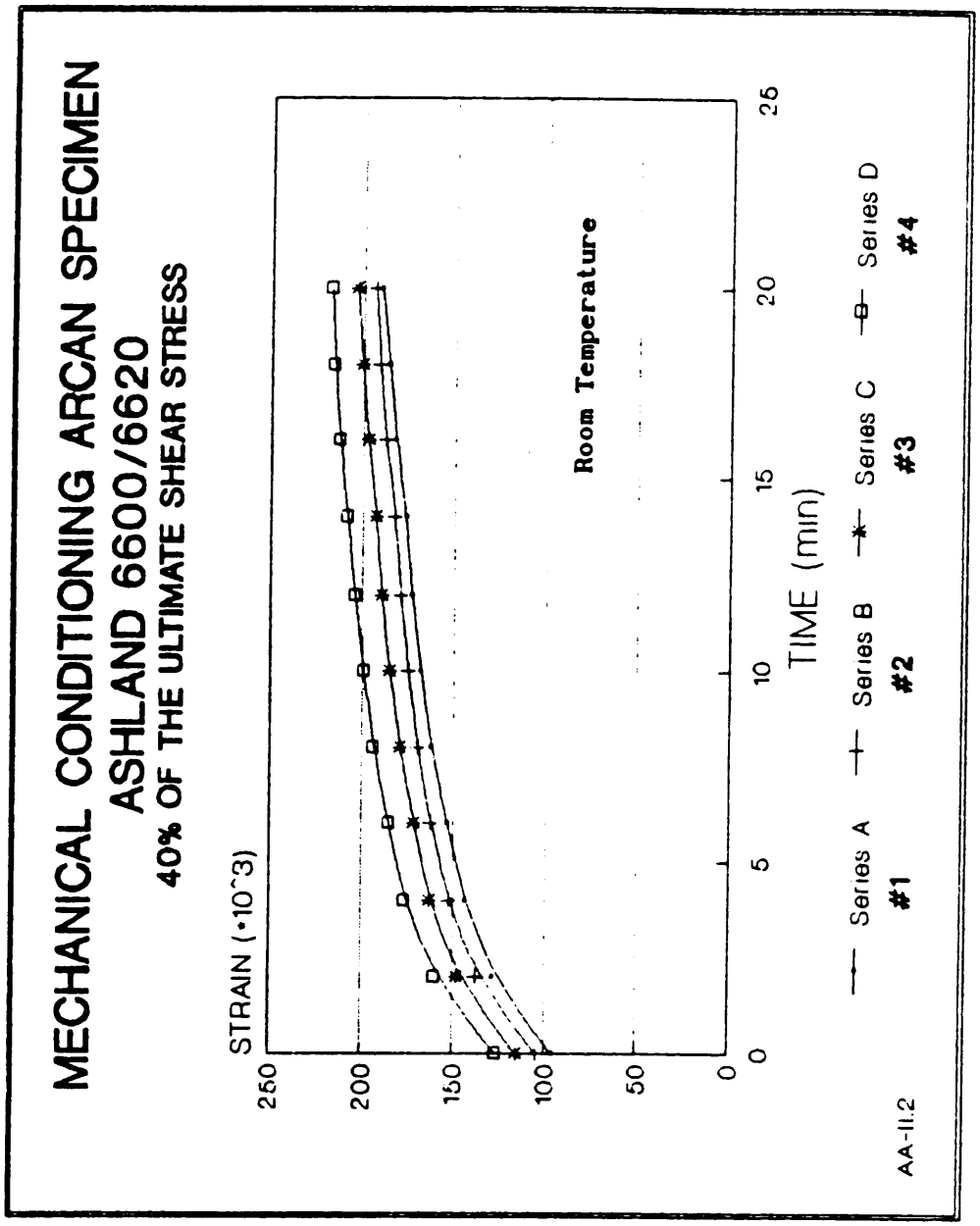

Figure 3.34: Mechanical Conditioning of Arcan Specimen, for Ashland Plyogrip 6600/6620.

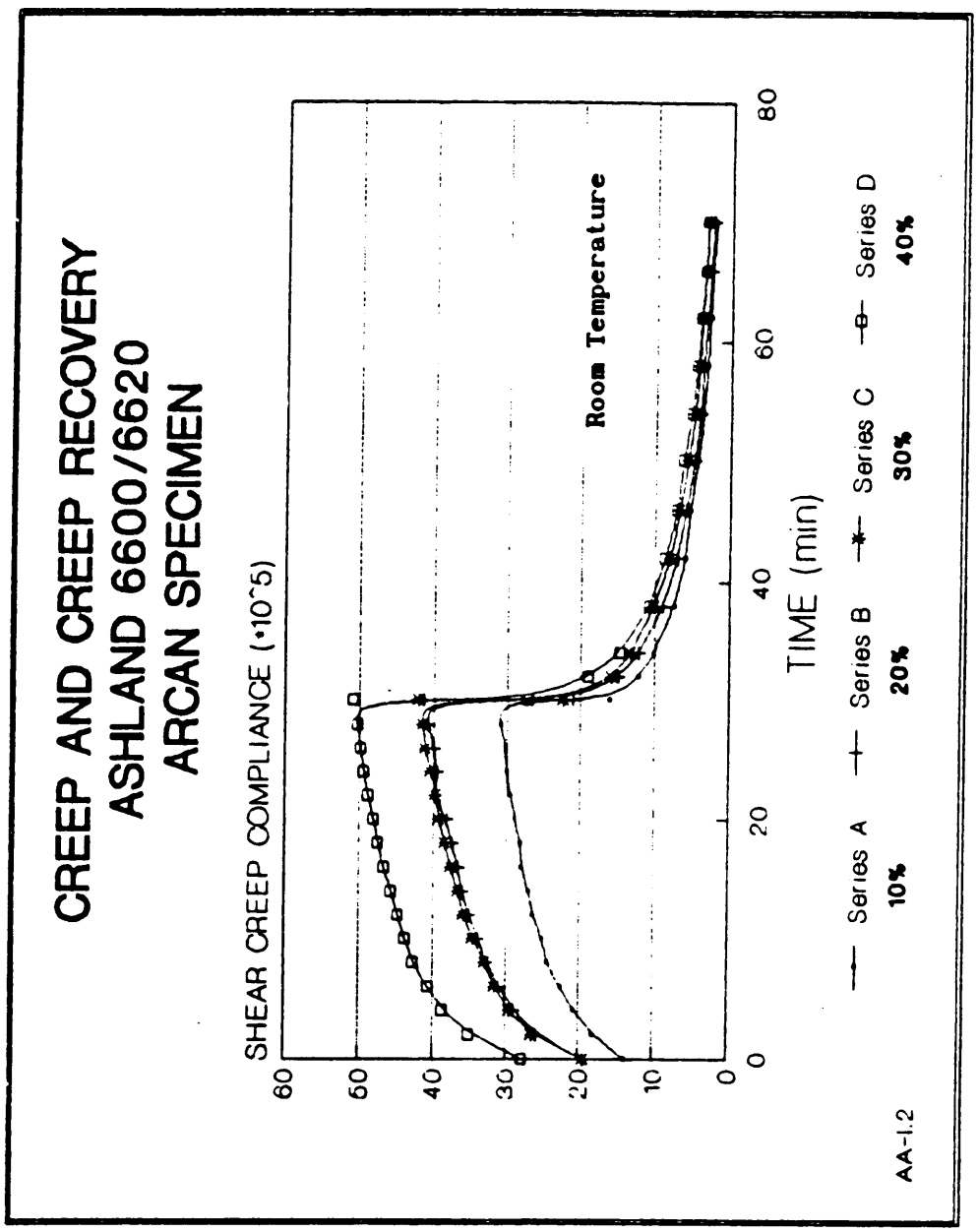

Figure 3.35: Creep and Creep Recovery of Arcan Specimen, for Ashland Plyogrip 6600/6620.

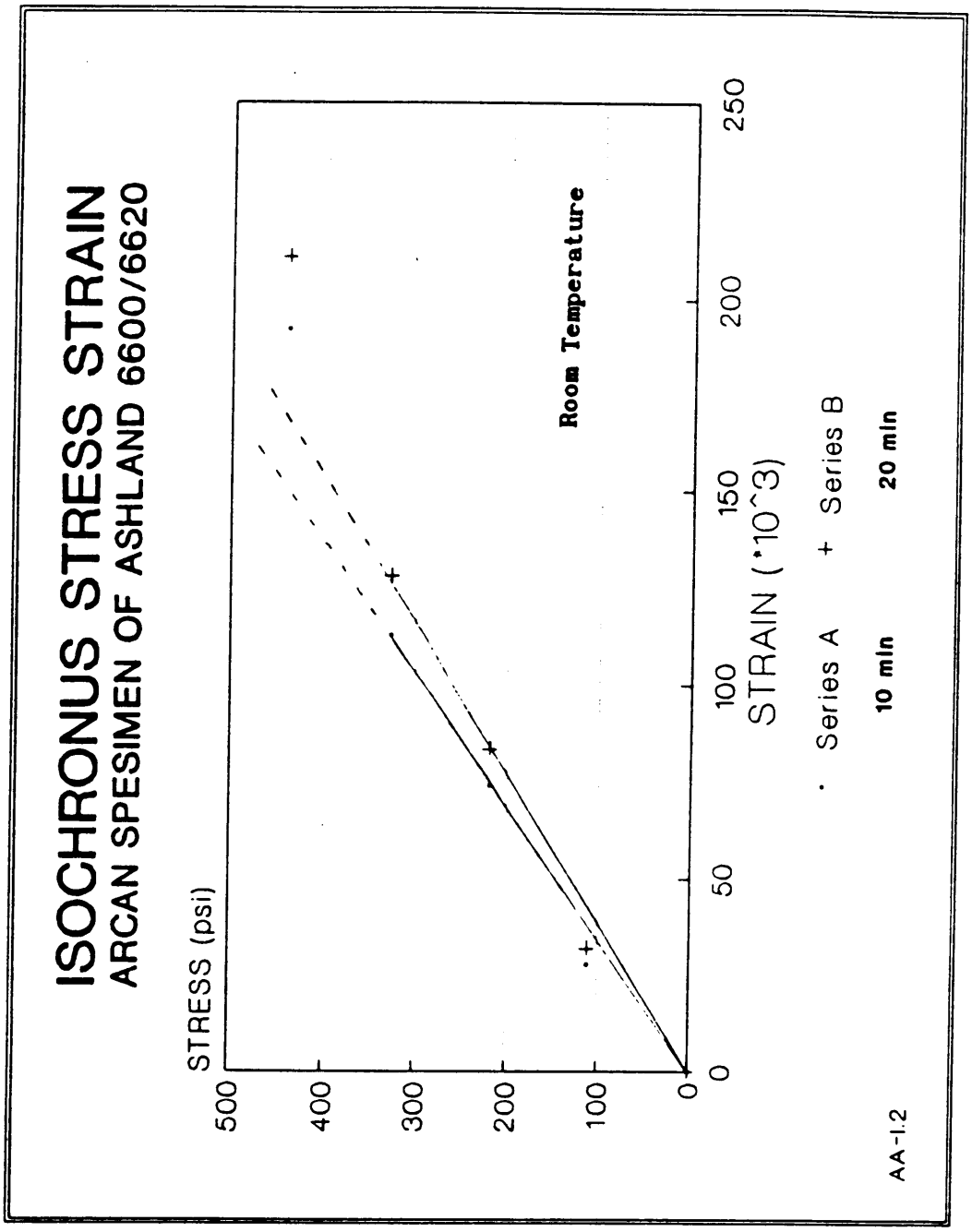

Figure 3.36: Isochronous Stress Strain curve for Ashland Plyogrip 6600/6620.

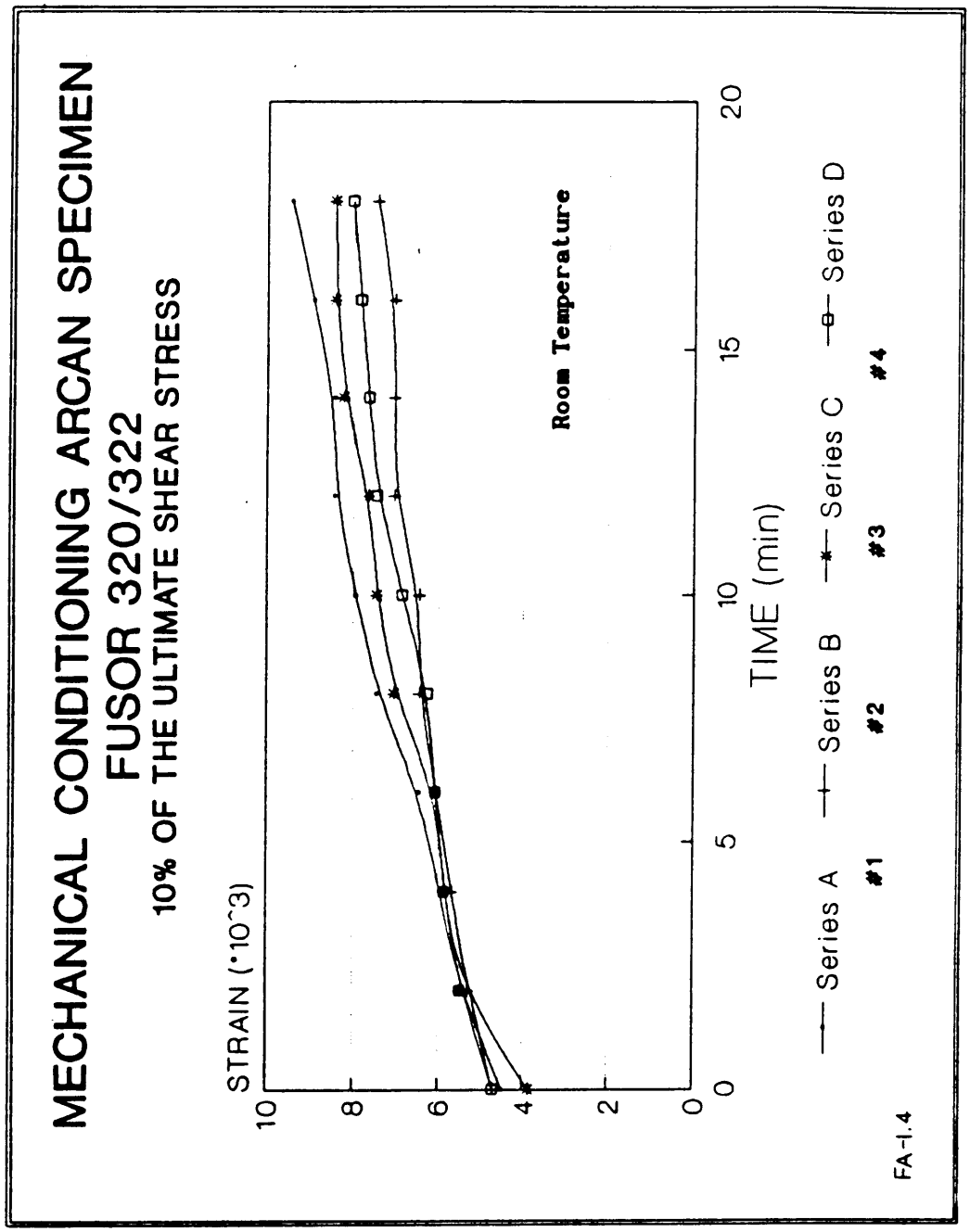

Figure 3.37: Mechanical Conditioning of Arcan Specimen, for Lord Fusor 320/322.

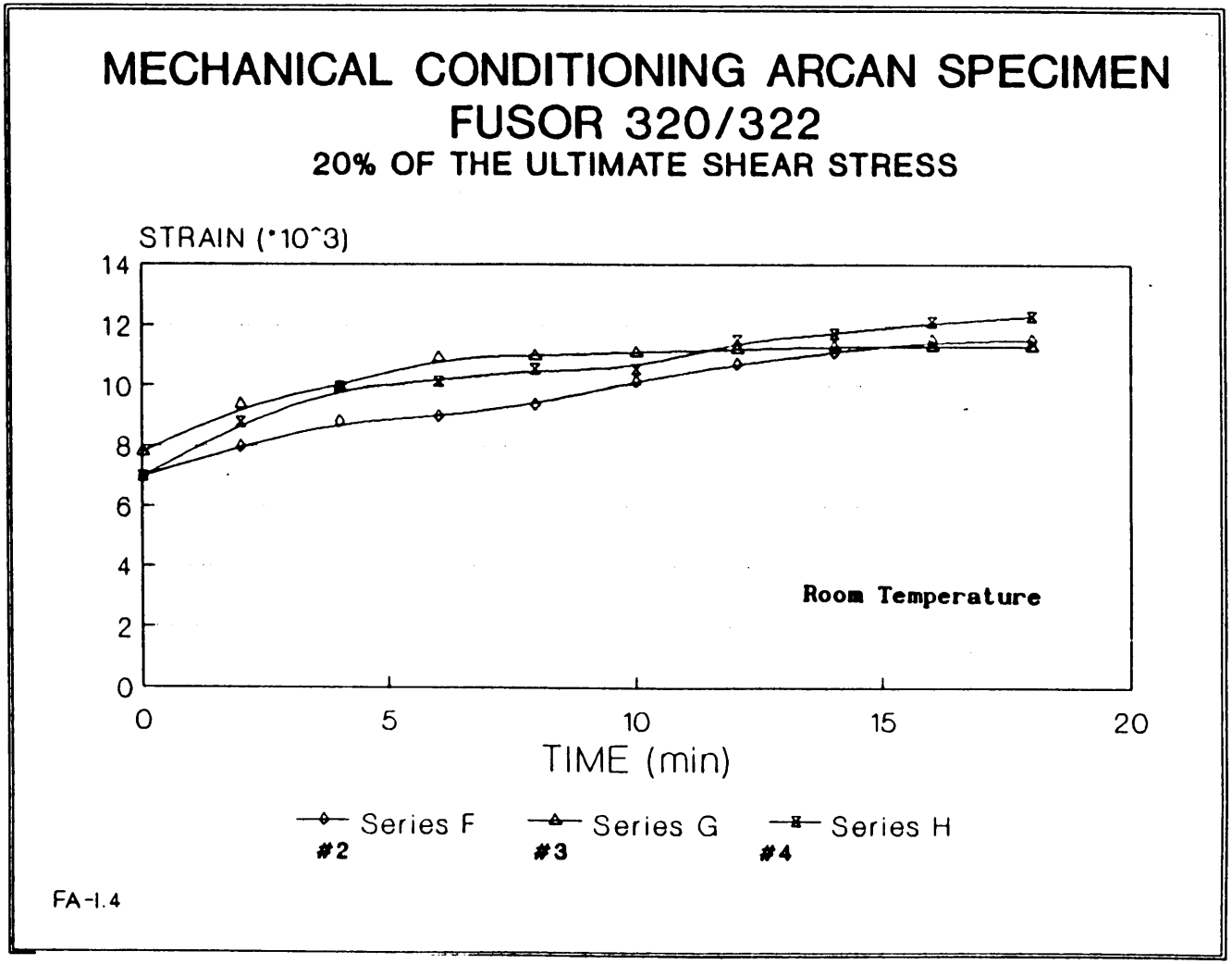

Figure 3.38: Mechanical Conditioning of Arcan Specimen, for Lord Fusor 320/322.

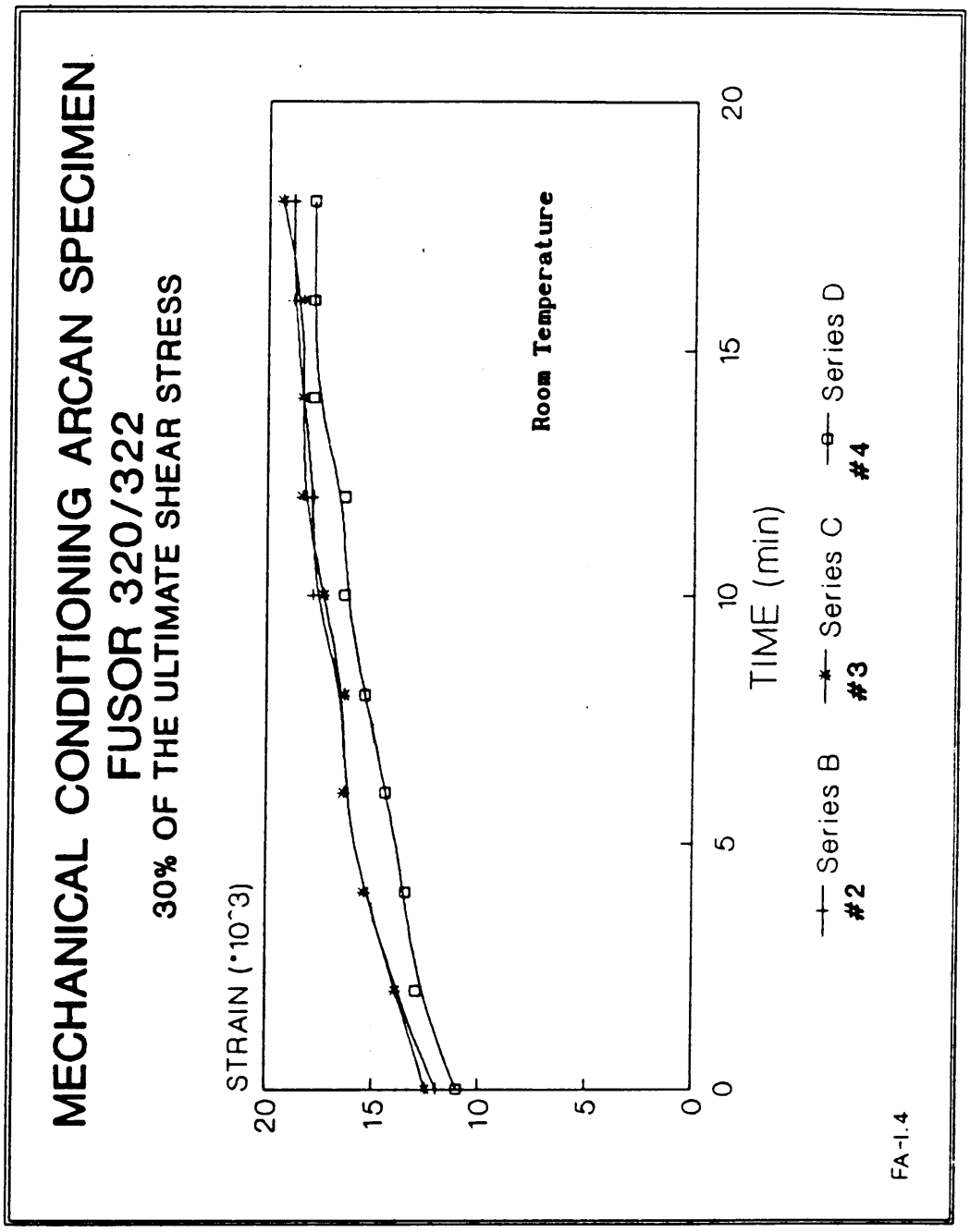

Figure 3.39: Mechanical Conditioning of Arcan Specimen, for Lord Fusor 320/322.

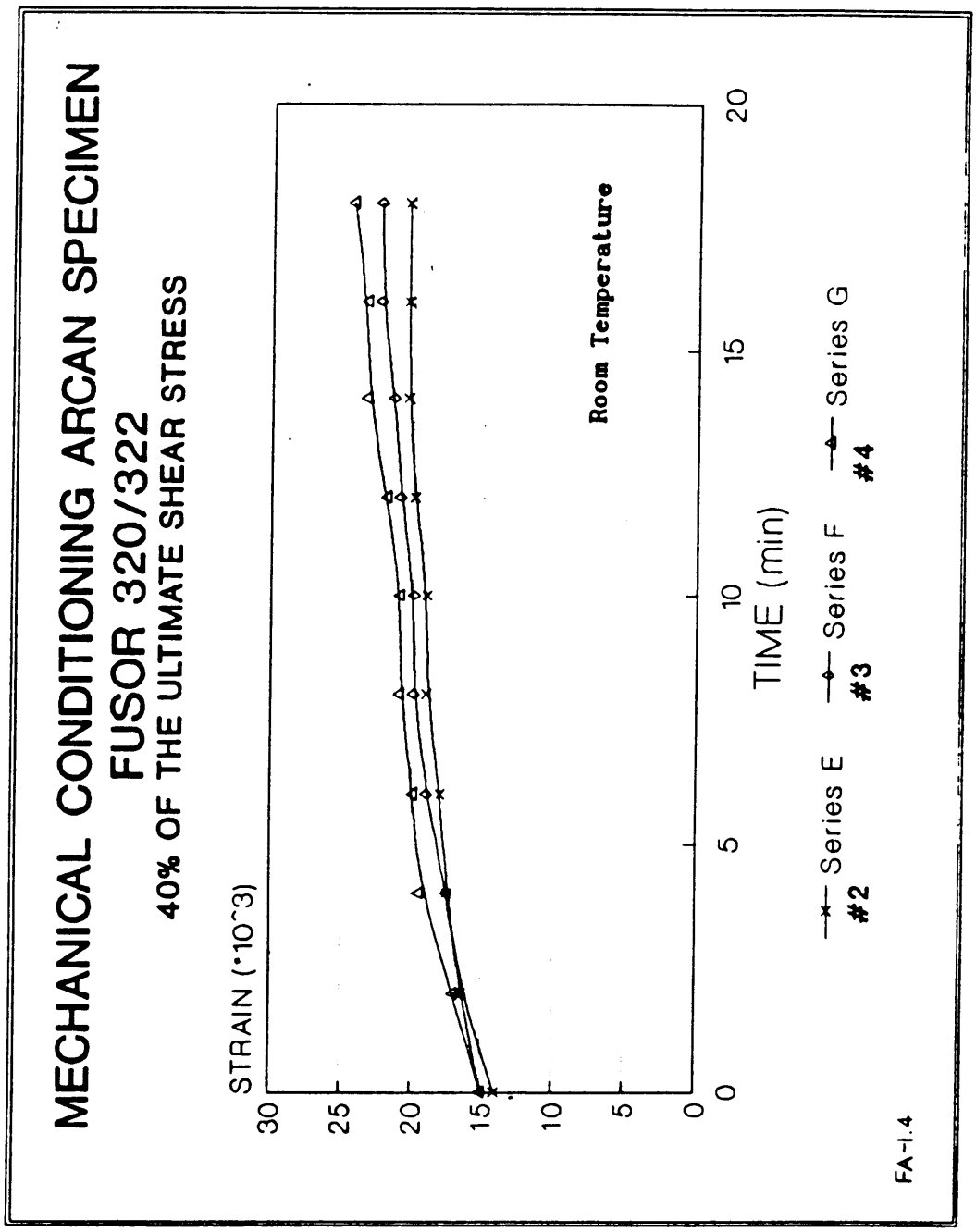

Figure 3.40: Mechanical Conditioning of Arcan Specimen, for Lord Fusor 320/322.

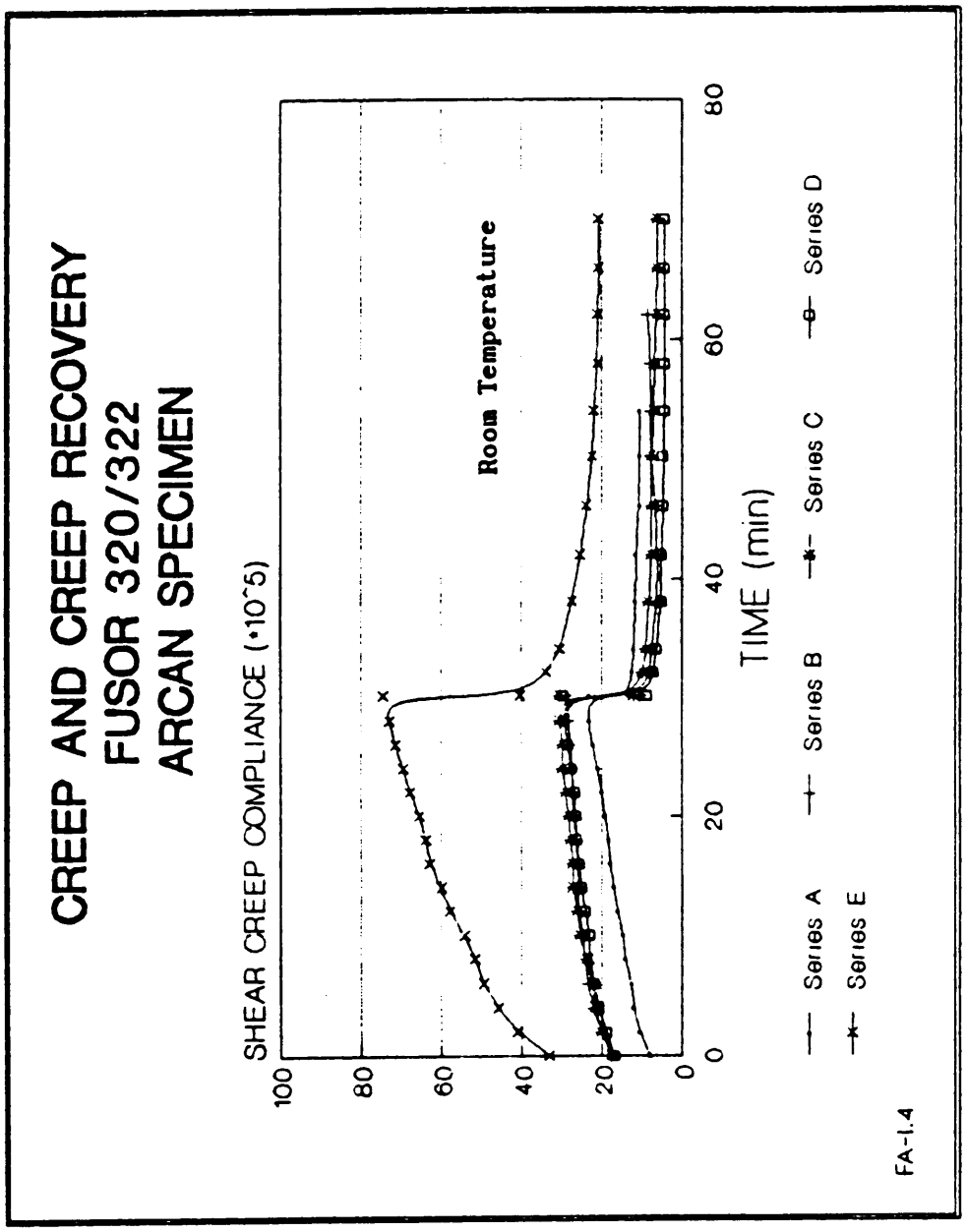

Figure 3.41: Creep and Creep Recovery of Arcan Specimen, for Lord Fusor 320/322.

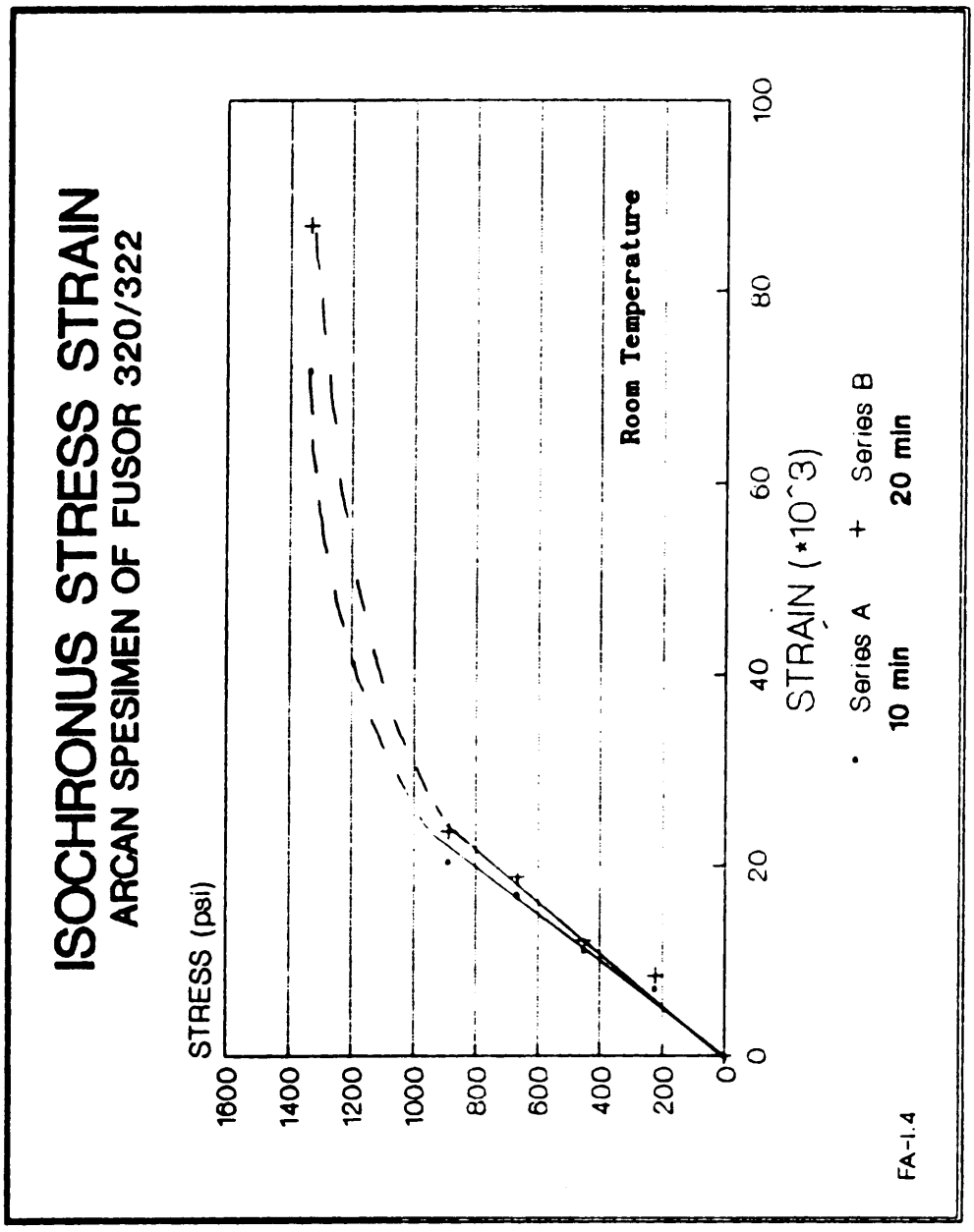

Figure 3.42: Isochronous Stress Strain curve for Lord Fusor 320/322.

3.2.3.4 Isochronous Stress Strain Curves

The isochronous stress strain curves for the Arcan tests are presented in figures 3.36 and 3.42 .

3.2.4 Discussion

The mechanical conditioning curves for both adhesives show good agreement between the third and fourth cycles. Furthermore, there is fair agreement among all four conditioning cycles. This may indicate that in the case of creep experiments of Arcan joint geometry, it may not be necessary to use the mechanical conditioning procedure to obtain consistent results. Further and thorough studies should be made to investigate the effect of the mechanical conditioning process for stiff adherent joints, such as the Arcan specimen.

3.2.4.1 Ashland Plyogrip 6600/6620 urethane

A specimen bonded with Ashland 6600/6620 was tested at 10%, 20%, 30% and 40% of the ultimate shear stress. At 60% the specimen failed. The shear creep compliance presented in fig 3.35 indicates linear behavior up to 30% of the ultimate shear stress. Nonlinearity is observed beyond that stress level.

The slight deviation at 10% of the Ultimate Shear Stress from

linear behavior may be regarded as experimental error, probably due to the small magnitude of the measured strain values.

3.2.4.2 Lord Fusor 320/322 epoxy

The Arcan specimen bonded with Fusor 320/322 FA-I.4 was tested at 10%, 20%, 30%, 40%, and 60% of the ultimate tensile shear stress.

Examining figures 3.41 and 3.42, it is apparent that the adhesive in the joint behaves in a linear viscoelastic manner at stress levels up to 40% of the ultimate shear stress. Above that level the material exhibits nonlinear viscoelastic behaviour.

The curve corresponding to 10% of the Ultimate Shear Stress deviates from linear behavior, as observed for the urethane adhesive. Again, it may be regarded as experimental error.

The results of the tests conducted on Arcan test specimens are compared with the Finite Element predictions for the same geometry and loading conditions in Chapter 4 of this report.

Chapter 4

FINITE ELEMENT ANALYSIS

The finite element analysis was performed in three stages. In the first stage the geometry of the Arcan test joint was examined, using elastic analysis only. In the second, the nonlinear viscoelastic properties of the bulk adhesives were modeled. The last step was to combine these two models in order to predict the creep compliance response of an adhesively bonded Arcan joint.

4.1 ANALYSIS OF THE ARCAN TEST JOINT GEOMETRY

Version 4.5 of the ABAQUS finite element program that was utilized in this study contains a mesh generator that cannot be used for the modeling of complicated configurations. Thus, in order to simplify the modeling process, the presence of the specimen load frame was neglected, and only the butterfly joint was modeled. The configurations of the butterfly joint and the specimen load frame are presented in figures 3.26 and 3.29.

Figure 4.1 shows the mesh utilized in the modeling of the stiff adherend Arcan butterfly joint. The model consists of 200 eight node biquadratic, reduced integration, plane strain elements. The adhesive

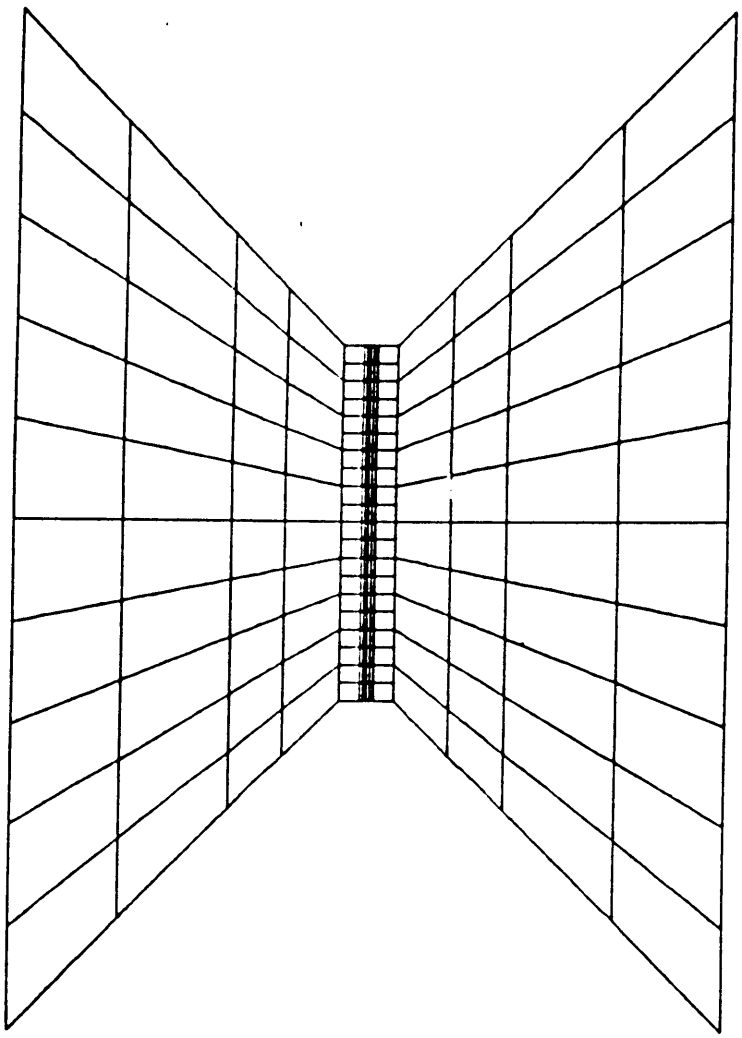

Figure 4.1: Finite Element Mesh of Arcan Specimen.

Figure 4.2: Enlarged View of the Finite Element Mesh of the Adhesive Layer in Arcan Specimen.

layer consists of 20 elements along the bondline length and four elements across the width. The aspect ratio of the bondline elements was 5.25. The analysis presented in this work is two dimensional, and the thickness of the joint was considered to be of unity magnitude or (1 inch). A detailed description of the bondline mesh is given in fig 4.2 .

The left and right hand sides of the adherends were constrained to move in the loading direction (the 2 direction) only, and the center point was constrained in both 1 and 2 directions.

Concentrated shear loads were applied to the nodes on the left and right hand sides of the specimen, using the CLOAD option.

The validity of the geometrical model was confirmed in two ways:

a) Material properties of steel were assigned to the Arcan model and the results obtained by the finite element analysis were compared with those obtained in a test of a steel specimen. Fig 4.3 shows that there is a perfect agreement between the calculated and the measured displacements, for such a specimen.

b) In his work, Cooper [10], presents a finite element analysis obtained, using a code named VISTA, of an aluminum joint bonded with AF 163-2U epoxy adhesive. His analysis was repeated using the ABAQUS F.E code. The shear stress across the bondline calculated by the two Finite Element codes, presented in fig 4.4 , shows that there is a good agreement between the two methods. It should be noted that although Cooper included the specimen load frame in his model,

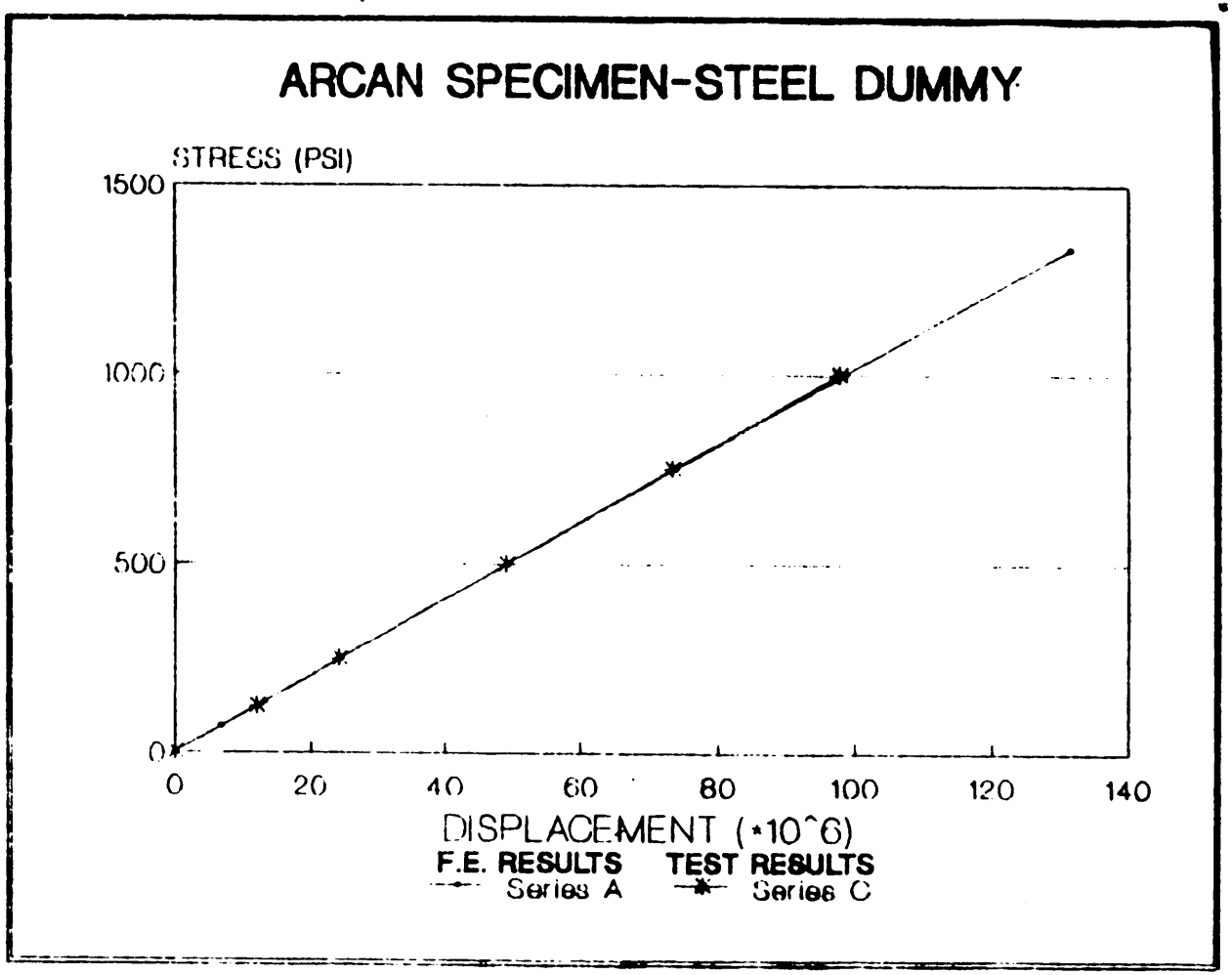

Figure 4.3: Comparison Between Finite Element Prediction and Measured Displacements in a Steel Arcan Specimen.

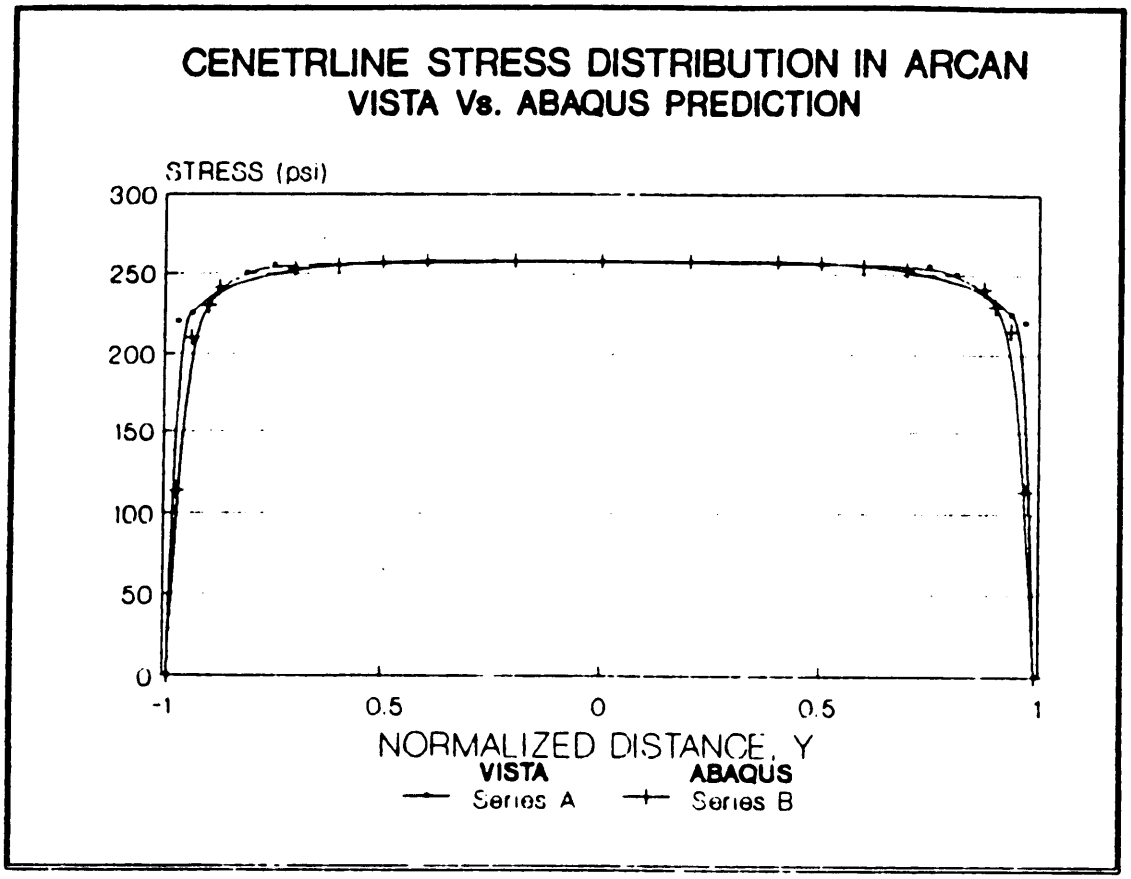

Figure 4.4: Adhesive Centerline Shear Stress Distribution in Arcan Specimen.

the model used in this study only represents the butterfly joint.

4.2 ANALYSIS OF THE VISCOELASTIC RESPONSE

The version of ABAQUS used in this study, version 4.5, enables the user to input isotropic viscoelastic material properties through a "creep" subroutine. The material properties as obtained from creep experiments conducted on bulk materials were introduced in the appropriate form of creep rate functions.

The equation for creep compliance, $D(t,\sigma)$, in the form of a Quadratic Power Law, (equation 2.6), was converted into an equation for the strain, by multiplying through by σ :

$$\varepsilon = (\sigma + g\sigma^3)\, D_0 + (\sigma + f\sigma^3)\, m\, t^n \qquad (4.1)$$

This representation of the stress, which is a non strain hardening expression, is valid only for cases where the stress remains constant with time. In this study, constant stress creep tests were conducted. The configuration of the Arcan joint results in constant shear stress along the bondline.

An example of such a subroutine is given in Appendix A.

The subroutines are constructed in such a way that the initial instantaneous response, i.e.the term $(\sigma + g\,\sigma^3)\, D_0$, does not appear. This initial responce is introduced through the Young's Modulus for the initial elastic response. The analysis was set up in two stages. First, the specimen is elastically loaded for one second. Then, the

viscoelastic analysis is performed. Creep behaviour was predicted for a period of 1800 seconds.

The initial Young's Modulus was obtained by using the following relationship for t=1 (the time for the elastic response) :

$$E^{*} = \frac{1}{D\ (t=1)} \qquad (4.2)$$

substituting for D (t=1)

$$E^{*} = \frac{1}{(1 + g\ \sigma_{eq}^{2})\ D_{0} + (1 + f\ \sigma_{eq}^{2})\ m} \qquad (4.3)$$

Where σ_{eq} is the equivalent stress as expressed by Kraus [4]

$$\sigma_{eq} = \left(\frac{1}{\sqrt{2}}\right)\left[(\sigma_{11} - \sigma_{22})^{2} + (\sigma_{33} - \sigma_{22})^{2} + (\sigma_{11} - \sigma_{33})^{2} + 6(\sigma_{12}^{2} + \sigma_{23}^{2} + \sigma_{13}^{2})\right]^{1/2} \qquad (4.4)$$

For the case of a uniaxial tensile creep test, as conducted on the bulk adhesive specimens, $\sigma_{eq} = \sigma_{11}$ (σ applied). Whereas, for the Arcan specimen, $\sigma_{eq} = \sqrt{3}\ \sigma_{12}$, where σ_{12} is the applied shear stress. Assuming f and g do not change with σ_{eq}.

In order to confirm the validity of the creep subroutine, the ABAQUS F.E. code was used to model the bulk adhesive coupon. A mesh of one quadrant of the actual coupon was modeled constraining the left nodes to move only in the load direction (the 1 direction) the bottom

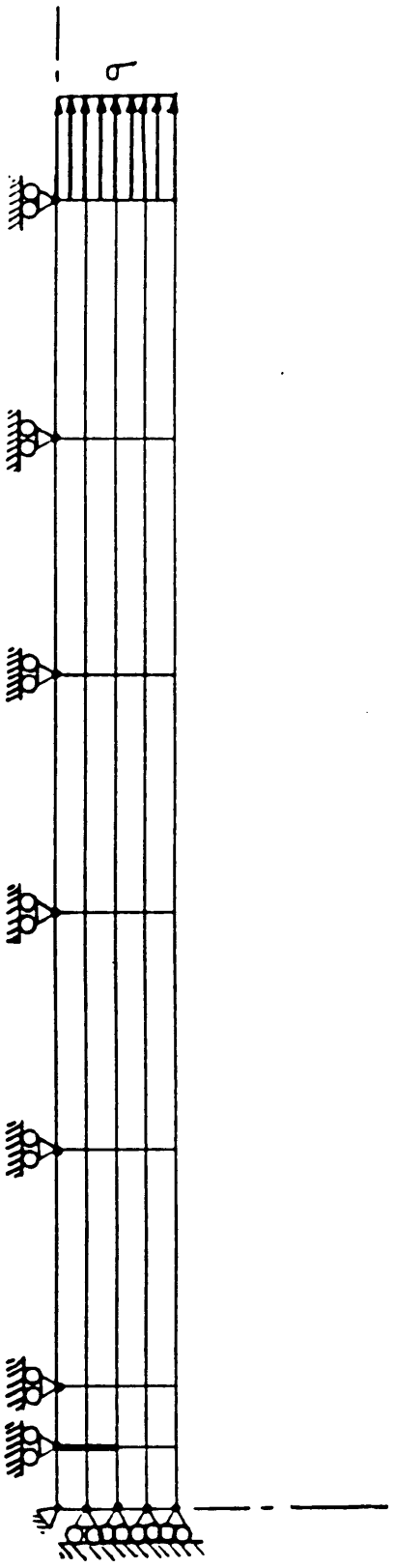

Figure 4.5: Finite Element Mesh of a Quarter of an Adhesive coupon.

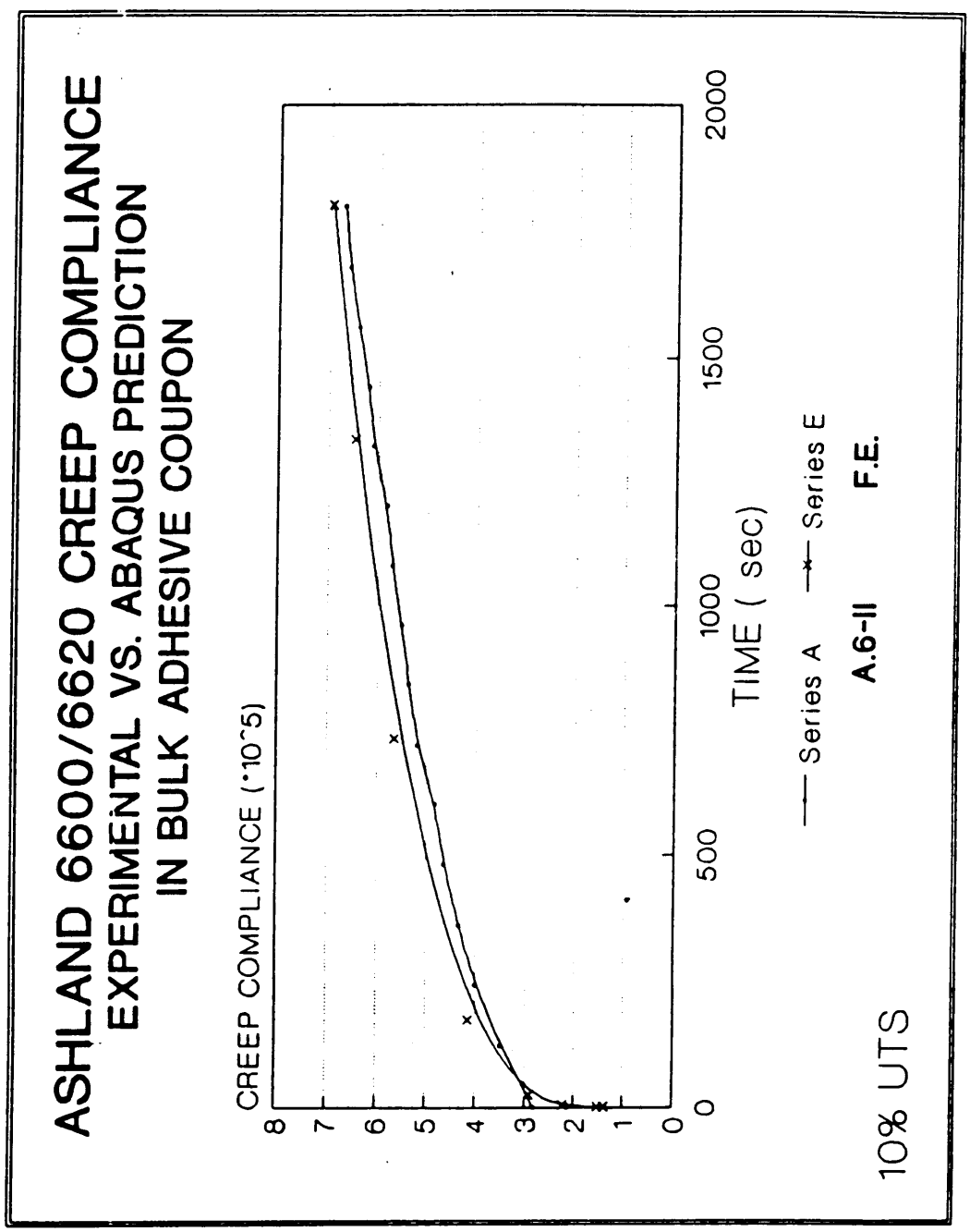

Figure 4.6: Creep Compliance in Bulk Adhesive Coupon, F.E. Versus Experimental Data, for Ashland Plyogrip 6600/6620.

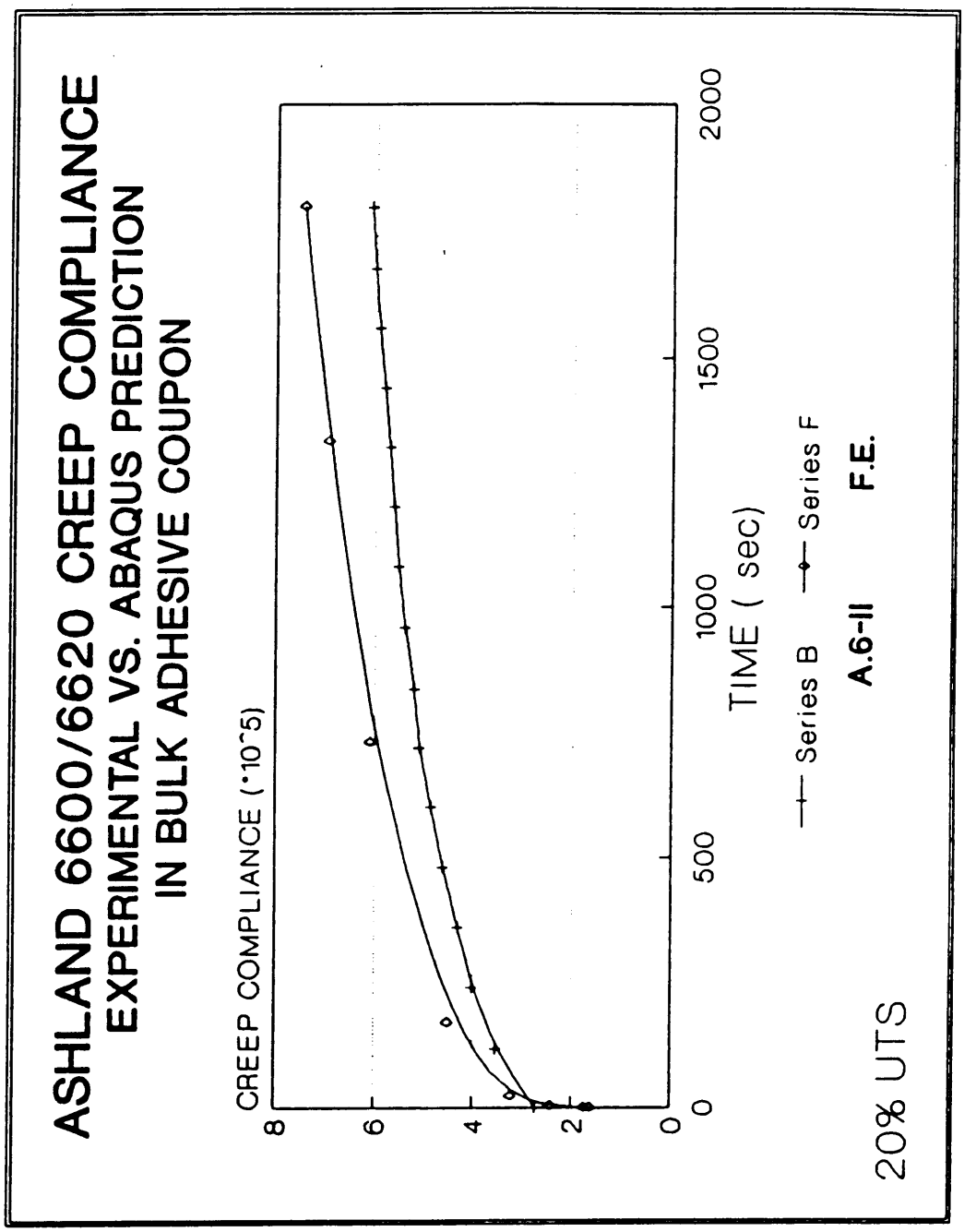

Figure 4.7: Creep Compliance in Bulk Adhesive Coupon, F.E. Versus Experimental Data, for Ashland Plyogrip 6600/6620.

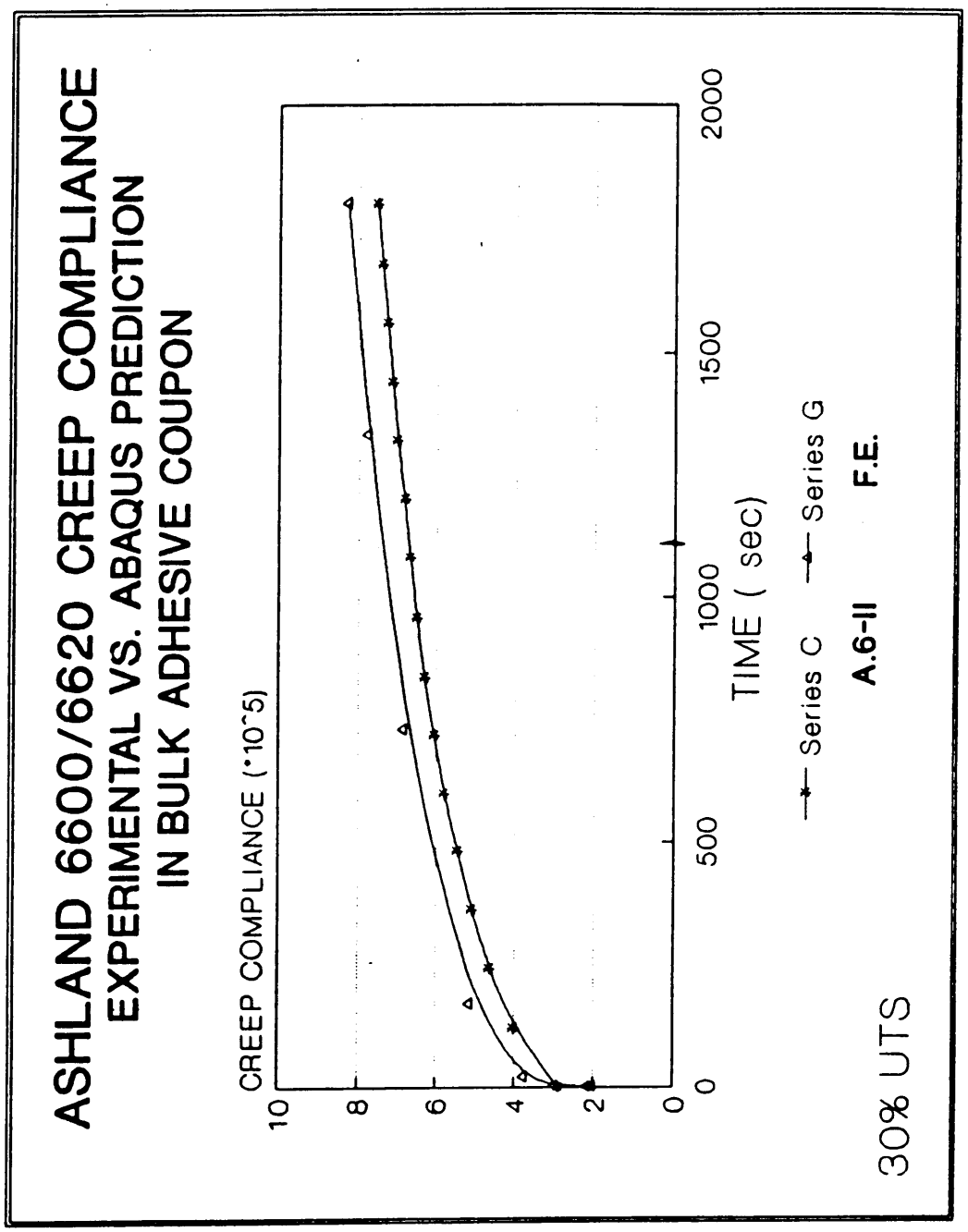

Figure 4.8: Creep Compliance in Bulk Adhesive Coupon, F.E. Versus Experimental Data, for Ashland Plyogrip 6600/6620.

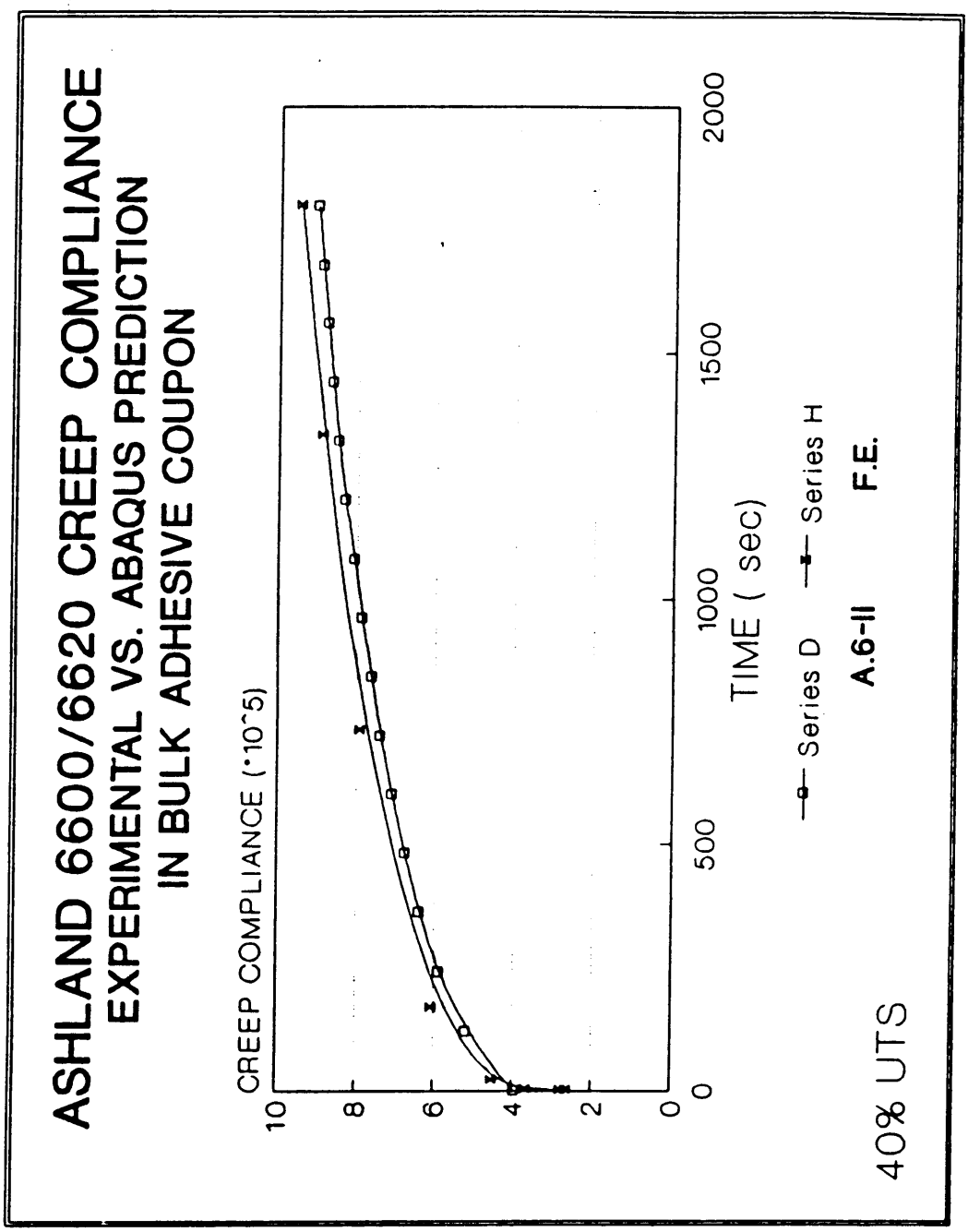

Figure 4.9: Creep Compliance in Bulk Adhesive Coupon, F.E. Versus Experimental Data, for Ashland Plyogrip 6600/6620.

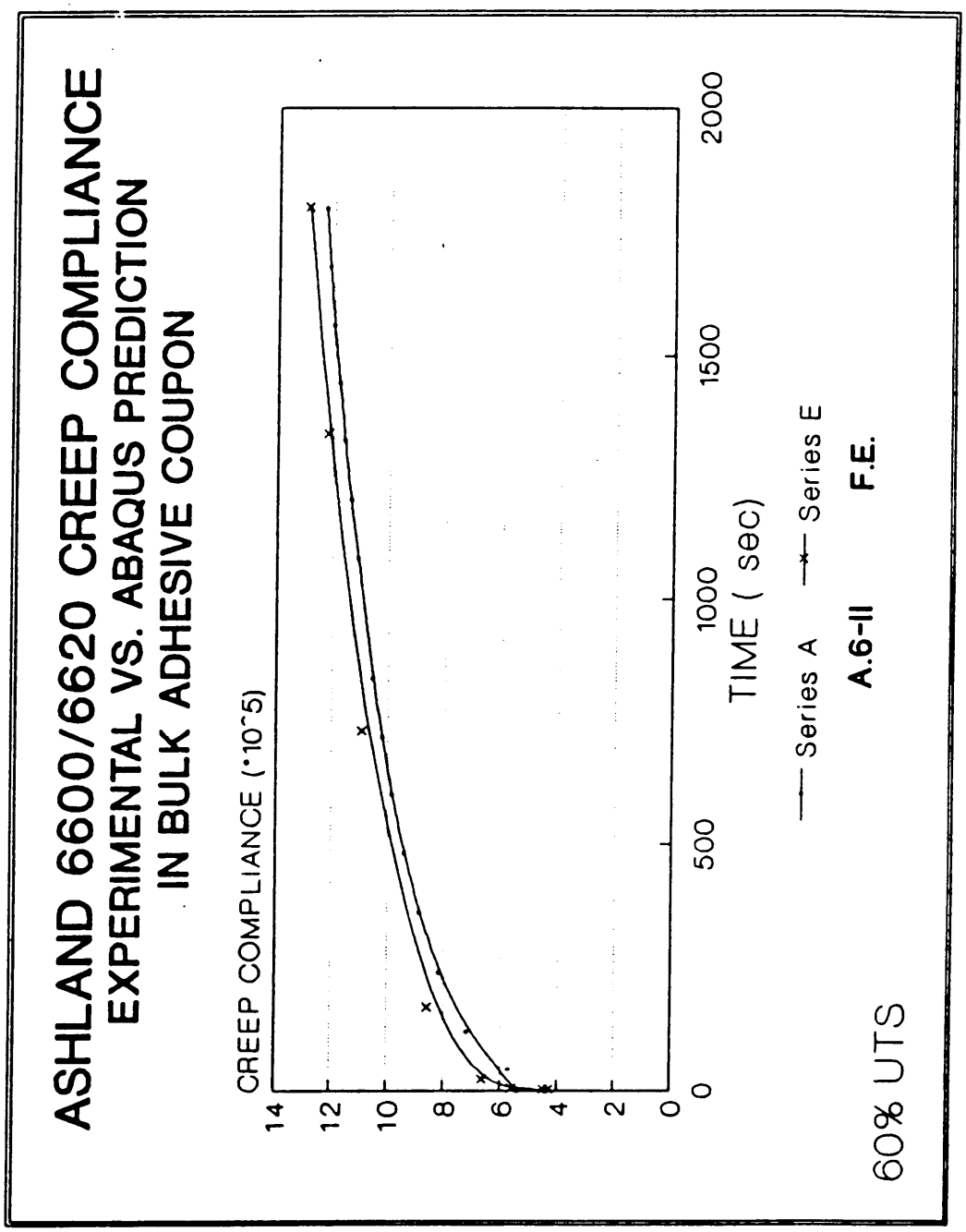

Figure 4.10: Creep Compliance in Bulk Adhesive Coupon, F.E. Versus Experimental Data, for Ashland Plyogrip 6600/6620.

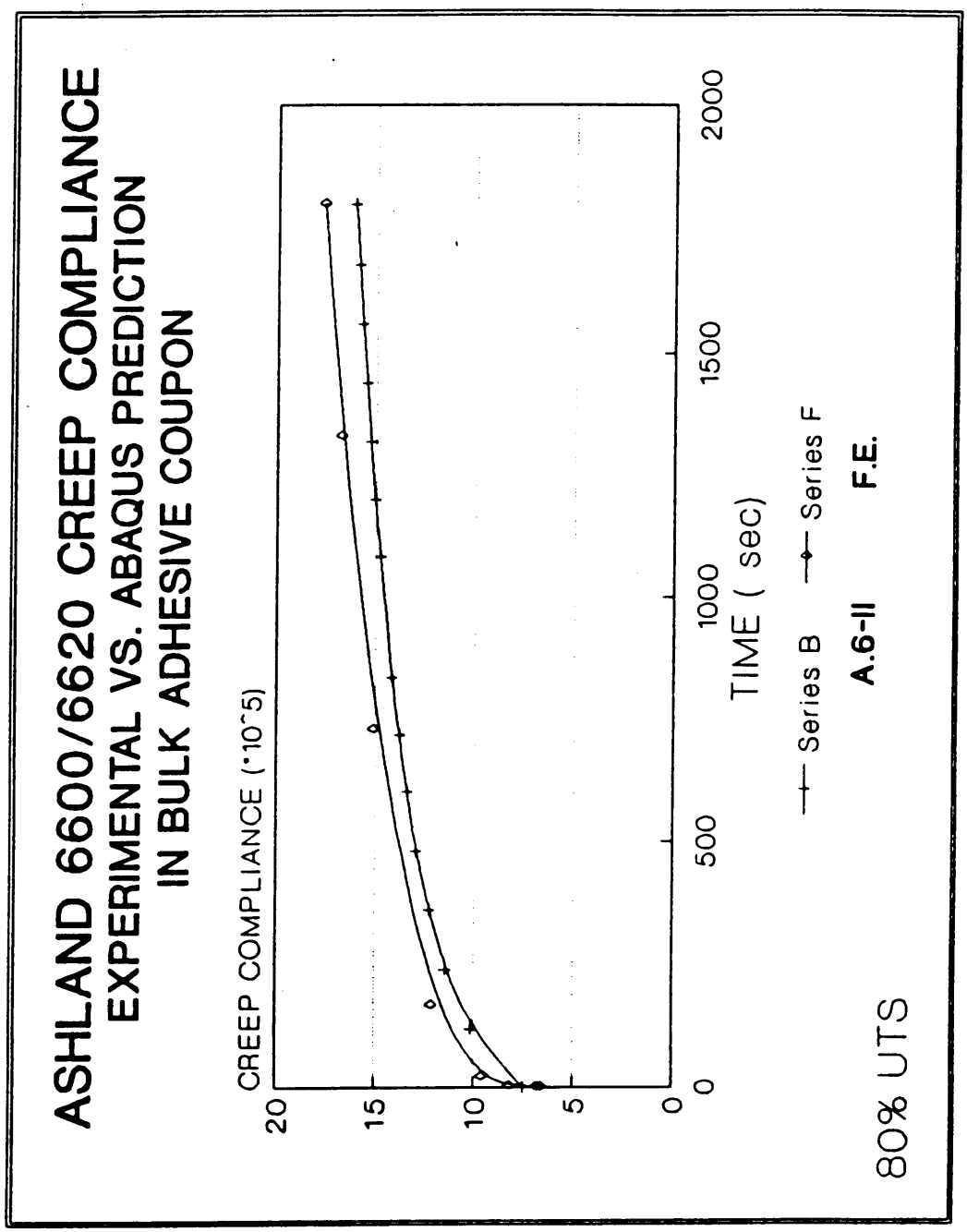

Figure 4.11: Creep Compliance in Bulk Adhesive Coupon, F.E. Versus Experimental Data, for Ashland Plyogrip 6600/6620.

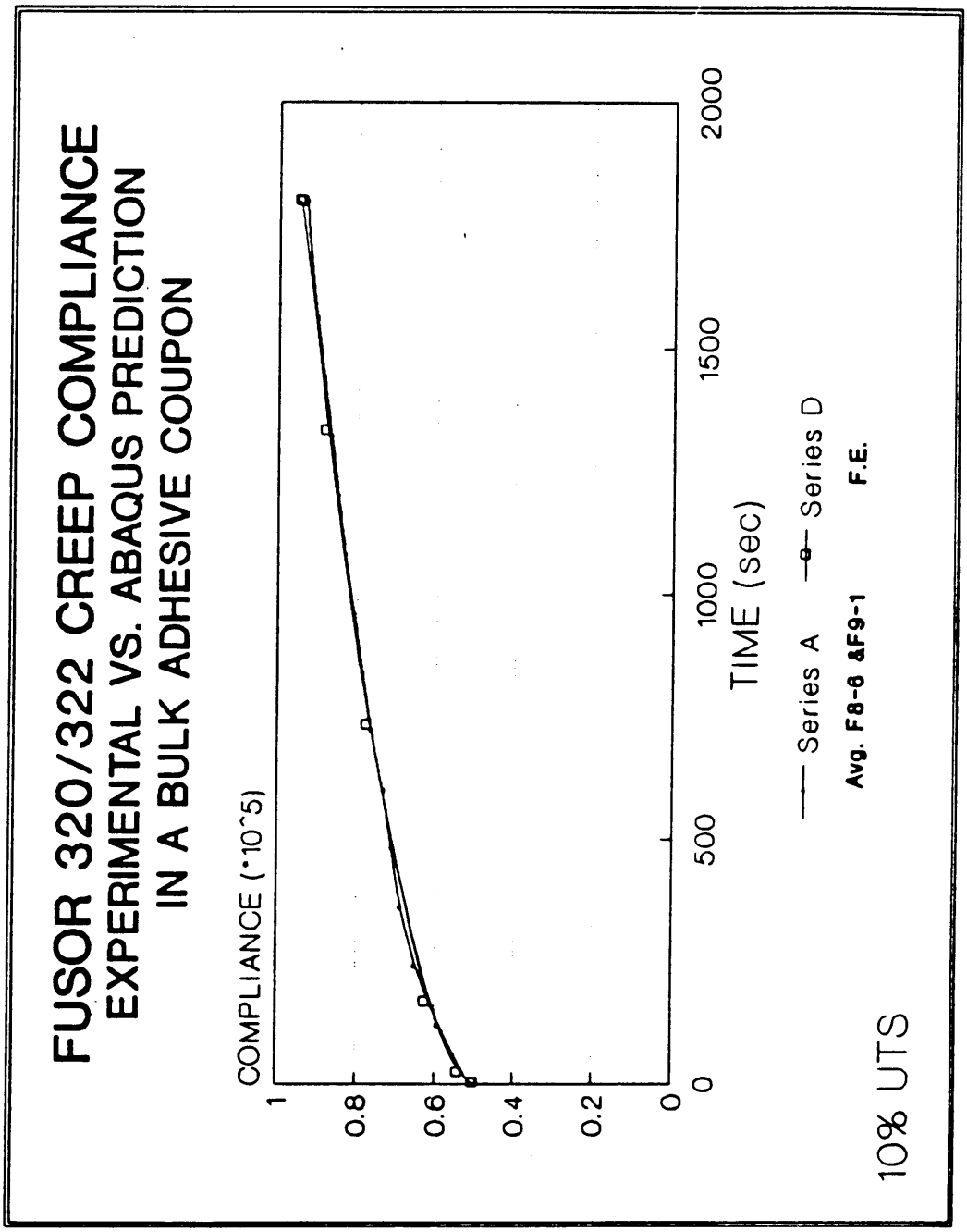

Figure 4.12: Creep Compliance in Bulk Adhesive Coupon, F.E. Versus Experimental Data, for Lord Fusor 320/322.

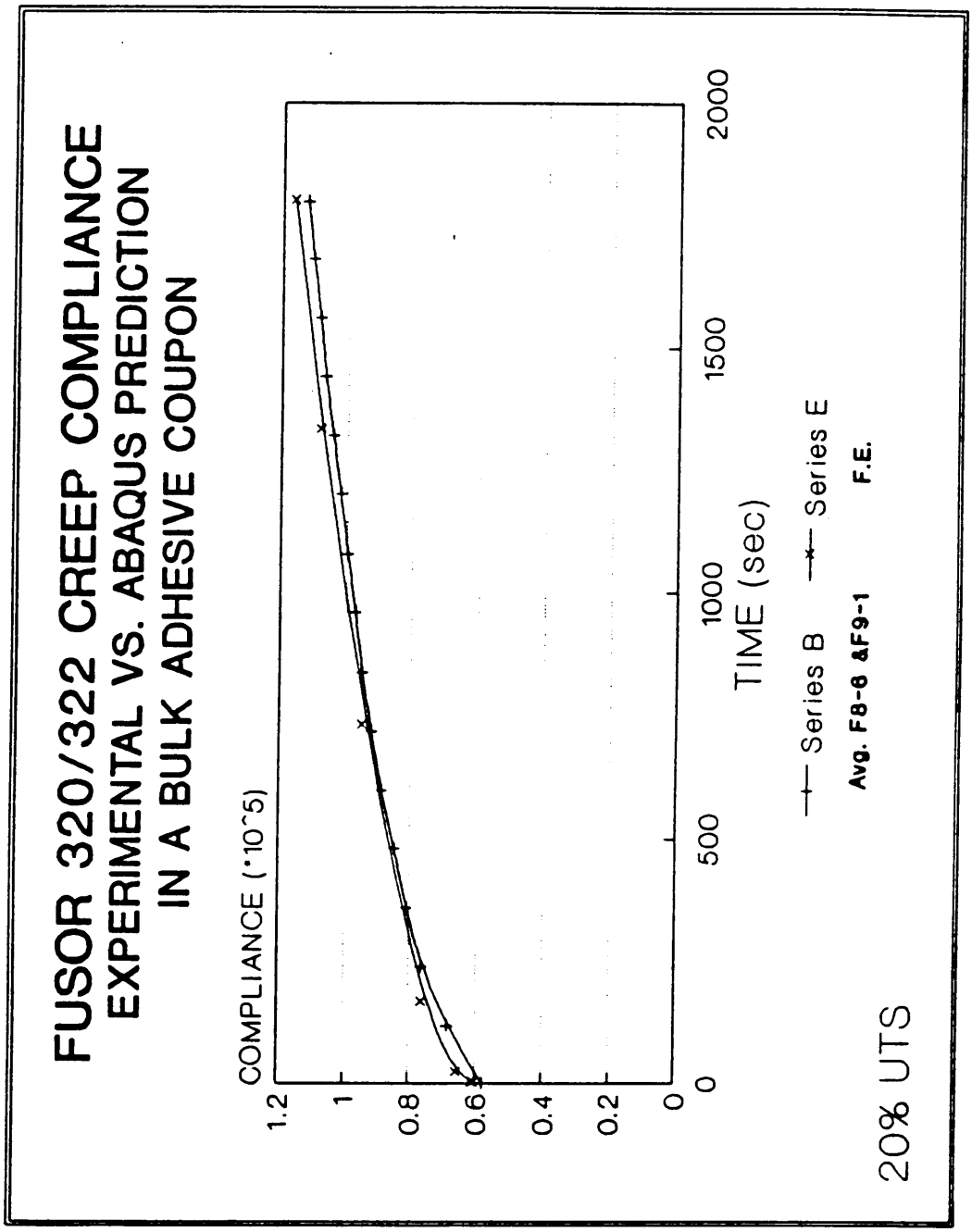

Figure 4.13: Creep Compliance in Bulk Adhesive Coupon, F.E. Versus Experimental Data, for Lord Fusor 320/322.

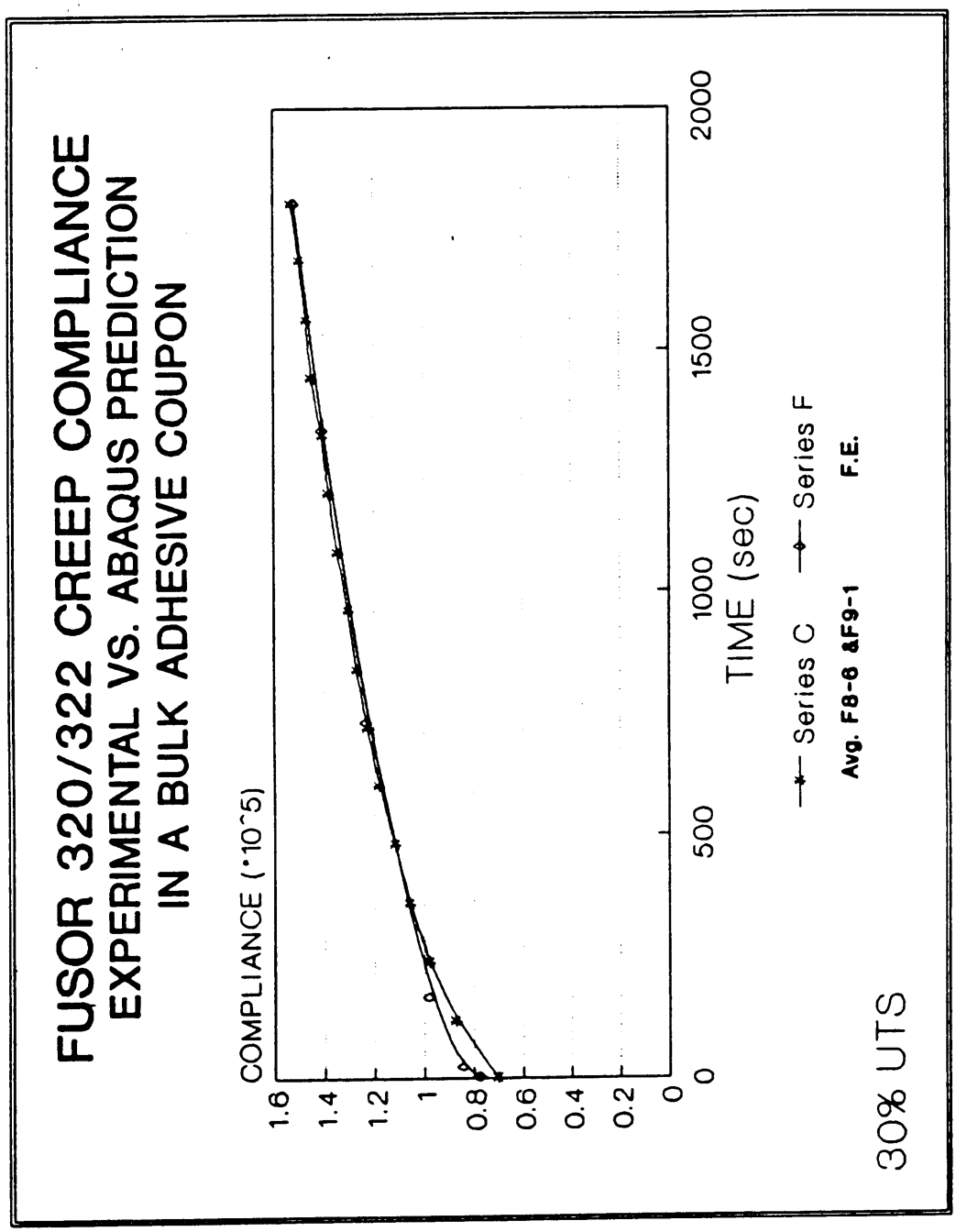

Figure 4.14: Creep Compliance in Bulk Adhesive Coupon, F.E. Versus Experimental Data, for Lord Fusor 320/322.

nodes to move only in the transverse direction (the 2 direction) and, fixing the left bottom corner node (the center point in the entire specimen).

The model was constructed of 28 four noded elements as shown in fig 4.5 . The creep subroutine was used to discribe the viscoelastic material response. The finite element prediction was compared to the measured creep compliance.

Figures 4.6 through 4.11 show the test results and the finite element predictions for Ashland Plyogrip 6600/6620 urethane adhesive. Figures 4.12 through 4.14 present the test results and the finite element predictions for Lord Fusor 320/322 epoxy adhesive at various stress levels. Good agreement was observed between the calculated and measured curves. The small differences between the curves, are mainly due to the errors introduced through the curve fitting of the test results.

4.3 ANALYSIS OF THE ADHESIVELY BONDED ARCAN TEST SPECIMEN

Having completed the two previous steps, the complete bonded joint was analyzed. The bulk viscoelastic response of the adhesives was assigned through creep subroutines, using the geometric model described in sections 4.1 and 4.2 of this chapter.

a) Ashland Plyogrip 6600/6620 urethane:

The results of the analysis using the material viscoelastic response

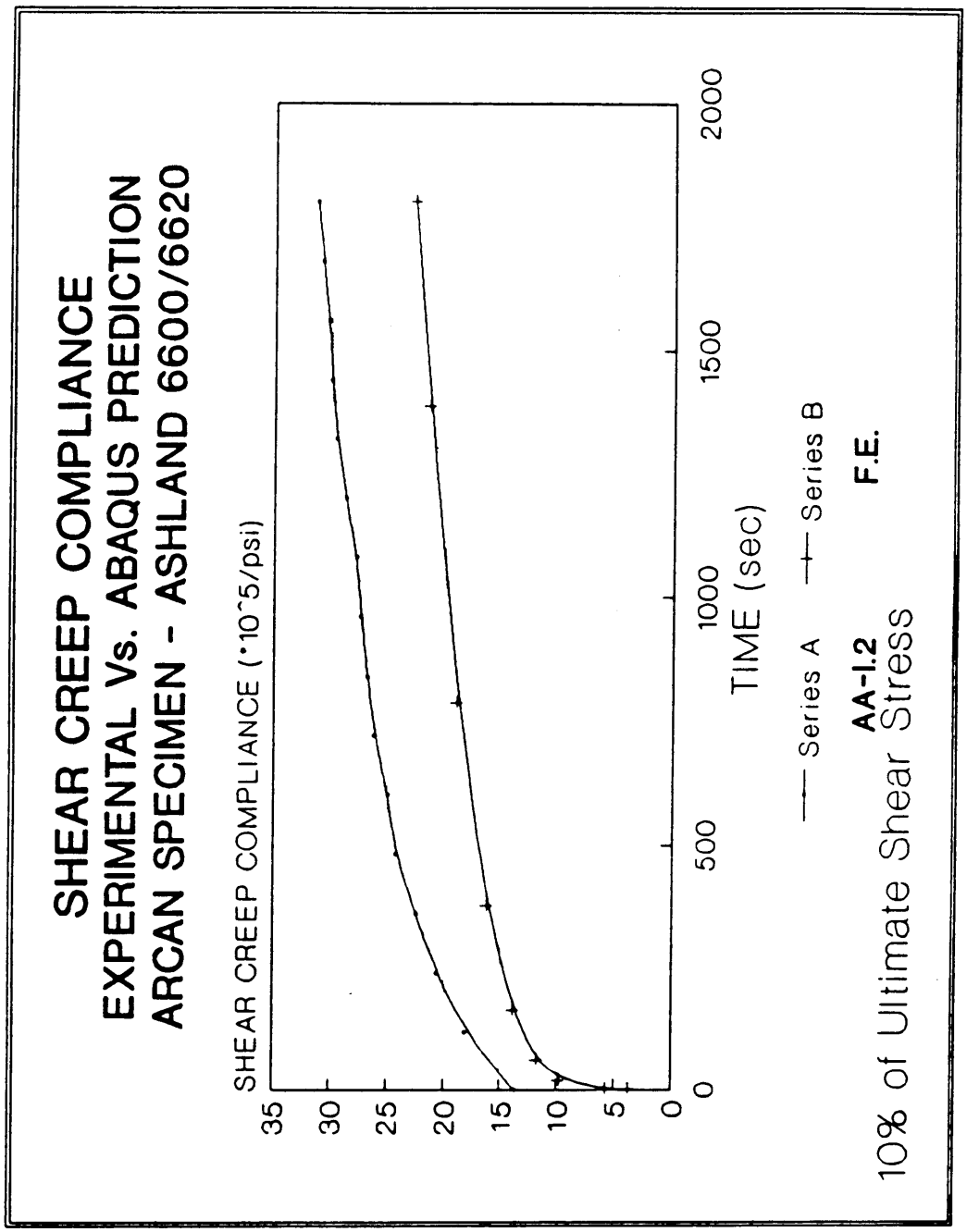

Figure 4.15: Shear Creep Compliance for Arcan Specimen, F.E. Versus Experimental Data, for Ashland Plyogrip 6600/6620.

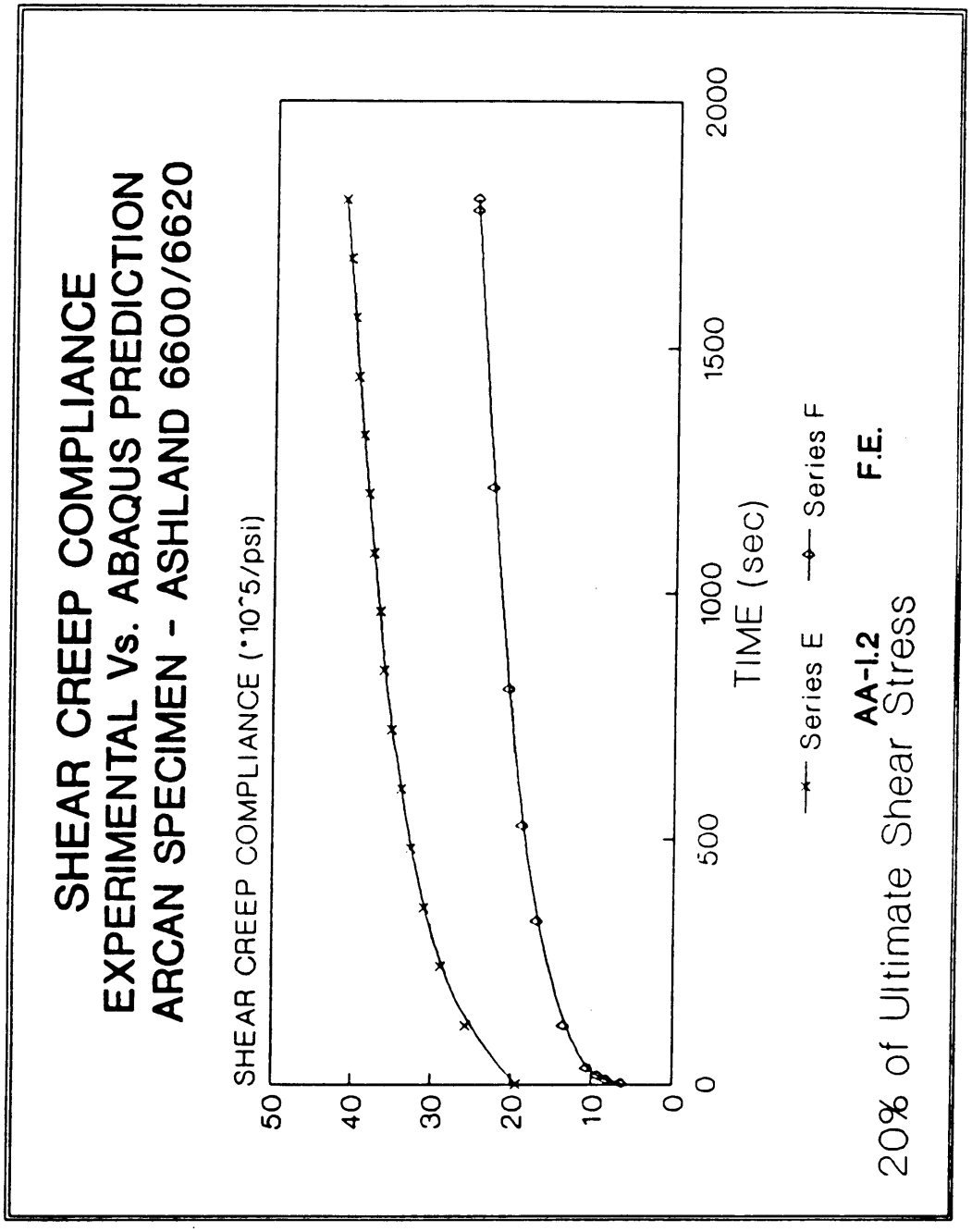

Figure 4.16: Shear Creep Compliance in Arcan Specimen, F.E. Versus Experimental Data, for Ashland Plyogrip 6600/6620.

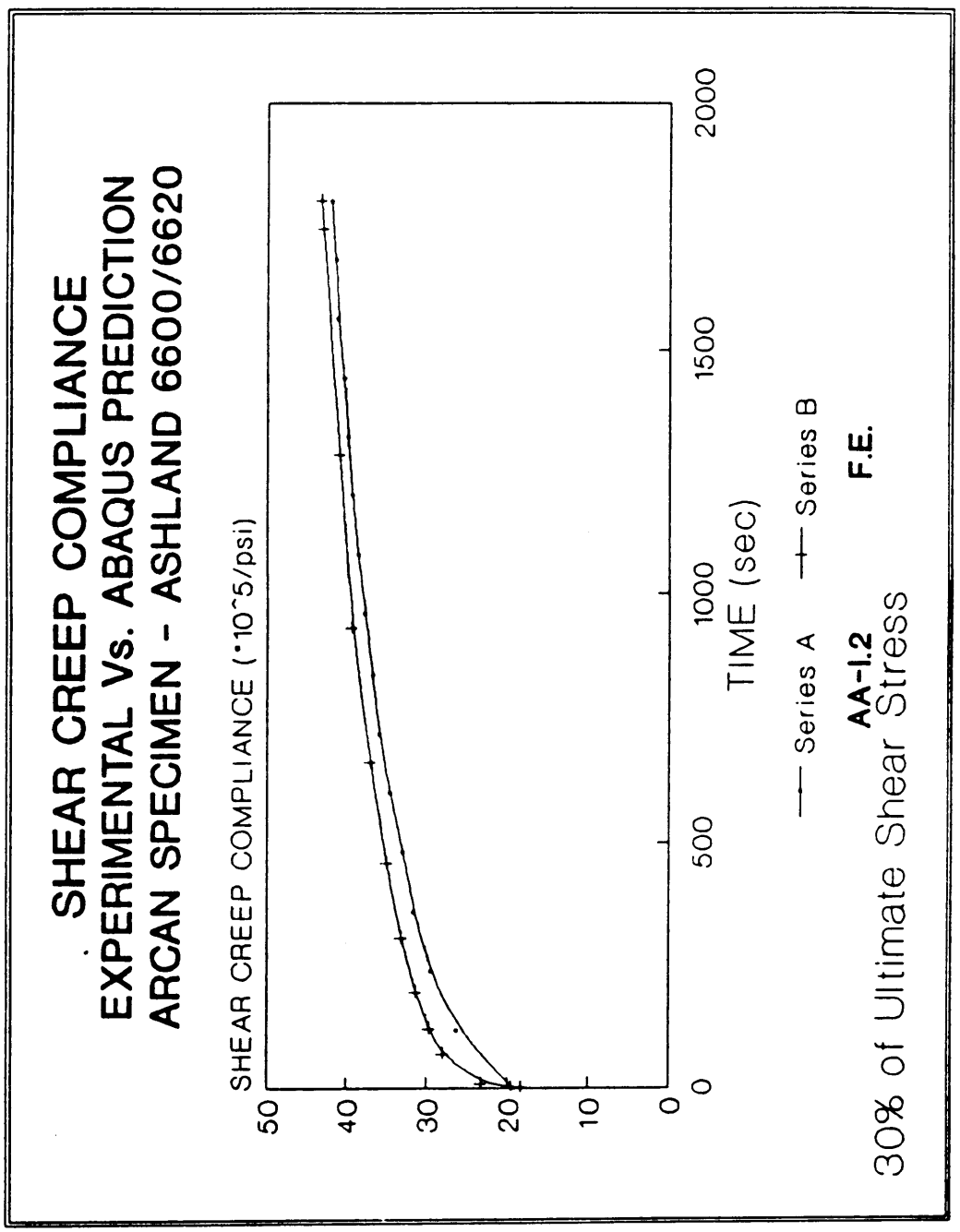

Figure 4.17: Shear Creep Compliance in Arcan Specimen, F.E. Versus Experimental Data, for Ashland Plyogrip 6600/6620.

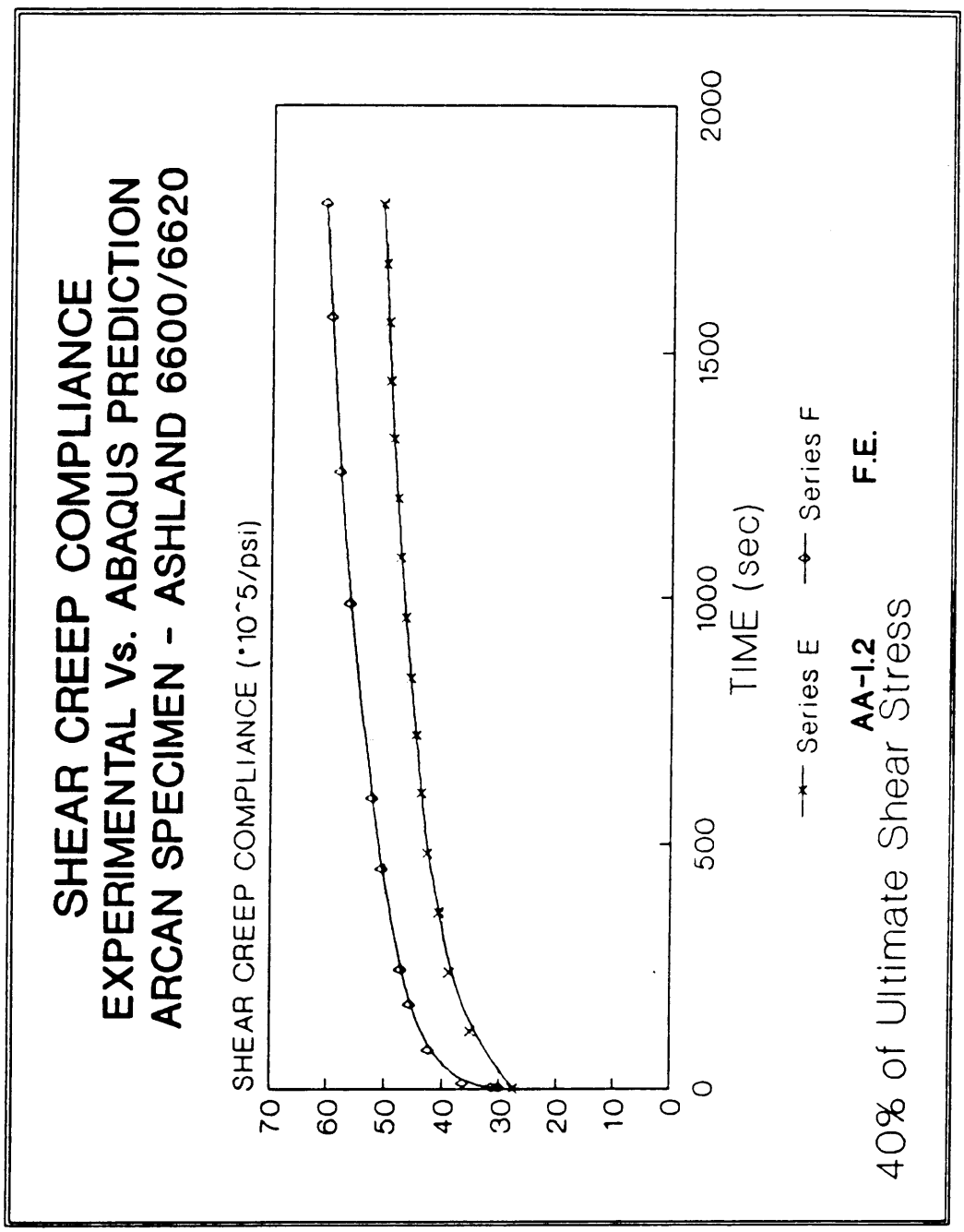

Figure 4.18: Shear Creep Compliance in Arcan Specimen, F.E. Versus Experimental Data, for Ashland Plyogrip 6600/6620.

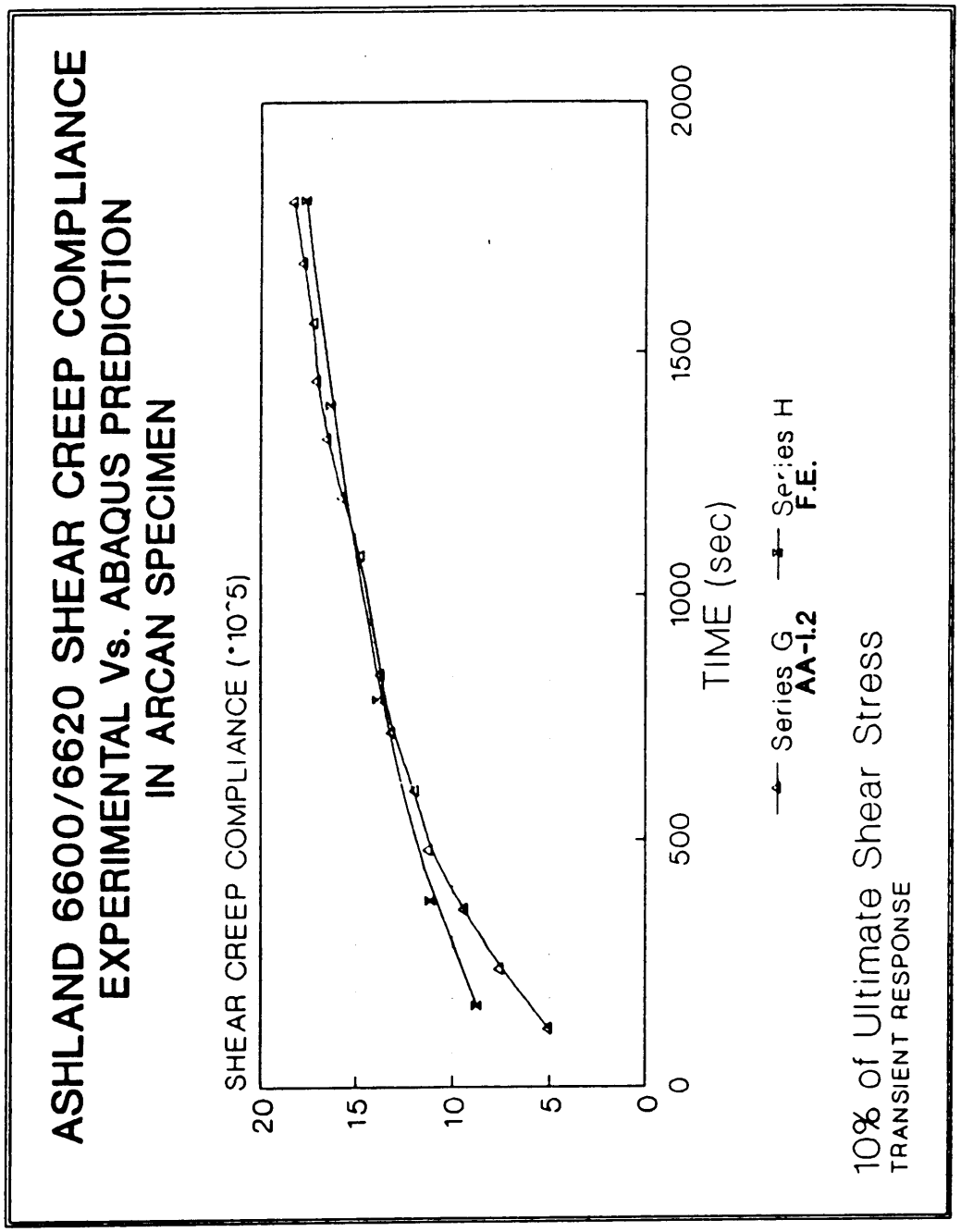

Figure 4.19: Transient Response in Arcan Specimen, F.E. Versus Experimental Data, for Ashland Plyogrip 6600/6620.

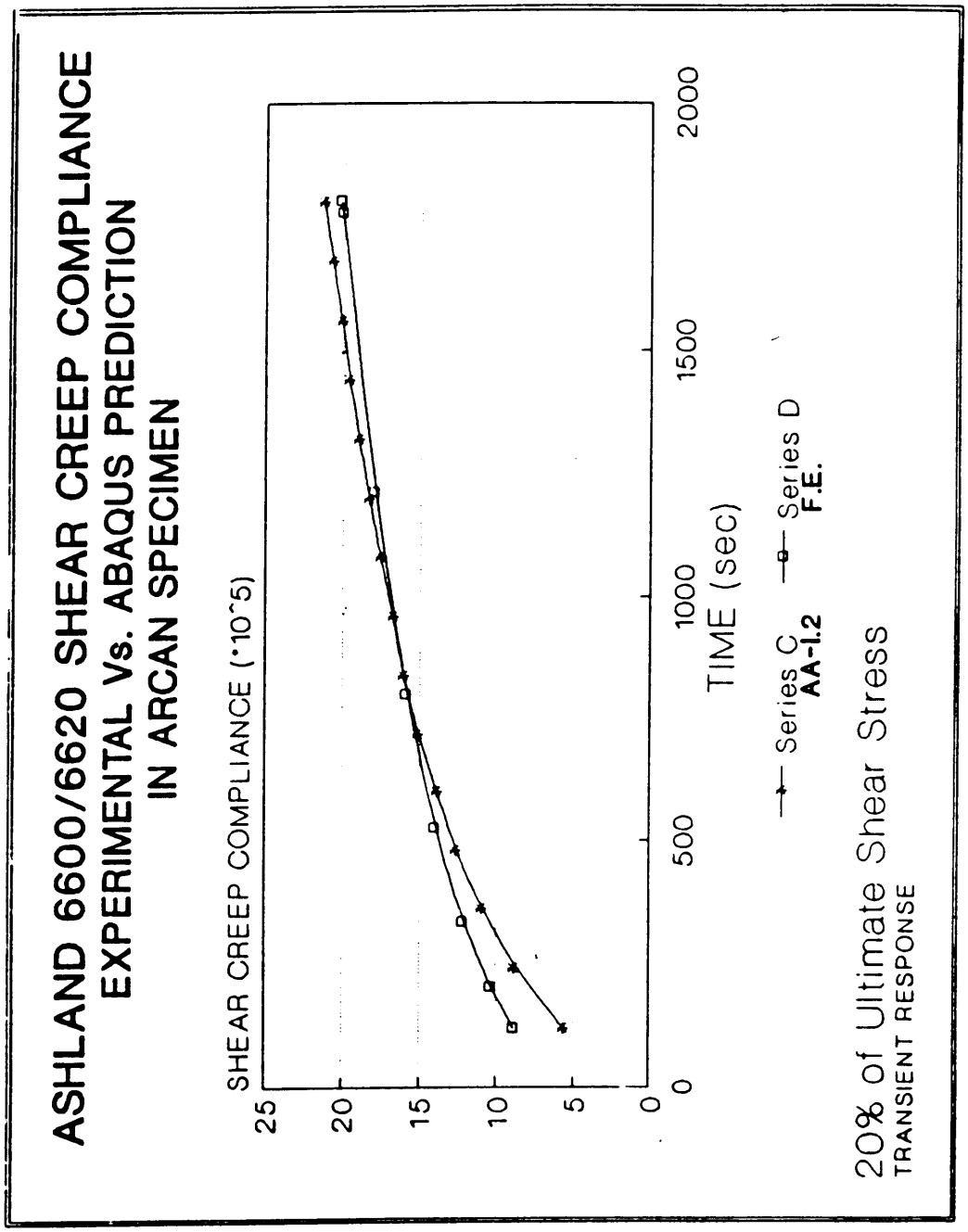

Figure 4.20: Transient Response in Arcan Specimen, F.E. Versus Experimental Data, for Ashland Plyogrip 6600/6620.

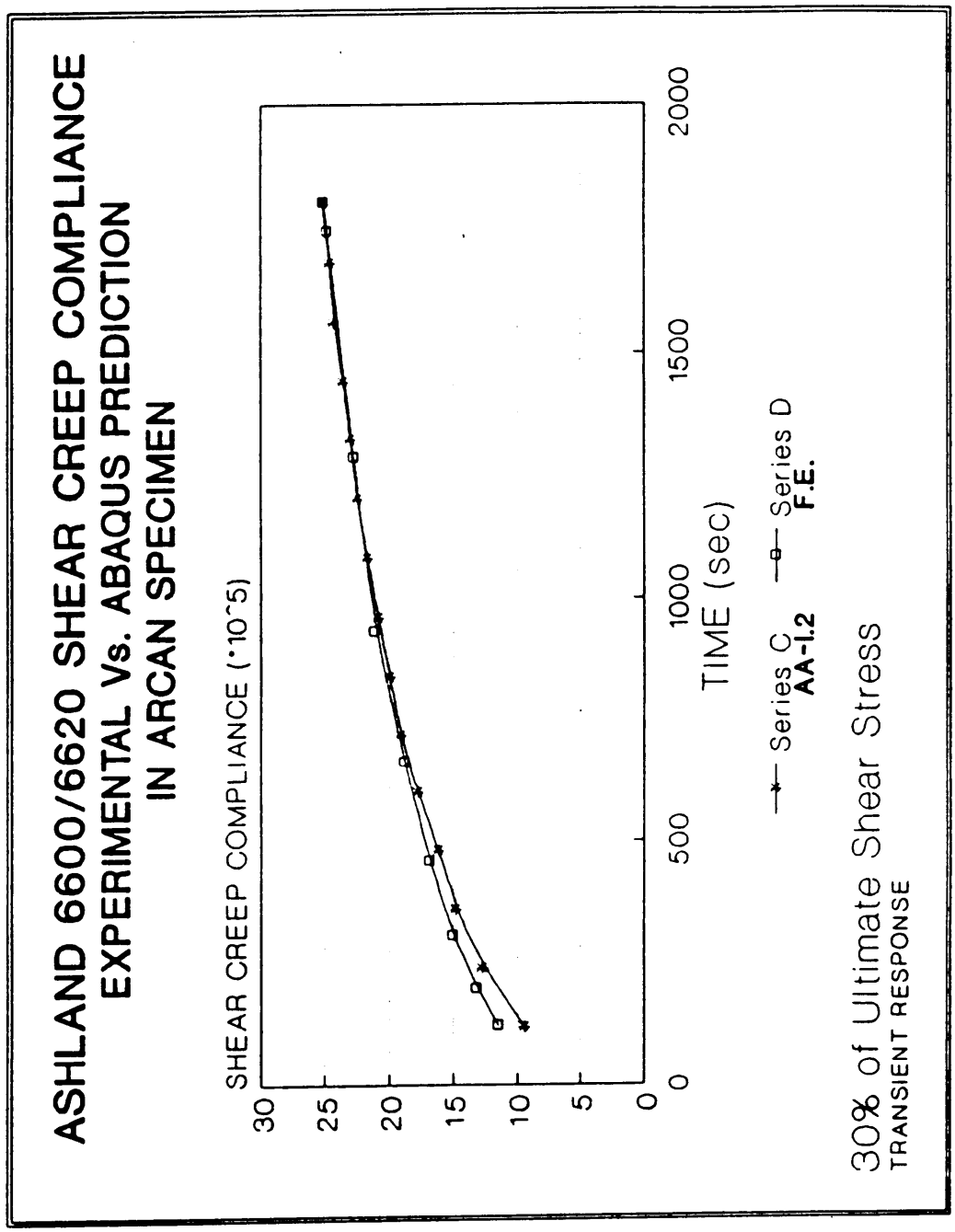

Figure 4.21: Transient Response in Arcan Specimen, F.E. Versus Experimental Data, for Ashland Plyogrip 6600/6620.

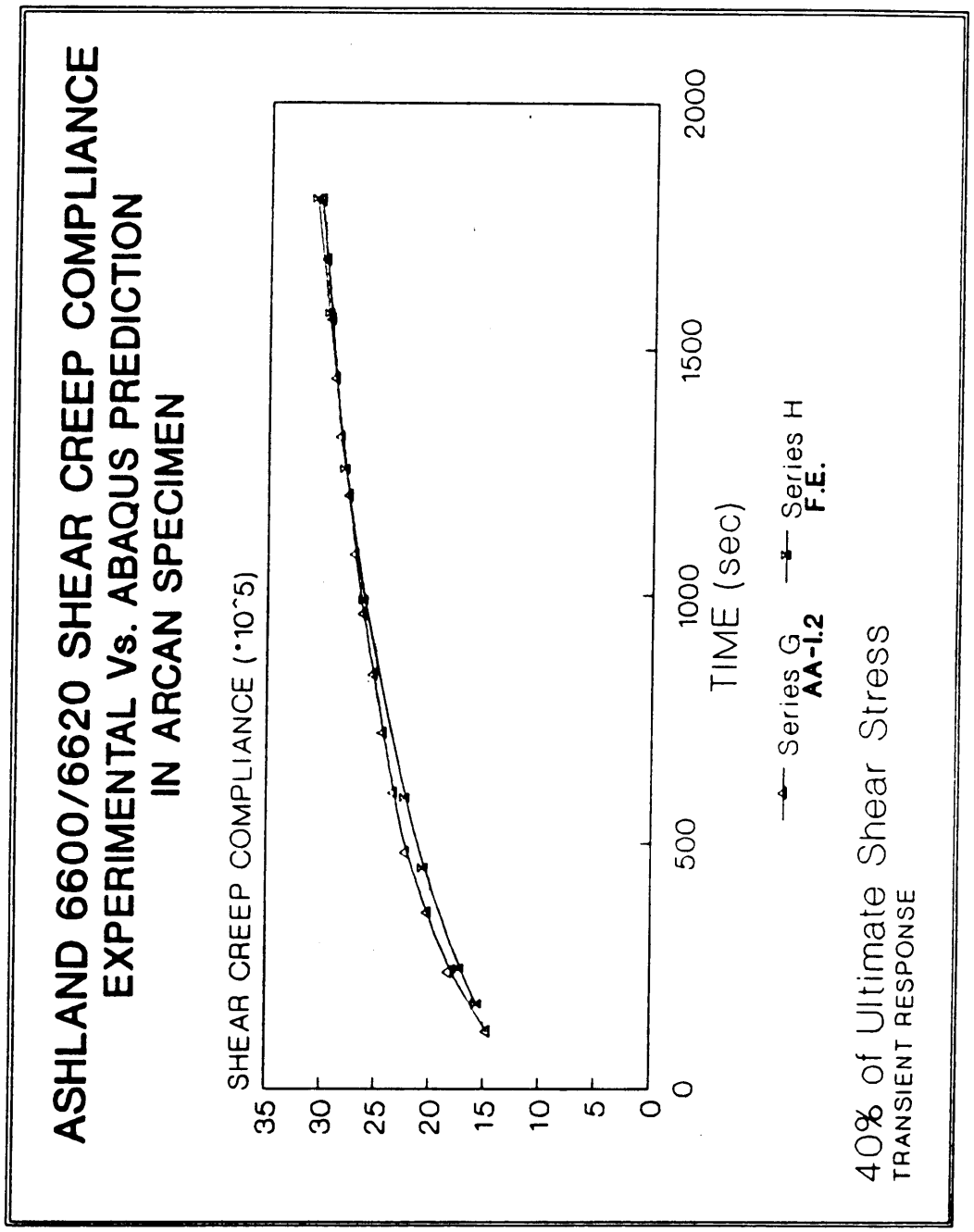

Figure 4.22: Transient Response in Arcan Specimen, F.E. Versus Experimental Data, for Ashland Plyogrip 6600/6620.

of this adhesive are presented in figures 4.15 through 4.18 . For the case where the applied shear stress is 30% of the ultimate shear stress, good agreement is observed between the measured and the Finite Element calculated shear creep compliance. For the other cases, 10% 20% and 40%, of the ultimate shear stress, the curves for the predicted shear creep compliance deviate from the curves for the experimental shear creep compliance. It is possible that the post curing in the bonded Arcan joint locks in much more free volume than in a bulk coupon. This may result in experimental values for the shear creep compliance that are greater than the values predicted by the finite element analysis.

A closer study of the results indicates that the transient deformation of each of the pairs presented are in good agreement. In figures 4.19 through 4.22 only the transient response is plotted at each stress level. These plots confirm that indeed the finite element prediction of the transient response is similar to the measured response. Using the curve fitting program written by Gramoll [6], the value of n, the exponent in creep compliance power law fit, for the creep comliance curves of the Arcan joint was obtained. This value of n, was found to be the same as the value obtained for the bulk adhesive.

b) Lord Fusor 320/322 :

Figures 4.23 through 4.27 show the shear creep compliance obtained by

testing Arcan joint bonded with Fusor 320/322 and the shear creep compliance obtained from the finite element analysis. There is not a good agreement between the two sets of results. Furthermore the transient response of the calculated and the measured curves do not exhibit the same behaviour. The curves corresponding to the finite element predictions have a steeper slope than the curve corresponding to the actual test results. When comparing the values of n, the exponent in creep compliance power law, it was found that n has different values for the bulk adhesive and the Arcan bonded joint.

The value of n was determined by curve fitting the experimental data to a power law. In the case of the bulk Lord Fusor 320/322, creep compliance curves were obtained only for three low stress levels. Thus the value of n obtained from this data may not be accurate. This may be the reason for the deviation of the values of n obtained for the Arcan specimens and those of the bulk adhesive coupons.

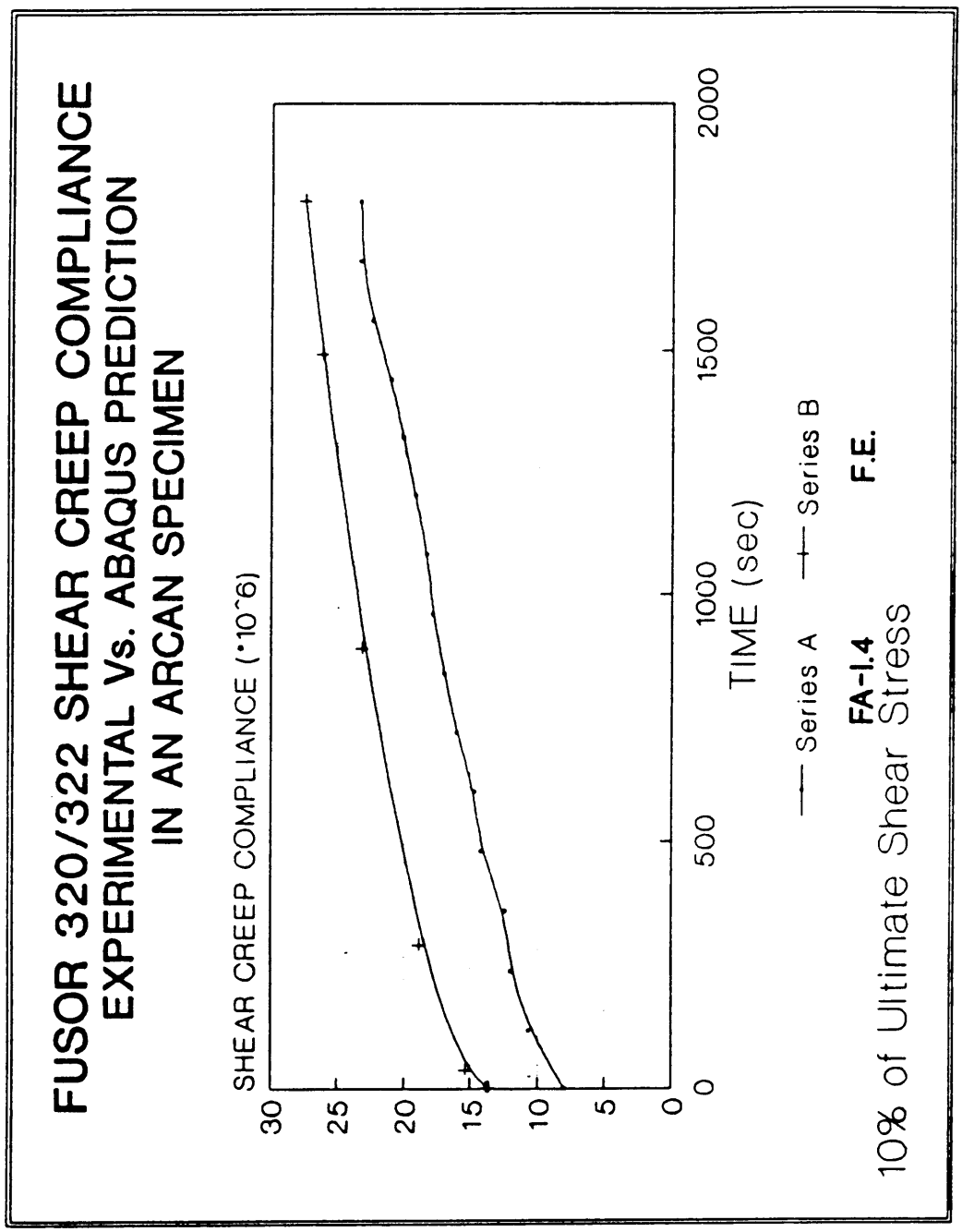

Figure 4.23: Shear Creep Compliance in Arcan Specimen, F.E. Versus Experimental Data, for Lord Fusor 320/322.

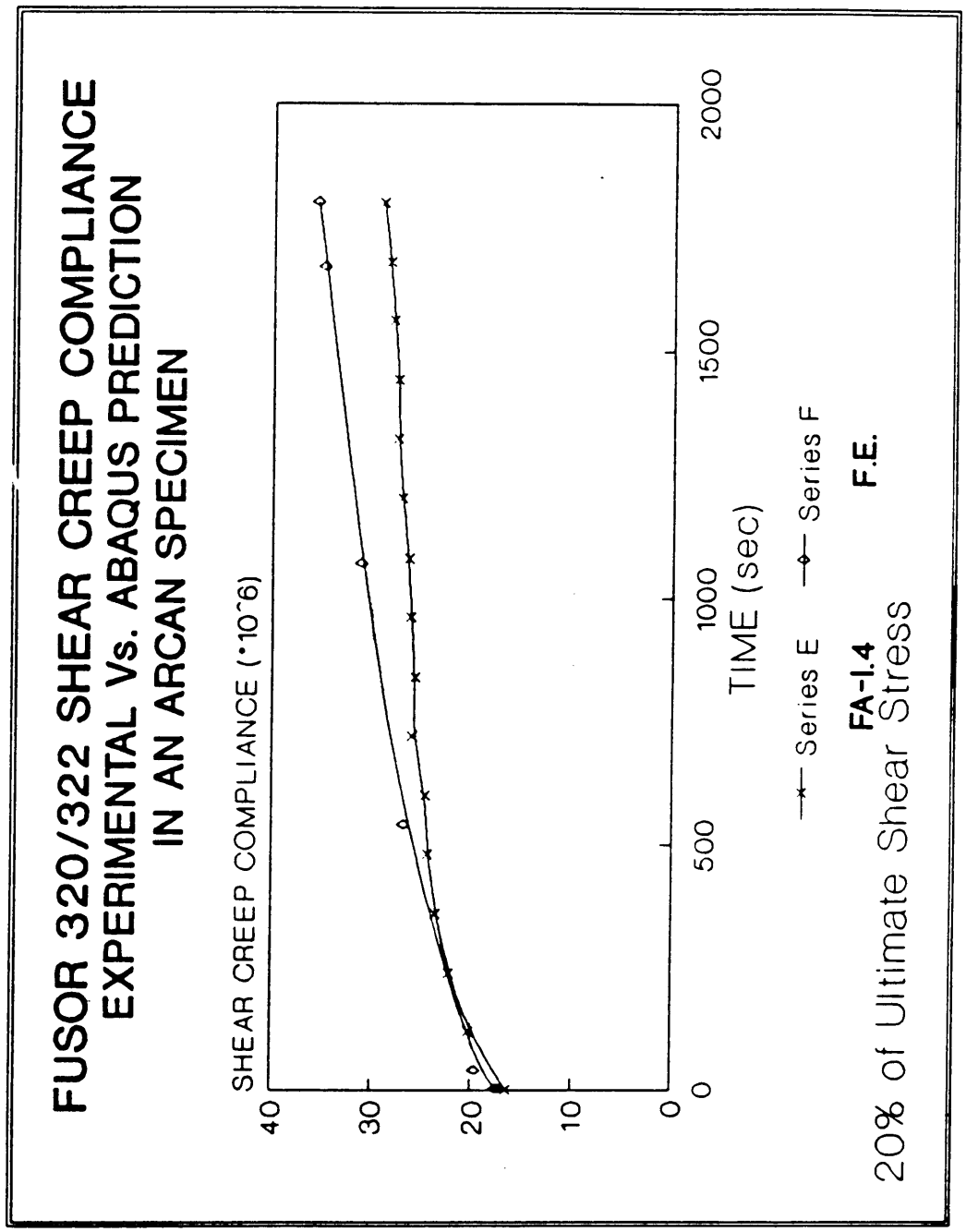

Figure 4.24: Shear Creep Compliance in Arcan Specimen, F.E. Versus Experimental Data, for Lord Fusor 320/322.

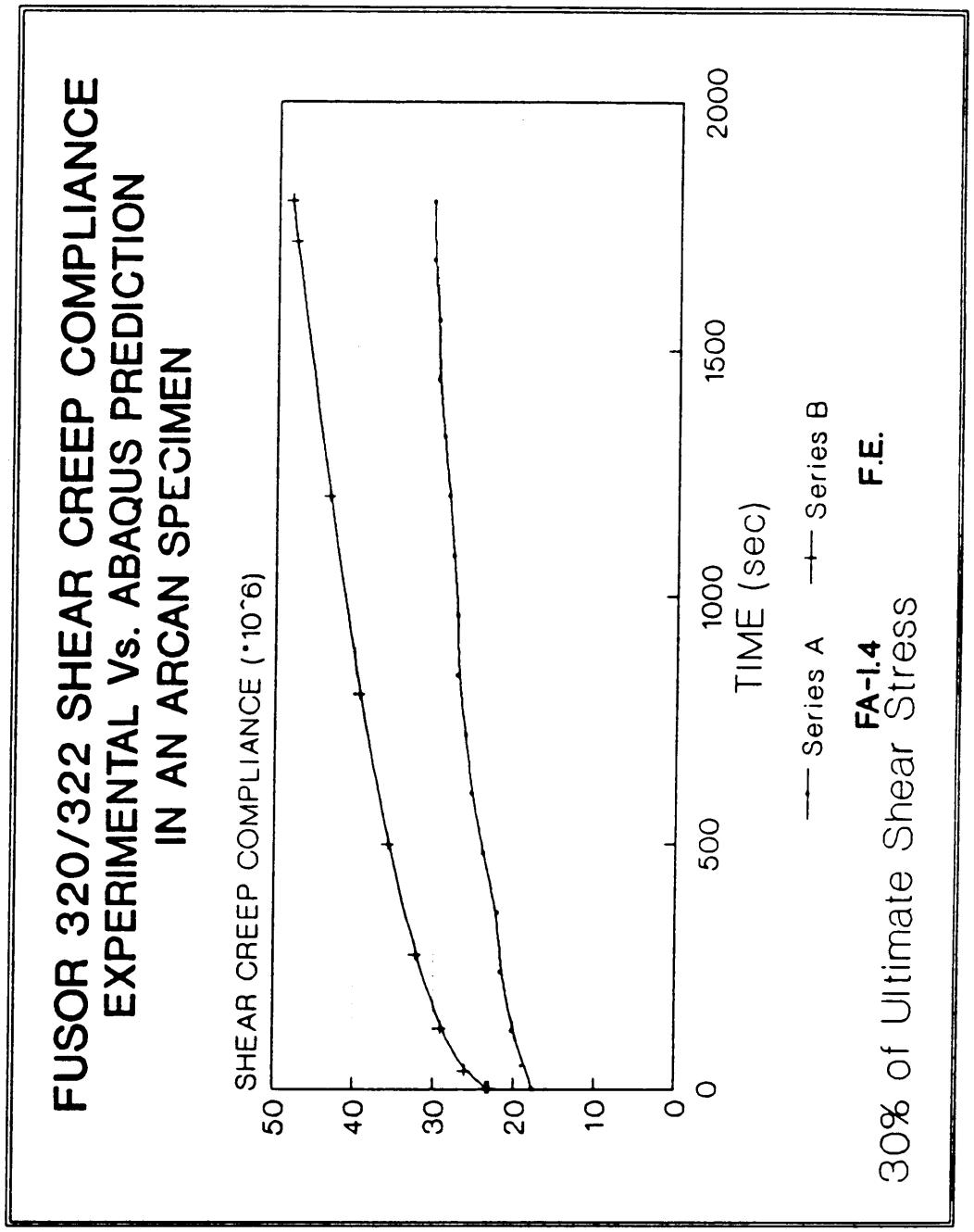

Figure 4.25: Shear Creep Compliance in Arcan Specimen, F.E. Versus Experimental Data, for Lord Fusor 320/322.

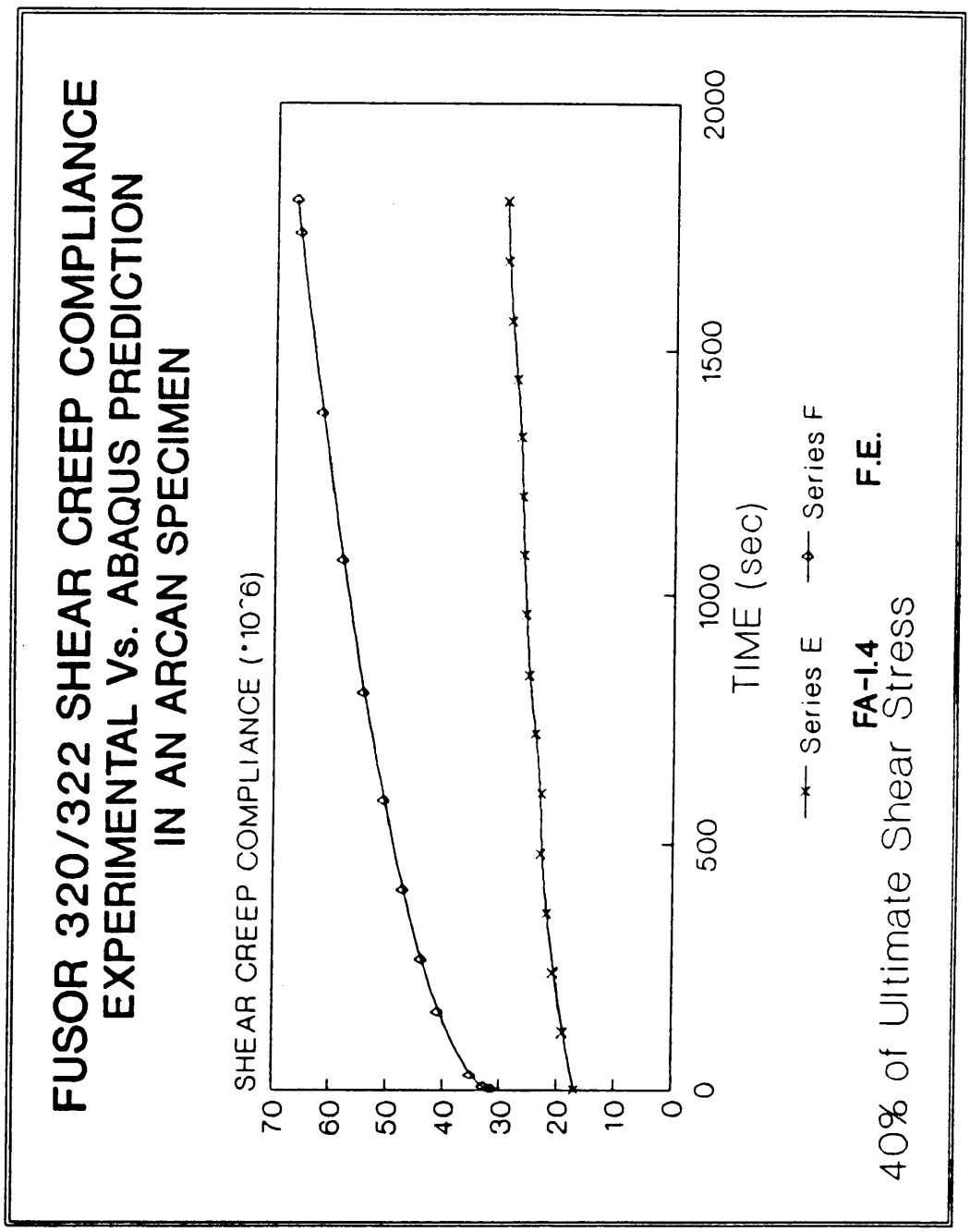

Figure 4.26: Shear Creep Compliance in Arcan Specimen, F.E. Versus Experimental Data, for Lord Fusor 320/322.

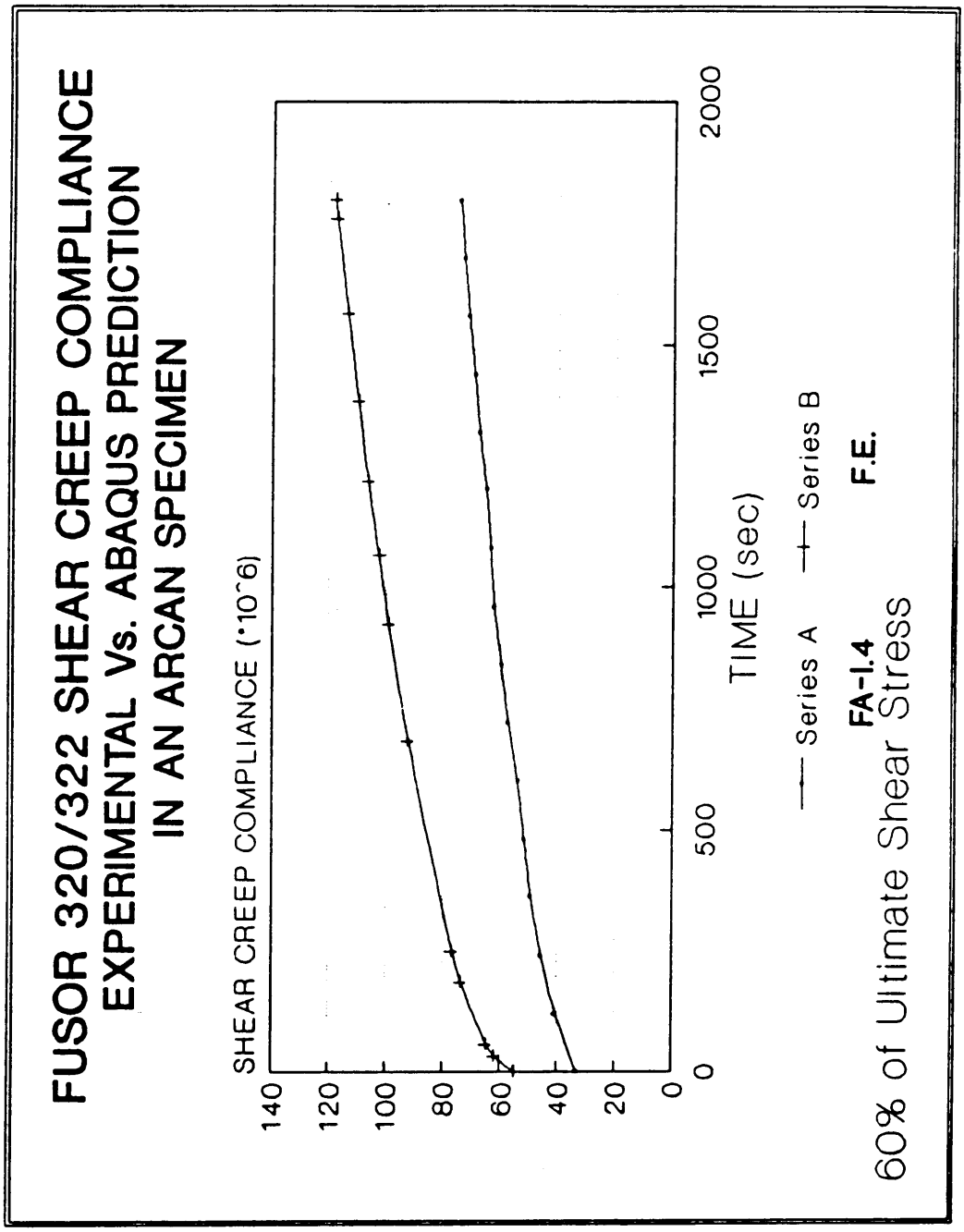

Figure 4.27: Shear Creep Compliance in Arcan Specimen, F.E. Versus Experimental Data, for Lord Fusor 320/322.

Chapter 5

SUMMARY, DISCUSSION AND CONCLUSIONS

5.1 Summary of Results

In this study, the nonlinear viscoelastic creep compliance characteristics of bulk adhesive specimens were obtained from a series of tensile creep tests conducted on cast adhesive coupons. The time dependent behavior was then incorporated in a finite element analysis of adhesively bonded joints, in order to predict the deformational behaviour. The final step was to compare the finite element predictions with test results.

5.1.1 Bulk Material Testing

Bulk adhesive coupons were cast using a procedure which involved bag mixing and degasing with the aid of a centrifuge. The specimens were not completely free of voids. These imperfections affect the tensile creep behavior due to the plasticizing effect of the voids and

the alteration of the failure mode, from cohesive rupture to void propagation. Due to the repeating occurance of such voids in specimens of the Lord Fusor 320/322 epoxy adhesive (very high mixed viscosity and short pot life), data could be collected only at three low stress levels; 10, 20 and 30 percent of the Ultimate Tensile Strength.

When testing at low stress levels, especially with compliant adhesives such as the Ashland Plyogrip 6600/6620 urethane, it was necessary to place a dummy extensometer on the specimen to counterbalance the active extensometer.

Displacements for the various stress levels were recorded over a period of 1800 seconds at each load. The loads were applied using the manual option of the M.T.S tensile testing machine. The adjusted reference time was assumed to be approximately five times the ramping time.

Transient strain curves were measured and creep compliance was calculated for each individual test. In order to obtain consistent creep test results, a mechanical conditioning procedure was employed. The use of such a procedure enabled us to obtain repeatable results.

Ashland Plyogrip 6600/6620 urethane adhesive, exhibits linear viscoelastic behaviour when tested at stresses up to 20% of the ultimate tensile stress. At higher stress levels nonlinear viscoelastic behaviour was observed. The viscoelastic creep compliance was fitted with a quadratic power law. The following relationship was

obtained,

$$D(\sigma,t) = (1 + g\sigma^2)\ 6.817E\text{-}6 + (1 + f\sigma^2)\ 6.08E\text{-}6\ t^{0.29343} \left[\frac{in^2}{lb}\right] \quad (3.4)$$

where,

$$g = 1.0663E\text{-}5 \left[\frac{in^4}{lb^2}\right]$$

$$f = 1.6134E\text{-}6 \left[\frac{in^4}{lb^2}\right]$$

Although a number of Lord Fusor 320/322 epoxy adhesive specimens have been tested, and an effort was made to detect imperfections; the specimens failed at the site of air bubbles when testing at 40% of the ultimate tensile stress.

The creep compliance and the isochronous stress - strain curves indicate nonlinear behaviour beginning at the lowest stress level tested (10% of the UTS). Based on the results at 10, 20 and 30% of UTS (average of two specimens), the following relationship was obtained,

$$D(\sigma,t) = (1+ g\sigma^2)\ 4.559E\text{-}6 + (1+ f\sigma^2)\ 7.317E\text{-}6\ t^{0.53743} \left[\frac{in^2}{lb}\right] \quad (3.5)$$

where,

$$g = 6.327E\text{-}7 \left[\frac{in^4}{lb^2}\right]$$

$$f = 7.669E\text{-}7 \left[\frac{in^4}{lb^2}\right]$$

5.1.2 Arcan Specimen

The test procedure used for bulk adhesive specimens was repeated using bonded Arcan joints. As for the coupons, the specimens were mechanically conditioned. However, observing the results of the conditioning cycles, it appears that the curves repeat themselves, and mechanical conditioning is probably not necessary to obtain consistent results.

The joint bonded with Ashland Plyogrip 6600/6620 urethane was tested at 10%, 20%, 30% and 40% of the ultimate shear stress. At 60% the specimens failed at the site of small air bubbles in the adhesive. The creep compliance curves corresponding to 20% and 30% of the ultimate shear stress agree perfectly, which indicates linear viscoelastic behaviour up to 30%. The creep compliance curve corresponding to 10% of the Ultimate Shear Stress is a little lower, probably due to experimental errors.

For the Arcan joints bonded with Lord Fusor 320/322 epoxy adhesive, loads up to 60% of the ultimate shear stress were applied before rapid failure occurred. The adhesive in the joint behaved in a linear viscoelastic manner at stress levels up to 40% of the ultimate shear stress. Beyond 40% of the ultimate shear stress nonlinear behavior was measured.

As observed in the joint bonded with Ashland 6600/6620 urethane, the shear creep compliance curve at 10% of the ultimate shear strength is lower than the curves at 20%, 30% and 40%. This repeated occurrence reinforces the assumption that experimental error is relatively large for tests conducted at low loads and it does not reflect true material behavior.

5.1.3 Finite Element Analysis

The geometry of the Arcan test joint was modeled. In order to simplify the model the presence of the load frame was neglected. The validity of the geometrical model was confirmed in two ways :

(i) by comparing the finite element results with those obtained in a test of a steel specimen.

(ii) by analyzing an aluminum joint bonded with AF 163-2U epoxy adhesive. The results obtained with the ABAQUS finite element code were compared to the analysis of the same joint peformed with the VISTA finite element code by Cooper [10].

In both cases good agreement between the two sets of results was observed.

The material viscoelastic characteristics, as obtained from creep experiments conducted on bulk materials, were introduced into the ABAQUS finite element code through "creep" subroutines. Time dependent behavior is expressed in the form of creep rate functions.

The above subroutines are constructed in such a way that the initial instantaneous response does not appear explicitly. This initial response is evaluated using the Young's Modulus for the initial elastic response.

The finite element analysis is set up in two stages. First the specimen is elastically loaded for one second. Then, the viscoelastic analysis is performed. Deformations were predicted for a period of 1800 seconds.

In order to confirm the validity of the creep subroutine, the ABAQUS F.E. code was used to model the bulk adhesive coupon. The F.E. prediction was compared to the measured creep compliance. Good agreement was observed between the calculated and the measured curves. The small differences between the curves arise mainly due to the errors introduced through the curve fitting procedure of the test results. The coefficient of variation for each of the steps of the curve fitting procedure, is indicated in tables 3.1 through 3.4.

The complete bonded joint was analyzed by combining the previous steps. The bulk viscoelastic reponse of the adhesives were assigned through creep subroutines, using the relationships described in section 4.1.

i) When comparing the results of the F.E. prediction with those obtained experimentally for Ashland 6600/6620 urethane, it is eveident that the F.E. prediction for 10%, 20% and 40% of the Ultimate Shear

Stress deviate slightly from the experimental values. The prediction at 30% of the Ultimate Shear Stress is in good agreement with the measured values. However, the F.E. prediction of the transient response at each stress level is in excellent agreement with the measured transient response. The value of the exponent n, in the creep compliance power law fit, has the same value for the bulk adhesive and the Arcan joint.

ii) The results obtained in the analysis of a joint bonded with Lord Fusor 320/322 epoxy, are not in good agreement with the corresponding test results. Furthermore, the transient response of the calculated and measured curves do not exhibit similar behaviour. The slope of the curves predicted by the finite element analysis are steeper than the slope of the curves obtained from test results.

5.2 Sources of experimental error and recommendations

Creep compliance tests are susceptible to experimental error arising from various sources. In general terms, the errors fall into the following categories;

1. Material variations, inhomogeneities and imperfections.
2. Measuring devices and their calibration.
3. Variations in testing conditions within an individual test or group of tests.
4. Data interpretation.
5. Analytical tools.

A brief discussion of such effects and suitable recommendations follow in the next few paragraphs.

Material variations and inhomogeneities due to the mixing and casting process are certain to be present. Although the process was carefully repeated in each instance, the high viscosity of the components and short pot life of the mixed adhesive hamper the possilbilities to control the quality of the specimens. The short gelling time does not allow for a complete elimination of voids, especially in the Arcan joints. It has been found that voids greatly influence the time dependent behavior, alter the geometry, and disrupt the test, causing premature failure.

In future studies it is recommended that:

1. Adhesive with the lowest possible viscosity be used.
2. A longer pot life adhesive should be used.
3. Mix and degas at low temperature for a prolonged period of time.
4. Cast and place the mold in vacuum to extract entrapped air bubbles.
5. Analyze cured material. Determine crosslink density T_g and/or other parameters that may help characterize the state of the material.
6. Use nondestructive techniques to detect flaws in bonded joints and castings. Techniques that involve immersion of the specimen in water should not be used to avoid moisture uptake in the specimen.

It is assumed that the M.T.S. load cell is properly calibrated and

detailed calibration of the extensometers was performed. Even so, at small strains and loads, the noise introduced by the pertinent channel amplifiers is significant when compared to the signal itself. Nonconstant load and noisy strain measurements accentuate the difficulty in obtaining accurate results at very low load levels.

There are no simple recommendations to be made. It would seem necessary to stay away from the lower limits of detection. A suitable change of specimen dimensions and geometry, especially for very compliant materials, might help. For example, the use of bulk specimens with larger cross sectional area, would imply an increase in the applied loads. Thus, eliminating some of the difficulties of obtaining accurate results at low stress levels.

The variations in testing conditions may be further subdivided into procedural and environmental.

The most important procedure in creep testing is the loading of the specimen. Manual ramping up to the prescribed constant load introduces a significant deviation from the step loading conditions assumed by the finite element code. The absolute value of such deviation may be evaluated analytically for simple cases and depends on material properties. In appendix B such analysis is performed for a three parameter viscoelastic solid subjected to step loading and constant strain rate loading. The magnitude of the error is different at short and long times (when compared to the loading time), and dependent on material properties. Numerical examples are presented

in appendix B.

Environmental variations include temperature and moisture fluctuations during an individual test or group of tests on the same specimen. After being cured the specimens are allowed to cool in the oven and stored in ambient conditions. The specimens are assumed to have reached equilibrium by the time the test begins.

Both equilibrium temperature and moisture content are known to affect viscoelastic behavior. Even more drastic are the effects of transient changes in temperature and ambient relative humidity.

It is recommended that;

1. Loading is applied by a controlled and recorded device, in such a way as to minimize the error induced.
2. Use the recorded loading history in future finite element analysis.
3. Monitor and, if possible, control, the environmental parameters. All tests should be conducted at the same constant temperature and relative humidity.
4. Measure moisture content of specimens at different times during the testing process, to evaluate the effect of moisture uptake.
5. Store specimen in a temperature and humidity controlled enviroment. This will minimize the physical aging effect.

Data interpretation is not always a simple task. In this study the limitations were set by the available finite element code. The ABAQUS code accepts time dependent behavior in a very simplistic manner. Creep behavior is represented by tensile creep rate functions and the

initial response is evaluated over a period of one second according to an artificial value of the Young's modulus. Immediately an important difficulty surfaces:

Data interpretation and the analytical tools are linked in this study. Accordingly, the following recommendations can be made;

1. Repeat the tests with different specimens.
2. Examine the possibility of characterizing the material in more than one pure mode of loading, for example compression or shear.
3. Consider long term testing in order to improve the accuracy and validity of the above relationships.
4. Examine the necessity and effects of the mechanical conditioning procedure, in both tensile and shear loading modes.
5. Use a finite element code that allows for nonlinear viscoelastic behavior and accepts complete characterizations as expressed in equations (3.4) and (3.5).
6. Do not employ codes that require an initial "elastic" response since this may introduce a large error.

5.3 Conclusion

The results of the analysis presented in this study indicate that it may be possible to predict the viscoelastic behaviour of any adhesively bonded joint based on the viscoelastic characterization of

the bulk adhesive. This is of great engineering significance since it will enable the designers of bonded joints to incorporate time dependent behaviour in their designs without having to conduct actual tests for each joint at all possible loading modes and levels.

Future work should concentrate in obtaining a more accurate and controlled viscoelastic characterization of the adhesive, including modelling the effects of temperature and moisture, and the use of more adequate analytical tools, such as the newer versions of ABAQUS.

REFERENCES

1. Christensen, R.M., Theory of Viscoelasticity - An Introduction, 2nd edition, New York: Academic Press, 1982.
2. Flügge, W., Viscoelasticity, 2nd edition, New York: Springer-Verlag, 1975.
3. Findley, W.N., J.S. Lai and K. Onaran, Creep and Creep Relaxation of Nonlinear Viscoelastic Materials, North Holland Publishing Company Amsterdam, New York, 1972.
4. Kraus, H., Creep Analysis, John Wiley, New York, 1980.
5. Cagle, C.V.(ed.), Handbook of Adhesive Bonding, McGraw-Hill, 1982.
6. Gramoll K.C., D.A. Dillard, H.F. Brinson, "Thermoviscoelastic Characterization and Prediction of Kevlar/Epoxy Composite Laminates", Virginia Polytechnic Institute and State University, VPI-E-88-12; CAS/ESM-88-5, May 1988.
7. Tuttle, M.E., and H.F. Brinson, "Accelerated Viscoelastic Characterization of T300/5208 Graphite - Epoxy Laminates", Virginia Polytechnic Institute and State University, VPI-E-84-9, March 1984.
8. Heil, C. ,A.H. Cardon and H.F. Brinson, "The Nonlinear Viscoelastic Response of Resin Matrix Composite Laminates", Virginia Polytechnic Institute and State University, VPI-E-83-6, March 1983.

9. Roy, S., J.N. Reddy, "A Finite Element Analysis of Adhesively Bonded Composite Joints Including Geometric Nonlinearity, Nonlinear Viscoelasticity, Moisture Diffusion, and Delayed Failure" Virginia Polytechnic Institute and State University, VPI-E-87-28;CAS/ESM-87-13, Dec. 1987.

10. Cooper, J.N., "The Effect of Residual Thermal Stress on the Viscoelastic Behaviour of Adhesively Bonded Joints", Virginia Polytechnic Institute and State University, MSc Thesis, 1987.

11. Fior, V.F., "A Beam Test For Adhesives", Virginia Polytechnic Institute and State University, VPI-E-88-21; CAS/ESM-88-8, July 1988.

12. Grant, J.W., "Measurement of In-Situ Adhesive Deformation Properties", Adhesion Science Review ,Vol. 1, 1987, pp. 187-196.

13. Alfey, T., in Treatise on Adehesion, Vol. 1, R.L. Patrick (ed.), New York: Mercel Dekker, 1961, p.151.

14. Hertzberg, R.W., Defotmation and Fracture Mechanics of Engineering Materials, 2nd edition, New York: John Wiley, 1983, pp. 193-200.

15. Ferry, J.D., Viscoelastic properties of Polymers, 3rd edition, New York: John Wiley, 1980.

16. Prertz, D. and Y. Weitsman, "The non linear thermo-viscoelastic characterization of FM 73 adhesive", J. Rheology, Vol. 26, 1983, pp.245-261.

17. Schapery, R.A., "Further development of a thermodynamic constituitive theory: stress formulation", Perdue Research

Foundation, Project no. 4958, 1969.

18. Kenner, V.H., W.G. Knauss, and H.Chai, "A Simple Creep Torsiometer and its Use in the Thermorheological Characterization of a Structural Adhesive", Experimental Mechanics, Vol. 22, 1982, pp. 75-80.

19. Lefebvre D.R. and H.F. Brinson, "Characterization of Structural Adhesives, FM 73 and FM 300", Oct. 1985, VPI-CAS/ESM-85-3.

20. Dolev, G. and O. Ishai, "Mechanical Characterization of Structural Adhesive Layers in-situ and as Bulk Material", J. Adhesion, Vol.12, 1981, pp. 283-294.

21. Stinger, L.G., "Comparison of the Shear Stress-Strain Behaviour of some Structural Adhesives", J. Adhesion, Vol. 18, 1985, pp. 185-196.

22. Knollman, G.C. and J.J. Hartog, "Experimental Determination of the Variation in Shear Modulus Through the Interfacial Zone of an Adhesive", J. Adhesion, Vol.17, 1983, pp. 251-272.

23. Green, A.E. and R.S. Rivlin, "The Mechanics of Nonlinear Materials with Memory", Arch. Rational Mech Anal, Vol 1, No.1, 1957, pp. 1-21.

24. Findley, W.N., and G. Khosla, "Application of the Superposition Principle and Theories of Mechanical Equation of State, Strain, and Time Hardening to Creep of Plastics Under Changing Loads", Journal of Applied Physics, Vol. 26, No. 7, 1955, pp. 821-831.

25. Findley, W.N., and J.S.Y. Lai, "A Modified Superposition Principle Applied to Creep Of Nonlinear Viscoelastic Materials

Under Abrupt Changes in State of Combined Stress", Transaction of the Society of Rhology, Vol. 11, No. 3, 1967, pp.361-381.

26. Lai, J.S. and W.N. Findley, "Creep of 2618 Aluminum Under Step Stress Changes Predicted by a Viscous-Viscoelastic Model", Journal Of Applied Mechanics, Vol. 47, No. 21, Mar 1980, pp. 21-26.

27. Findley W.N., U.W. Cho and J.L. Ding, "Creep of Metals and Plastics Under Combined Stresses, A Review", Journal of Engineering Materials and Technology, Vol. 101,Oct. 1979, pp. 365-368.

28. Banks-Sills, L., M. Arcan, and Y. Bortman, "AMixed Mode Fracture Specimen for Mode II Dominant Deformation", Eng. Fract. Mechanics, Vol. 20, 1984, pp. 145-157.

29. Weissberg, V. and M. Arcan, "A Uniform Pure Shear Testing Specimen for Adhesive Characterization", ASTM STP 981, 1988, pp. 28-38.

30. ABAQUS Version 4.5, User's Manual, July 1985.

31. Ward, T.C., A. Wood Brinkley, M. Sheridan and P. Koning, "Effect of Molecular Orientation on Bonded Joints", Polymer Preprints (American Chemical Society Division of Polymer Chemistry), 1983, Vol. 24(2) pp. 119-121.

32. Ward, T.C., M. Sheridan and D.K. Kotzev, "Nondestractive Evaluation of Some Bonded Joints", Organic Coating and Applied Polymer Science Proceedings, 1982, Vol. 47, pp. 467-470.

APPENDIX A

CREEP SUBROUTINE

The creep subroutine defines a creep law. It is called during steps where creep occurs (when the step '*visco' is defined), in each of the elements having the '*creep' material option, with law = user parameter.

In order to use the subroutine, define the following:

a) ERATE (1) - the equivalent (uniaxial) creep strain rate, $\frac{\partial \bar{\varepsilon}^{cr}}{\partial t}$

b) SINV2 - Mises equivalent stress, $\tilde{q}$.

c) TIME - total time.

d) DTIME - current time increment.

e) $\Delta\bar{\varepsilon}^{cr}$ - creep strain increment, ERATE (1) * DTIME

f) ERATE (5) - derivative of the equivalent creep strain incement with respect to the equivalent stress, $\tilde{q}$, at the end of the time increment, $\frac{\partial \Delta\bar{\varepsilon}^{cr}}{\partial \tilde{q}}$

The following creep subroutine describs the creep properties of Lord Fusor 320/322 :

```
      SUBROUTINE CREEP (ERATE,ECR,EQUIVE,STRESS,NDI,NSHR,SINV1,SINV2,
     * TEMP,PREDEF,TIME,DTIME,MATERL,SVAR)
C
C     INCLUDE THE FOLLOWING STATMENT FOR DOUBLE PRECISION
      IMPLICIT REAL*8(A-H,O-Z)
      DIMENTION ERATE(5),ECR(1),STRESS(1),PREDEF(1),SVAR(1)
      F=7.6690E-7
      M=7.3166E-8
      XN=0.53743
C     QUADRATIC POWER LAW CURVE FIT - FUSOR 320/322
      TERM1=M*(SINV2+F*SINV2**3)
      TERM2=M*(1.+3.*F*SINV2**2)
      ERATE(1)=TERM1*((TIME+DTIME)**XN-TIME**XN)
      ERATE(5)=ERATE(1)*TERM2/TERM1
      ERATE(1)=ERATE(1)/DTIME
      RETURN
      END
```

For the subroutine which describes the viscoelastic behaviour of Ashland Plyogrip 6600/6620 urethane, only the values of the coefficients F, M and XN are changed..

APPENDIX B

EFFECT OF RAMP LOADING

The magnitude of the experimental error introduced due to the manual loading procedure is unknown, and it cannot be deduced from the data. In order to find a first crude approximation and evaluate the role of the different parameters (loading rate and material properties), a simple analysis of a three parameter viscoelastic solid is performed.

The model consists of a free spring, denoted E_0, and a Kelvin element represented by a second spring, E_1, and dashpot, μ_1, in series. The constitutive equation of such a simple model is given by,

$$\sigma + \overset{\circ}{\sigma} p_1 = \varepsilon q_0 + \overset{\circ}{\varepsilon} q_1 \qquad \text{(B1)}$$

where the superscript $\circ$ represents a time derivative and,

$$p_1 = \frac{\mu_1}{E_1 + E_0}, \quad q = \frac{\mu_1 E_0}{E_1 + E_0} \quad \text{and} \quad q_0 = \frac{E_0 E_1}{E_1 + E_0} \qquad \text{(B2)}$$

In the case of instatntaneous loading up to a constant load σ_0, equation (B1) reduces to,

$$\dot{\varepsilon} + \varepsilon\frac{q_0}{q_1} = \frac{\sigma}{q_1} \qquad \text{(B3)}$$

with the initial condition,

$$\varepsilon(0) = \frac{\sigma_0}{E_0} \qquad \text{(B4)}$$

The solution to equation (B3) and the above initial value is,

$$\varepsilon(t) = \sigma_0\left[\frac{1}{E_0} + \frac{1}{E_1}\left[1 - \exp\left(-\frac{E_1}{\mu_1}t\right)\right]\right] \qquad \text{(B5)}$$

or,
$$\varepsilon(t) = \varepsilon(0)\left[1 + \frac{E_0}{E_1}*\left[1 - \exp\left(-\frac{E_1}{\mu_1}t\right)\right]\right] \qquad \text{(B6)}$$

For the case of manual loading, the loading rate could be idealized as constant load rate up to σ_0, achieved at time t_0.

$$\sigma = Rt \qquad \text{for } t < t_0 \qquad \text{(B7)}$$

Then for t<t0, $\dot{\sigma} = R$ (B8)

Substituting in (B1),

$$Rt + Rp_1 = \varepsilon q_0 + \dot{\varepsilon} q_1 \qquad \text{(B9)}$$

A first order nonhomogeneous differential equation with the initial condition,

$$\varepsilon(0) = 0 \qquad \text{(B10)}$$

The solution to (B9) and the above initial condition is,

$$\varepsilon(t) = \frac{R\mu_1}{E_1^2}\left[\exp\left(-\frac{E_1}{\mu_1}t\right) - 1\right] + \frac{R(E_1+E_0)}{E_1E_0}\,t \qquad (B11)$$

At $t=t_0$ the strain is,

$$\varepsilon(t_0) = \frac{R\mu_1}{E_1^2}\left[\exp\left(-\frac{E_1}{\mu_1}t_0\right) - 1\right] + \frac{R(E_1+E_0)}{E_1E_0}\,t_0 \qquad (B12)$$

Substituting in equation (B6) for the initial strain, then complete response at $t>t_0$ is,

$$\varepsilon(t) = \varepsilon(t_0)\left[1 + \frac{E_0}{E_1}\left[1 - \exp\left(-\frac{E_1}{\mu_1} * (t-t_0)\right)\right]\right] \qquad (B13)$$

It is worthwhile to notice that for the case where $t_0 \longrightarrow 0$, then expression (B13) reduces to (B6).

To evaluate the two different responses it is useful to examine the ratio of the creep strains obtained from (B5) and (B13), denote $\phi(t)$, at two points in time, at $t \longrightarrow \infty$ and after the load has reached its constant value.

For the case of instatntaneous loading,

$$\lim_{t\longrightarrow\infty} \varepsilon(t) = \sigma_o \frac{E_0+E_1}{E_0E_1} \qquad (B14)$$

For the case of ramp loading,

$$\lim_{t\longrightarrow\infty} \varepsilon(t) = \sigma_o \frac{E_0+E_1}{E_0E_1}\left[\frac{E_0\mu_1}{t_0E_1^2}\left[\exp\left(-\frac{E_1}{\mu_1}t_0\right) - 1\right] + \frac{E_1+E_0}{E_1}\right] \qquad (B15)$$

Dividing (B15) by (B14), the ratio is,

$$\phi(t\rightarrow \infty) = \frac{E_0\mu_1}{t_0E_1^2}\left[\exp(-\frac{E_1}{\mu_1}t_0) - 1\right]+\frac{E_1+E_0}{E_1} \qquad (B16)$$

Again, this ratio appraches unity for $t_0\rightarrow 0$.

The ratio of (B12) and (B4) represents the ratio of strains when the stress reaches its constant value for both cases. After deriving the ratio it was found that

$$\phi(\sigma_0) = \phi(t\rightarrow \infty) \qquad (B17)$$

and, in fact, after the load has reached its constant values,

$$(\varepsilon(t))_{creep} = \propto (\varepsilon(t-t_0))_{ramp} \qquad (B18)$$

Coefficient of proportionality is given by (B16).

It is apparent that the amount of error introduced due to ramp loading depends on a complicated function of the material properties (E_0, E_1 and μ_1) and the loading rate, t_0. As it was observed above, for $t_0\rightarrow 0$, the ratio reduces to 1. Although the number of combinations is infinite, the two following numerical examples are presented to help understand the magnitudes involved. For both examples, t_0=30 seconds.

Example 1: Stiff epoxy adhesive

$E_0=52\times10^3$ psi, $E_1=1\times10^5$ psi, $\mu_1=7.5\times10^7$ psi$\times$sec

then, $\phi(t) = 1.01$ for $t>t_0$

Example 2: Compliant urethane adhesive

$E_0=33\times10^3$ psi, $E_1=18.7\times10^3$ psi, $\mu_1=48.5$ psi$\times$sec

then, $\phi(t) = 2.62$ for $t>t_0$

Obviously, ramp loading may have a small or large impact on the quality of the test. It is especially significant when the initial compliance needs to be evaluated, as is the case for the finite element code.

The vita has been removed from the scanned document